Performance of MIMO Cognitive Ad-hoc Networks

Amiotosh Ghosh

A Thesis

in

The Department

of

Eletrical and Computer Engineering

Presented in Partial Fulfillment of the Requirements
for the Degree of Doctor of Philosophy at
Concordia University
Montreal, Quebec, Canada

April 2013

CONCORDIA UNIVERSITY
SCHOOL OF GRADUATE STUDIES

This is to certify that the thesis prepared

By: Amiotosh Ghosh

Entitled: Performance of MIMO Cognitive Ad-hoc Networks

and submitted in partial fulfillment of the requirements for the degree of

DOCTOR OF PHILOSOPHY (Electrical & Computer Engineering)

complies with the regulations of the University and meets the accepted standards with respect to originality and quality.

Signed by the final examining committee:

Dr. C. Assi   Chair

Dr. H. S. Hassanein   External Examiner

Dr. I. Hassan   External to Program

Dr. D. Qiu   Examiner

Dr. Y. R. Shayan   Examiner

Dr. W. Hamouda   Thesis Supervisor

Approved by

_____
Chair of Department or Graduate Program Director

_____   _____
                                            Dean of Faculty

Abstract

Performance of MIMO Cognitive Ad-hoc Networks

Amiotosh Ghosh, PhD

Concordia University, 2013

Cognitive ad-hoc networks are able to share primary user frequency bands following certain interference preconditions. For considered cognitive network, cognitive communication is limited by the interference imposed on the primary user. Probability of channel availability for cognitive nodes for such opportunistic access is determined. Furthermore, this probability of channel availability is used for the performance analysis purpose. A Carrier Sense Multiple Access (CSMA) Media Access Control (MAC) protocol for the cognitive network is considered and for that the embedded Markov model of cognitive nodes is determined. This Markov model is used to determine the average channel access delay, throughput and service rate of cognitive nodes.

This network is further extended to consider multiple frequency bands for cognitive access. For this propose algorithms are proposed to address the channel allocation and fairness issues of multi-band multiuser cognitive ad-hoc networks. Nodes in the network have unequal channel access probability and have no prior information about the offered bandwidth or number of users in the multiple access system. In that, nodes use reinforcement learning algorithm to predict future channel selection probability from the past experience and reach an equilibrium state. Proof of convergence of this multi party stochastic game is established. Nevertheless, cognitive nodes can reduce the convergence

time by exchanging channel selection information and thus further improve the network performance.

To further improve the spectrum utilization, this study is extended to include Multiple-input Multiple-output (MIMO) techniques. To improve the transmission efficiency of the MIMO system, a cross-layer antenna selection algorithm is proposed. The proposed cross-layer antenna selection and beamforming algorithm works as the data link layer efficiency information is used for antenna selection purpose to achieve high efficiency at the data link layer.

Having analyzed the cognitive network, to consider more realistic scenario primary users identification method is proposed. An artificial intelligent method has been adopted for this purpose. Numerical results are presented for the algorithm and compare these results with the theoretical ones.

Acknowledgments

I owe my gratitude to all the people who have me this possible and because of whom my graduate experience has been one that I will cherish forever.

First of all I would like to express my deepest gratitude to my thesis supervisor, Dr. Walaa Hamouda, for his continuous guidance and support throughout my thesis work. During my work he always provides me key directions and inspiration with his great personality, vast experience and immense knowledge.

I would like also to express my thanks to my thesis committee for agreeing to serve on my thesis committee and for spearing their invaluable time reviewing the manuscript.

Also, I want to acknowledge my fellow graduate students who helped me a lot providing continuous support and advices during my thesis work. I also want to acknowledge the faculty members, staff and system administrators of Electrical and Computer Engineering Department for their cooperation

I am forever indebted to my parents for their support and inspiration.

<div align="right">AMIOTOSH GHOSH</div>

To my parents for their love and patience

Contents

List of Figures

xii

List of Algorithms

List of symbols

T_f — Channel unavailability time due to fading

F_i — Channel access state

B_i — Back-off state

C_i — Collision state

T — Transmission state

$\hat{C}$ — No. of unused frequency bands of primary user

$\hat{T}$ — No. of Cognitive pairs

N_t — Number of transmit antenna

N_r — Number of receive antenna

$\boldsymbol{G}_i$ — 'Cognitive-to-Primary user' $1 \times N_t$ channel vector

$\mathbf{x}$ — $N_t \times 1$ cognitive user transmit symbol vector

$\mathbf{y}_{pl}^i$ — Interference signal at any primary user l from cognitive user $i \in \hat{T}$

I_i^l — Interference at lth primary user due to cognitive user $i \in \hat{T}$

$p_{\sigma_{eff}}(u)$ — pdf of interference power

I_{th} — Interference threshold at the primary user

σ — Cognitive SNR

$\hat{\rho}$ — Conditional collision probability

P — Probability of successful transmission

m — Maximum number of back-off stage

K — Maximum number of retransmission event

w — Minimum value of contention window size

T_s — Holding time in transmission state

T_c — Holding time in collision state

$E(p)$ — Expected packet transmission time

P_s — Probability of successful transmission

P_c	Probability of collision
P_i	Probability of channel being idle
d	Interval time between two successive back-off timer
t_{slot}	duration of a time slot
Ew_i	Average value of back-off counter
P_a	Probability of channel availability
Y_i	Holding time at back-off stage
D_i	Channel access delay
$E(D)$	Average channel access delay
π_{C_i}	Steady state probability of collision state
π_{F_i}	Steady state probability of fading state
π_{B_i}	Steady state probability of back-off collision state
π_T	Steady state probability of transmission state
$\hat{\tau}_c$	Holding time in state C
$\hat{\tau}_T$	Holding time in state T
$\hat{\tau}_f$	Holding time in state F
$\hat{d}$	Holding time in state B
$\bar{\pi}_T$	Service probability or rate
η	Normalized throughput
$Q(.)$	Q value
$\hat{P}$	Exact potential game
θ	Cardinality function
$E(.)$	Expectation operator
$O(.)$	Complexity function
M	No. of RF Chain
K	Number of selected transmit antenna
$\boldsymbol{H}$	$N_r \times N_t$ 'Cognitive-to-Cognitive' channel matrix

$\boldsymbol{H}_p$	$N_r \times K$ 'Cognitive-to-Cognitive' channel sub-matrix
$\boldsymbol{\Pi}$	Channel dependent permutation matrix for greedy QR detection ordering
$\boldsymbol{n}$	Complex Gaussian noise vector with zero mean and variance N_o
$\mathbf{y}_c$	$C^{N_r \times 1}$ Received signal at cognitive receivers
$\mathbf{A}$	Beamforming precoding matrix.
τ_i	Transmission probability of ith cognitive node
ρ_o	Average received SNR per receive antenna
ρ_j	Received SNR at jth subchannel
r_{jj}	Diagonal elements of the matrix $\boldsymbol{R}_p$ calculated using $\boldsymbol{H}_p\boldsymbol{\Pi} = \boldsymbol{Q}_p\boldsymbol{R}_p$
χ	LLC sublayer achievable data rate
U_i	Utility of channel
$\beta, \gamma, \& \delta$	User defined parameters for the utility function
S_i	Set of strategies for node $i \in \hat{T}$
s_a	Strategy to select channel $a \in \hat{C}$
$p_i^{t+1}(s_a)$	Probability to select strategy s_a
α	Learning rate
$\hat{C}_{xy}$	Cumulant of order x with degree y
$\hat{M}_{xy}$	Moment of order x with degree y

List of Acronyms

ANN	Artificial Neural Network
AMC	Automatic Modulation Classification
BPSK	Binary Phase Shift Keying
BER	Bit-Error Rate
CR	Cognitive Radios
CSI	Channel State Information
CSMA/CA	Carrier Sense Multiple Access with Collision Avoidance
CTS	Clear to send
CTMC	Continuous Time Markov Chain
CLAS	Cross Layer Antenna Selection
CLBF	Cross Layer antenna selection and Beamforming
DFD	Decision Feedback Detection
D − DMI	Direct Digital Modulation Identification
DSA	Dynamic Spectrum Access
DIFS	Distributed coordination function Inter Frame Space
ECs	European Commissions
ED	Energy Detection
FCC	Federal Communication Commission
GBN	Go-Back-N
HOS	Higher Order Statistics
i.i.d.	Independent and Identically Distributed
ISM	Industrial, Scientific and Medical
LLC	Logical Link Control
KCC	Korea Communications Commission
MIMO	Multiple-input Multiple-output

MAC	Media Access Control
MAS	Maximum Antenna Selection
$MBMMCAN$	Multi Band Multiuser MIMO Cognitive Ad-hoc Networks
ML	Maximum Likelihood
pdf	probability density function
PER	Packet Error Rate
QoS	Quality of Service
RTS	Request to send
RF	Radio Frequency
$RPROP$	Resilient Backpropagation Learning Algorithm
SNR	Signal-to-Noise Ratio
$SARSA$	State-Action-Reward-State-Action
SDR	Software Defined Radio
$SISO$	Single-Input and Single-Output
$TDMA$	Time-Division Multiple-Access
WAS	Without Antenna Selection
ZF	Zero-Forcing

Chapter 1

Introduction

1.1   Cognitive Radio

Traditionally, regulatory authorities applied fixed spectrum allocation policy to reduce chaos and to promote the development of inter operable wireless devices. But recent growth of wireless devices creates two challenges for the fixed spectrum allocation policy, namely: spectrum crisis and low spectrum utilization. Spectrum crisis situation arose as fixed allocation policy licensed out most of the available bands [1]. On the other hand, most of the licensed users either use the assigned spectrum for a small amount of time, or do not use the spectrum at all. As a result, new licensed applicants are denied, though some of the frequency bands are not utilized at all (Fig. 1.1 [2]). For example, armature radio band is utilized for a very small amount of time. Conversely, ISM (Industrial, Scientific and Medical), C, and L frequency bands are heavily utilized. This crisis situation prevailed so far, as the traditional wireless devices are designed for a particular frequency band which cannot operate in other bands. Fortunately, recent development of Software Defined Radios (SDR) eliminate the interoperability issues. Unlike the traditional hardware radios, SDRs are able to operate in a wide range of frequencies by switching the carrier frequency [3]. Motivated by these facts, the Federal Communication Commis-
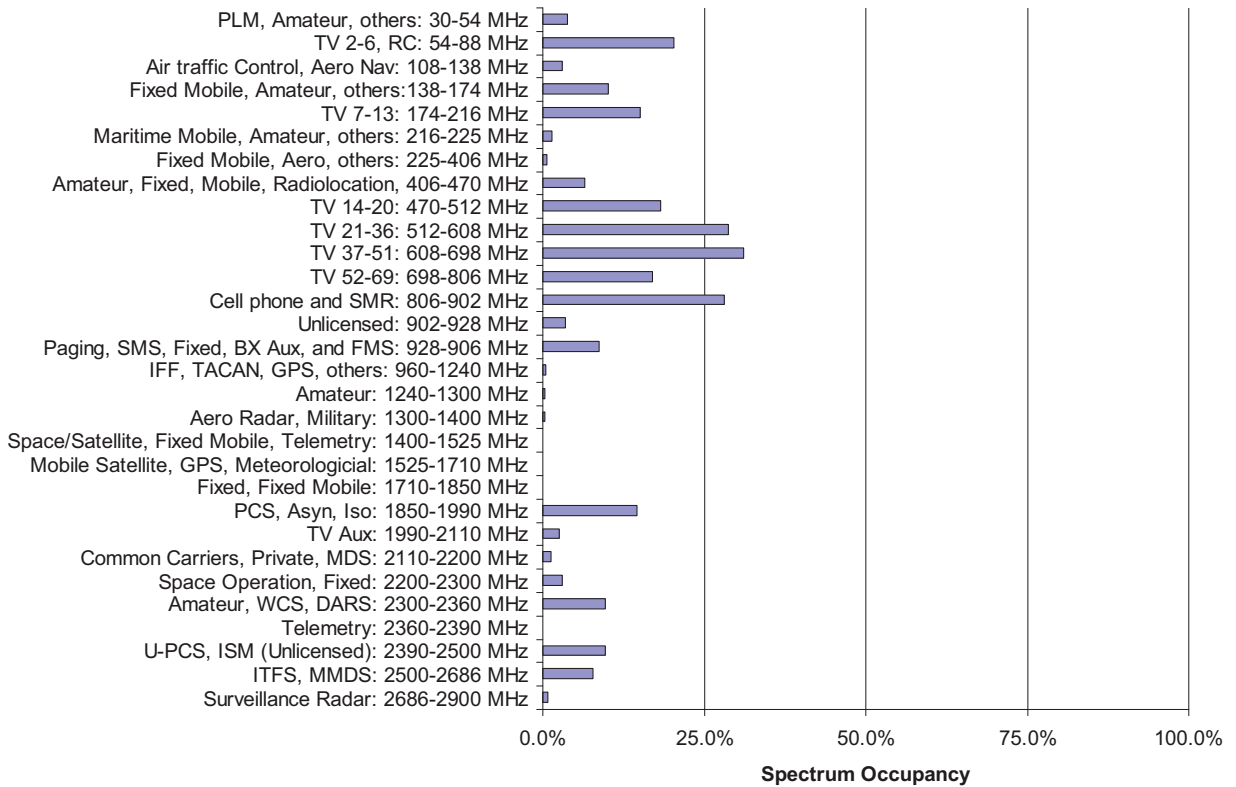
Figure 1.1: Average spectrum occupancy over six locations: Riverbend Park (Great Falls, VA), Tysons Corner (VA), NSF Roof (Arlington, VA), NRAO (Greenbank, WV), New York City, NRAO (Greenbank, WV), SSC Roof (Vienna, VA) and Chicago (IL) [2].

sion (FCC) in United States [1,4], Ofcom in United Kingdom [5], European Commissions (ECs) [6], and Korea Communications Commission (KCC) [7] have been considering more flexible and comprehensive usage of the available spectrum through the use of cognitive radio technology. Beyond policy establishments, we also find practical implementation of cognitive networks first in Claudvilla, Virginia in 2009, and later on a large-scale in Wilmington, North Carolina, in 2010 [8], which proved that cognitive networks are realizable and have real promise.

1.1.1   Classification

Cognitive radios apply two distinct approaches [9] for concurrent spectrum access, viz., spectrum overlay and spectrum underlay, described as follows:

- Underlay scheme, in which secondary users occupy the whole bandwidth and transmit at power lower than the noise floor of the primary user. As power is very low in these schemes, secondary users communication appears as white noise at the primary user.

- Overlay scheme, in which secondary users use opportunistic or adaptive techniques to determine when and where to transmit. In this study, we will only focus on overlay communications of cognitive users.

1.1.2 Challenges for cognitive communication

Cognitive devices impose unique challenges due to the high fluctuation in the available spectrum, as well as the diverse Quality of Service (QoS) requirements of various applications. In order to address these challenges, each cognitive user in the cognitive network must perform [9]:

- Spectrum sensing, to determine which portions of the spectrum are available.

- Spectrum decision, to select the best available channel.

- Spectrum sharing, to coordinate access to this channel with other users.

- Spectrum mobility, to vacate the channel when a licensed user is detected.

1.2   Motivation

In this work, we will mainly focus on the above mentioned functionalities of cognitive networks. Spectrum decision of a cognitive network has two primary goals: fairness and utilization [3]. One of the prominent techniques to improve the spectrum utilization is through Multiple-Input and Multiple-output (MIMO) techniques. As cognitive radios are able to access very small amount of wireless resources, this high spectrum efficiency

makes MIMO systems extremely valuable for cognitive devices. Moreover, MIMO system efficiency can also be improved using techniques [10, 11], such as, space-time coding, antenna selection, etc. This motivates us to investigate the application of MIMO technology in cognitive networks.

Fairness among the cognitive nodes is another important issue for spectrum sharing. But, most of the existing works in the area of channel selection for cognitive networks assume that cognitive radios get access to channels having equal bandwidth [12–16]. Incidentally, bandwidth is not equally divided among the primary users. As a result, this equal bandwidth assumption is not realistic. For the unequal bandwidth scenario, nodes in a cognitive network may experience unequal data rate i.e., performance. Cognitive radios have to vacate the occupied spectrum on the presence of the primary user. In such case, cognitive nodes may switch to another spectrum or interrupt service, if no opportunity is present.

Recently, the concept of cooperative communications has been introduced to gain benefits of MIMO through cooperation between wireless nodes [17]. It is envisioned to improve reliability and throughput in wireless networks. Similar to traditional cooperative networks in cognitive settings, nodes can cooperate by relaying to each other useful information about the network, while at the destination node, MIMO like diversity can be achieved by combining the original and relayed packets [18, 19]. Moreover, nodes can cooperative with each other in decision making and learning process of cognitive communication.

As indicated above, in cognitive settings, nodes may receive simultaneously signals from primary users and from other cognitive users. Early detection of primary users' presence is one of the most important tasks in cognitive communications. In the literature, available algorithms use a separate sensing time slot for this detection purpose [20, 21] . If cognitive users detect primary user signal while communicating, cognitive nodes can either reduce transmit power or stop transmitting to reduce unwanted interference on the

primary user.

1.3   Thesis Contributions

In light of motivation and challenges mentioned above, the objective of this work is to investigate the issues related to spectrum decision, sharing, and mobility functionalities of cognitive ad-hoc networks. We consider a cognitive ad-hoc network as shown in Fig. 1.2. Cognitive nodes use side by side frequency bands of the primary user. As a result, primary users experience interference due to spill over energy [22]. Depending on the amount of interference on primary users, cognitive nodes may need to turn off communication at some instance. We assume cognitive nodes measure this interference using pilot signaling of the primary user or blind channel estimation method. In this study, we consider physical layer, data link layer, and cross layer issues to improve network performance for this type of communication environment. At this end, we investigate the following topics as:

- We analyze the performance of interference-limited cognitive ad-hoc networks. In the cognitive network, cognitive nodes use a multiple access MAC protocol for chan-
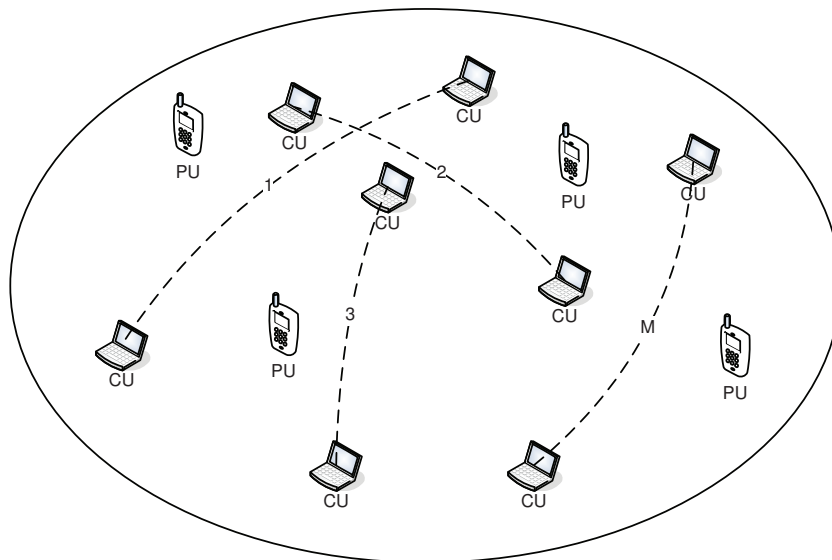
Figure 1.2: Cognitive network scenario.

nel access purpose while communication is limited by the interference imposed on primary users by the cognitive nodes. Cognitive users are able to access the channel if the interference imposed on primary users is below the specified threshold. For this opportunistic network, we determine the probability of accessing the channel under Rayleigh fading condition. We establish the embedded Markov model in the cognitive nodes for the modified MAC protocol. We present analysis for the Markov model to determine the average channel access delay, throughput and service rate of cognitive nodes.

- We extend our study for multi-band scenario. To address the channel allocation and fairness issues of multi-band multiuser cognitive ad-hoc networks (MBMMCAN), we propose machine learning based algorithm. Nodes in the network have unequal channel access probability and have no prior information about the offered bandwidth or number of users in the multiple access system. In that, nodes use reinforcement learning algorithm to predict future channel selection probability from the past experience and reach an equilibrium state. Proof of convergence of this multi party stochastic game is provided, and the throughput performance is analyzed and compared for Q learning, No-regret learning and learning automata algorithms. We further extend this study for cooperative communication context. Cognitive nodes use modified MAC protocol to achieve cooperative communication. In the process, nodes achieve diversity gain and exchange channel selection information to further improve the network performance.

- Efficient use of the spectrum is one of the key issues for cognitive communications. To address this issue, we consider a MIMO cross-layer transmit-antenna selection algorithm to improve the spectrum utilization between cognitive node pairs. We also consider the effect of antenna selection approaches on beamforming and pre-coding techniques. Antenna selection, beamforming and pre-coding at the physical layer

determine the performance of a particular channel. This allows us to apply these techniques combined with the channel selection algorithm to determine the network performance. For implementation point of view, we also determine the complexity of the proposed learning based channel selection and antenna selection algorithm.

- We propose primary user signal detection using modulation class identification method. We consider multiple transmit and multiple receive antennas for cognitive nodes. We employ machine learning approaches for the modulation identification purpose. The proposed algorithm works as higher order moments and cumulants are calculated from the received signal samples at each of the receiving branches of cognitive nodes. After this step, these features are fed to an Artificial Neural Network (ANN) to determine the presence of primary users. Final identification decision is mad using the decisions from all receiving branches. We also present numerical results of our algorithm and compare these results with the theoretical results of the energy detection algorithm [23].

Contributions of this thesis have been published in [24–31]. Throughout the thesis, bold-face letters are used to represent vectors and matrices.

1.3.1 Outline of the thesis

The rest of the thesis is organized as follows. In Chapter 2, we present literature review of cognitive ad-hoc networks, machine learning, game theory and MIMO.

In Chapter 3, we determine the average access delay, throughput and service time for interference-limited cognitive networks. For this purpose, we provide theoretical results for the probability of channel availability of cognitive networks in interference-limited communication. We present an embedded Markov model of the cognitive nodes. We use previously determined channel availability results in the embedded Markov model to determine the network performance metrics. Both simulation and analytical results are

presented to examine the performance under different network settings.

In Chapter 4, we present performance results for learning-based channel selection approaches in cognitive ad-hoc networks. First, we establish proof of convergence for the algorithms in multi-band cognitive ad-hod networks with heterogeneous nodes. We show that learning-based channel selection algorithms converge to a Nash equilibrium point for nodes having unequal packet arrival rate in multi-party multi-agent stochastic game. We also establish that learning-based algorithms can improve the average data rate of the network, and can reduce user satisfaction variance i.e., improve fairness among cognitive nodes. We further show that the convergence time and data rate improve for the cooperative learning case.

In Chapter 5, we investigate the performance of cross-layer antenna selection and channel selection approaches for cognitive ad-hoc networks. We present the average data rate objective function for multi-band cognitive ad-hod network that accounts for the interference constraint set by the primary user. It is shown that the proposed cross-layer antenna selection algorithm can improve the link layer transmission efficiency. Our results also indicate that when the cross-layer antenna selection algorithm is deployed with learning based channel selection algorithm, the average data rate of the network improves significantly. We further combine antenna selection with beamforming to gain high throughput in cognitive networks. Using beamforming, the combined algorithm allows cognitive users to access the channel with no interference effect on primary users. The developed cross-layer algorithm offers high throughput using low number of RF chains. Our results also show that the effect of imperfect channel-state information (CSI) and delayed estimates is not significant as the system still able to outperform other existing schemes.

In Chapter 6, we present an algorithm for primary user identification using modulation class detection. We also evaluate the effect of multiple receive antennas on identification probability. We present simulation results for both intra-class and inter-class

identifications. Our results indicate that neural networks can be adopted to identify primary users' presence with very high accuracy while cognitive users are communicating.

Finally, in Chapter 7 we present a brief summery of our investigation and some important conclusions. We also include recommendations for possible future areas of interest related to this thesis.

Chapter 2

Background

In this chapter, we first present a brief review on cognitive networks, machine learning, ANN, followed by an introduction to game theory, and finally on MIMO techniques. Our intention is to make the reader prepared for next chapters, where we use these techniques in our development.

2.1 Cognitive Ad-hoc Networks

An ad-hoc network is a collection of wireless mobile nodes that self-configure to form a network without any established infrastructure. A wireless link exists between each pair of nodes as there is no master node or base station. That is, communication is peer to peer. As every node may not be in the direct communication range of every other node, nodes can cooperate in routing each other's data. In addition, the nodes in an ad-hoc network may be mobile.

According to the features mentioned above, ad-hoc networks can be rapidly deployed and reconfigured, can be easily tailored to specific applications, and are robust due to the distributed nature and redundancy of nodes.

2.1.1 Classical ad-hoc networks vs. cognitive ad-hoc networks

The uncertain spectrum environment and the importance of protecting the transmission of the licensed users of the spectrum mainly differentiate classical ad-hoc networks from cognitive ad-hoc networks. We describe these unique features of cognitive ad-hoc networks [9, 32] compared to classical ad-hoc networks as follows:

- **Choice of transmission spectrum**: In cognitive radio networks, the available spectrum bands are distributed over a wide frequency range, which vary over time and space. Thus, each user sees different spectrum availability according to the primary user activity. This is different in classical ad-hoc networks where they generally operate on a pre-decided channel that remains unchanged with time. For the ad-hoc network with multi-channel support, all the channels are continuously available for transmission, though nodes may select few of the latter from this set based on self-interference constraints. A key distinguishing factor is the main consideration of protecting the primary user transmission, which is entirely missing in classical ad-hoc networks.

- **Topology control**: Ad-hoc networks lack centralized support, and hence must rely on local coordination to gather topology information. In classical ad-hoc networks, this is easily accomplished by periodic beacon messages on the channel. However, in cognitive ad-hoc networks, as the licensed spectrum opportunity exists over large range of frequencies, sending beacons over all the possible channels is not feasible. Thus, cognitive ad-hoc networks are highly probable to have incomplete topology information, which leads to an increase in collisions among cognitive users as well as interference to the primary users.

- **Multi-hop/multi-spectrum transmission**: The end-to-end route in the cognitive ad-hoc network consists of multiple hops having different channels according to the spectrum availability. Thus, cognitive ad-hoc networks require collaboration

11

between routing and spectrum allocation in establishing these routes. Moreover, the spectrum switching on the links are frequent based on primary users' arrivals. However, in classical ad hoc networks, maintaining end-to-end QoS involves not only the traffic load, but also how many different channels and possibly spectrum bands are used in the path, the number of primary users induced spectrum change events, and consideration of periodic spectrum sensing functions.

- **Distinguishing mobility from primary user activity**: In classical ad hoc networks, routes formed over multiple hops may periodically experience disconnection caused by node mobility. These cases may be detected when the next hop node in the path does not reply to messages and retry limit is exceeded at the link layer. However, in cognitive ad-hoc networks, a node may not be able to transmit immediately if it detects the presence of a primary user on the spectrum, even in the absence of mobility. Thus, correctly inferring mobility conditions and initiating the appropriate recovery mechanism in cognitive ad-hoc networks necessitate a different approach from the classical one.

2.1.2 Cognitive radio functions

To realize the above mentioned differences, cognitive radio devices use greater sense of self-awareness, learning and planning capabilities. The operation of cognitive radios can be best described by the cognition cycle. The cognition cycle is a state machine that shows the stages in the cognitive process as shown in Fig. 2.1 [33]. In simple terms, radio receives information about its operation environment - the outside world. This corresponds to the **Observe state**. This information is then evaluated to determine its importance during the **Orient state**. Based on this evaluation, the radio can either react immediately and enter the **Act state**, or it can determine its various options in a more considered manner during the **Decide state**, or it can **Plan** for the longer term before deciding and acting. Throughout the process, the radio uses these observations
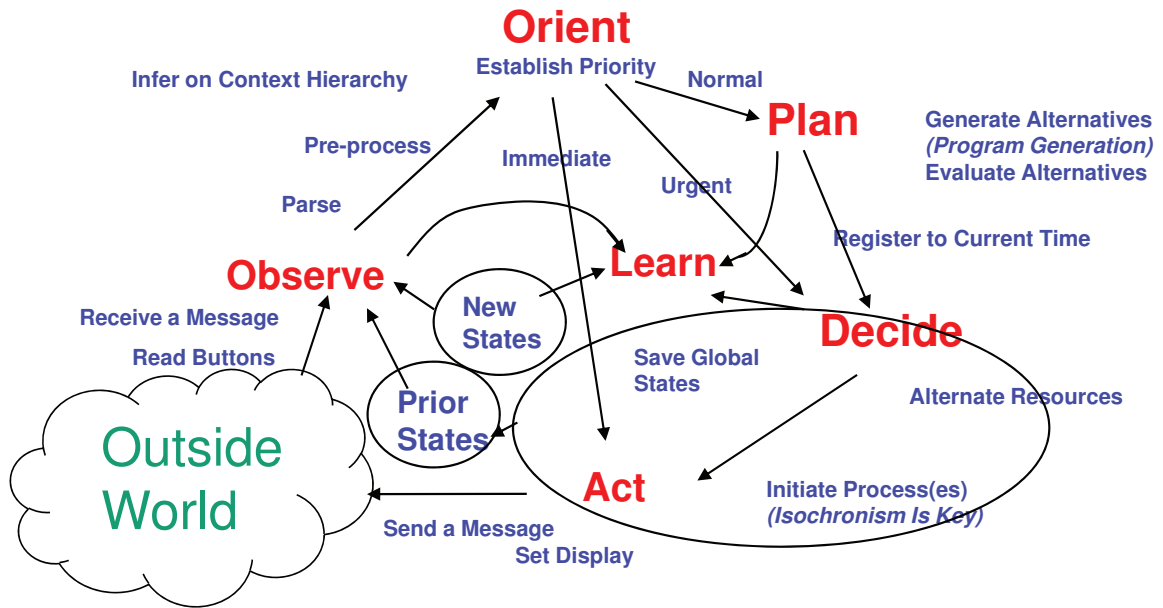
Figure 2.1: The cognition cycle proposed in [33].

and decisions to improve the operation and to **Learn**. The cognition cycle, though only approximating the process, has proved to be a very useful framework within which to analyze the concept of the cognitive radio. However, this model is further extended in [3] to include the physical layer perspectives as shown in Fig. 2.2 [3]. As indicated in the figure, physical layer parameters such as transmit power control, interference temperature measurement, channel state information estimation and spectrum hole detection tasks are included in the cognition cycle. This enable the cognition cycle to become the basis of large amount of works in this area. In the following subsections we will introduce machine learning, MIMO, game theory related to cognition cycle while we propose physical layer, data-link layer, and cross layer techniques to improve network performance in the following chapters.

2.2 Machine Learning

Machine learning is a branch of artificial intelligence, contains construction and study of systems that can learn from input data. For instance, a system could be trained

Radio Environment
(Outside world)

Action:
Transmitted
signal

RF
stimuli

Spectrum holes
Noise-floor statistics
Traffic statistics

Radio
scene
analysis

Transmit power
control and
spectrum
management

Interference
Temperature

Channel state
estimation,
and predictive
modeling

Quantized
Channel capacity

Transmitter

Receiver
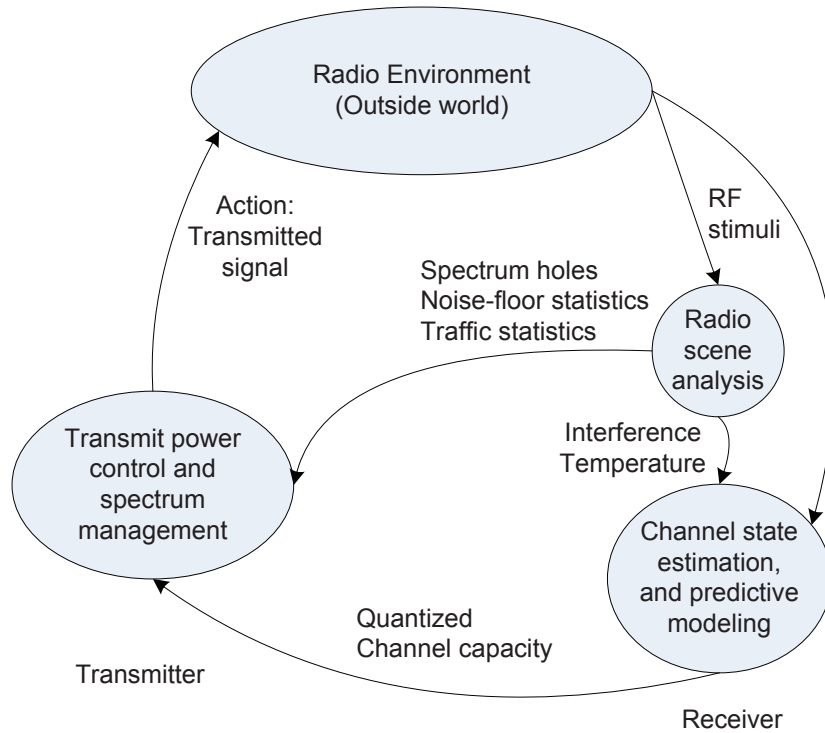
Figure 2.2: The cognition cycle proposed in [3].

to recognize characters by optical scanning. After the learning phase, it can be used to recognize printed characters automatically based on previous learning experience. Machine learning algorithms can be classified based on the desired outcome of the algorithms, learning process or types of input available during the training period.

2.2.1 Supervised learning

In this learning process, the system generates a function to map inputs to desired outputs. Human experts often provide outputs or labels for the systems. In order to solve a given problem of supervised learning, the following steps [34] are followed:

1. Determine data needed for the training set. For example, for the case of handwriting analysis, the training data can be an entire line of handwriting, a single handwritten character, or an entire handwritten word.

2. Gather necessary data for the training set. A good training set contains inputs and corresponding outputs and represents the real-world. These data can be collected either from human experts or from measurements.

3. Determine input features for the learned function. The learned function accuracy depends on how the input data is represented. In practice, a set of features are detected that properly represent the input data. The number of features are kept small to limit the dimensionality of the system. But, enough features are considered to accurately predict the output.

4. Determine the structure of the learning system i.e., learned function and corresponding learning algorithm. For instance, the designer may choose to use decision trees or support vector machines.

5. Complete the design and train the system using the gathered training set.

6. Evaluate the performance of the learned function. After learning and parameter adjustment, the performance of the resulting function is tested with a test input set that is separate from the training set.

There are many supervised learning algorithms available [35] viz., Analytical learning, Artificial neural network, Backpropagation, Decision tree learning, Inductive logic programming, Gaussian process regression, Learning Automata, Naive Bayes classifier, Nearest Neighbor Algorithm, etc. These algorithms are used in: Bioinformatics, Database marketing, Handwriting recognition, Information retrieval, Object recognition in computer vision, Optical character recognition, Spam detection, Pattern recognition, Speech recognition, etc.

2.2.2 Unsupervised learning

In this learning process, the goal of the system is to model a set of inputs. Unlike supervised learning, here outputs or labels are not known for learning systems. The learning systems have only input data and without the presence of supervisor, their goal is to identify the structure of the input space such as certain patterns of the input data i.e., clustering [35].

2.2.3 Semi-supervised learning

These algorithms combine both labeled and unlabeled examples to generate an appropriate function or classifier.

2.2.4 Reinforcement learning

In these algorithms the learner is a decision-making agent that takes actions in a environment and receives reward or penalty for its actions in trying to solve a problem. After a set of trial-and-error runs, it should learn the best policy, which is the sequence of actions that maximize the total reward (Fig. 2.3) [35]. Reinforcement learning differs from supervised learning in that correct input and output pairs are not presented. Moreover, the system is not trained prior to deployment. Here the main goal of the system is finding a balance between exploitation (of current knowledge) and exploration (of uncharted territory).

The basic reinforcement learning model consists of:

- a set of states S;

- a set of actions A;

- rules of transitioning between states;

- rules that determine the scalar immediate reward or penalty of a transition; and
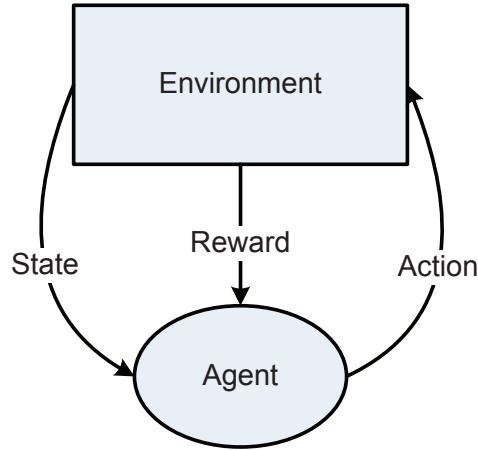
Figure 2.3: At any state of the environment, the agent takes an action that changes the state and returns a reward [35].

- rules that describe what the agent observes.

In a reinforcement learning process, an agent interacts with the environment in discrete time steps. At given time t, the agent receives an observation o_t, which includes the reward or penalty r_t. Based on the reward or penalty, the agent then chooses an action a_t from the set of available actions, which is subsequently sent to the environment. As a result, the environment moves to a new state s_{t+1} and the reward or penalty r_{t+1} associated with the transition (s_t, a_t, s_{t+1}) is determined. The goal of a learning agent is to explore as much states as possible to collect reward or penalty. The agent can choose any action as a function of the history, or it can even randomize its action selection for exploration purpose. When the agent's performance is compared to that of an agent with optimal action set, the difference in performance gives rise to the notion of regret. Note that in order to act near optimality, the agent must reason about the long term consequences of its actions. Thus, reinforcement learning is particularly well suited to problems which include a long-term versus short-term reward trade-off.

In the literature some of the well known reinforcement learning algorithms are: Temporal difference learning, Q-learning, State-Action-Reward-State-Action (SARSA) [35], Fictitious play [36], Learning automata [37], etc. These algorithms have been applied

successfully to problems such as, robot control, elevator scheduling, telecommunications.

2.3 ANN

Artificial Neural Networks are mathematical models based on organizational structure of the human brain. A neural network is an adaptive system that contains interconnected group artificial neurons or processing elements [38]. ANN can be trained with sample data using a teaching method to solve problems. Similarly, ANNs with identical features can be applied to perform different tasks depending on the received training [38, 39]. ANN can be applied to find patterns in data or model relationship between input and output data [40].

A neural network contains neurons to perform certain nonlinear mathematical operations. Each neuron produces an output signal based on the received signals from its inputs, and transmits that signal to all connected neurons or outputs. These neurons are arranged in layers (Fig. 2.4). Each layer performs non-linear functions and connected with a non-linear combination of the previous layer. The first layer, known as Input layer, receives input signal and interacts with the environment. The final layer known as Output layer, presents the processed data. Hidden layers do not have any interaction with the environment as they connects the input and the output layers. Computational capacity and complexity of an ANN depends on the number of hidden layers and neurons per layer [38].

Learning is the fundamental component for ANN systems [38]. Through learning, ANNs teach themselves to produce required outputs form inputs. In this step, ANNs are first provided with a set of input-output samples for learning. During the learning process, ANNs update inter neuron connection or synaptic weights to produce desired outputs from inputs. After this step, ANN goes to the production stage. Learning can also happen in the production stage. Learning can be supervised, unsupervised or hybrid [38].

18
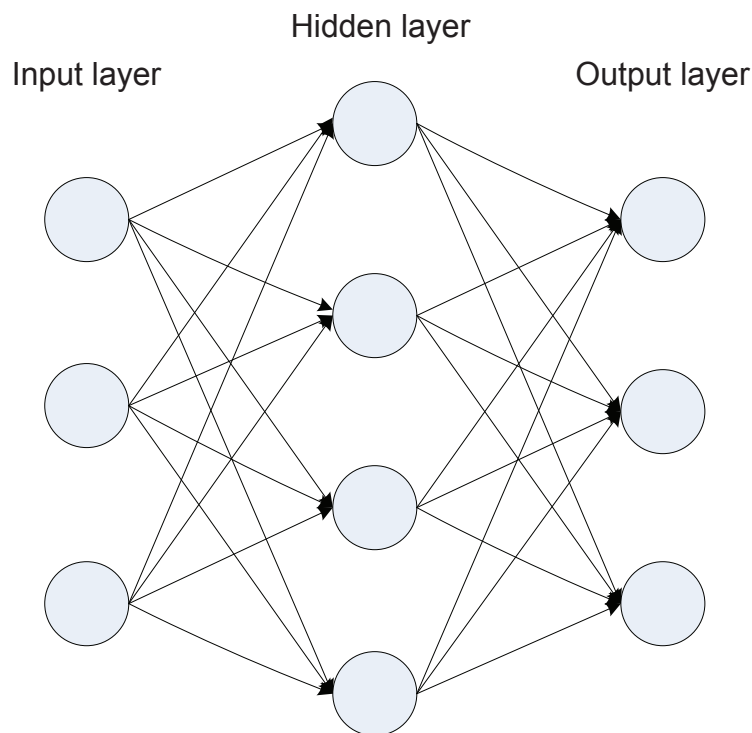
Figure 2.4: ANN model

In the ANN design process, several parameters are considered [38] such as, the number of inputs and outputs, the number of layers, the number of neurons per layer, minimum acceptable error, learning rate, and Epoch.

2.4   Game Theory

In applied mathematics, game theory is used to model multi person decision making situations. During the decision making process, player in the game pursue some rational strategies that take into account their expectations or knowledge of the other players' behavior. Besides many applications in economics, game theory has been applied to numerous fields such as law enforcement, voting decisions, telecommunications, etc.

Games can be classified into non cooperative or cooperative [41]. In non cooperative games, the actions of the single player is considered. On the contrary, in cooperative games the joint actions of groups are analyzed, i.e. what is the outcome if a group of players

cooperate. In telecommunications, most game theoretic research has been conducted using non cooperative games, but there are also approaches using coalition games.

A famous example of game theory is the prisoners dilemma [42]. In this game, two arrested criminals are charged with a crime. But, the police does not have enough evidence to convict the suspects, unless one of them confesses. The criminals are kept in separate cells and they are not able to communicate with each other during the process. In the process of conviction they are given the following choices:

1. If neither confesses, they will be convicted with minor crime and sentenced for one month.

2. If one confesses and the other does not, the confessing one will be released and the other will be sentenced for 9 months.

3. If both confess, both will be sentenced for six months.

The possible actions and corresponding sentences of the criminals are given in Fig. 2.5. Solution of the game is an outcome from which no player wants to deviate unilaterally. The best possible outcome of a game is the Pareto efficient point. At this point all players have better pay off. In the above mentioned prisoners dilemma, all the outcomes except (Confess; Confess) are Pareto efficient. However, as there is no communication between the prisoners, they are not able to reach this point. The prisoners are rational players and choose the strategy that provides better payoff for a particular strategy of another prisoner. This selfish behavior makes both prisoners to choose (Confess; Confess) strategy. This point is the well known **Nash** equilibrium point. In this example, the way prisoners or players choose a strategy is known as pure strategy game. However, in other forms of the game, players choose strategy with some probability, which is known as mixed strategy game.

We can also notice similar dilemma in the wireless environment. For instance, the **Multiple Access Game** addresses the problem of medium access of wireless networks.
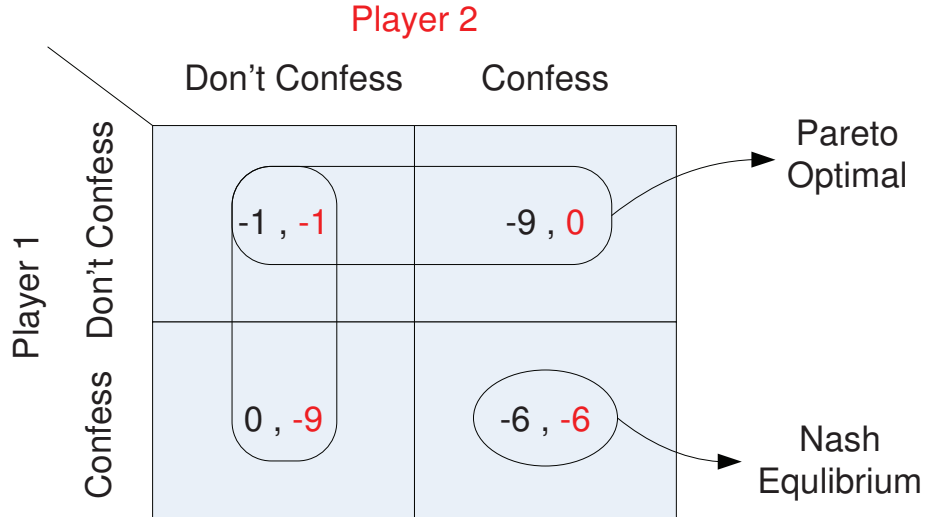
Figure 2.5: Example of Prisoner's dilemma game. The numbers represent the amount of jail terms in months.

We choose this example as it corresponds to the channel allocation problem that we will present in the next chapter. Consider a scenario of two players $p1$ and $p2$, who want to access a shared communication channel for their intended receivers $r1$ and $r2$. We assume that in each time slot each player has one packet to send and he/she can decide to access the channel to transmit it or to wait. Furthermore, let us assume that $p1, p2, r1$, and $r2$ are in the same power range i.e., collision domain. If player $p1$ transmits his/her packet and $p2$ does not transmit or wait, packet transmission of $p1$ becomes successful, otherwise there is a collision and both players lose wireless resources. The dilemma in this game is the following: Each player is tempted to transmit and involved in collision. But, if they wait for each other they can save resources. This Multiple Access Game serves as the basis of our proposed channel selection game in Chapter 3, a player switches channel to get the benefit of the dilemma. Reader can find a very good tutorial on game theory and its application in wireless environment in [41].

2.5 MIMO

In radio communications, MIMO refers to the technology where multiple antennas are employed at both the transmitter and receiver sides to improve performance. MIMO technology offers significant increases in data throughput and link range without additional bandwidth or transmit power [10,11]. That is MIMO systems are known to provide higher spectral efficiency and better link quality. Because of these properties, MIMO is an important part of modern wireless communication standards [43, 44] such as IEEE 802.11n (Wifi), 4G, 3GPP Long Term Evolution, WiMAX and HSPA+.

MIMO techniques can be sub-divided into three main categories, pre-coding, spatial multiplexing, and diversity.

- **Pre-coding**: In (single-layer) beamforming (Fig. 2.6), the same signal is emitted from each of the transmit antennas with appropriate phase (and sometimes gain) weighting such that the signal power is maximized at the receiver input. The benefits of beamforming are to increase the received signal gain, by making signals emitted from different antennas add up constructively, and to reduce the multi path fading effect. In the absence of scattering, beamforming results in a well defined directional pattern, but in typical cellular conventional beams are not a good analogy. When the receiver has multiple antennas, the transmit beamforming cannot simultaneously maximize the signal level at all of the receive antennas, and pre-coding is used (Fig. 2.7) [11]. This spatial processing occurs at the transmitter, and requires knowledge of channel state information (CSI) at the transmitter.

- **Spatial multiplexing** In spatial multiplexing, a high rate signal is split into multiple lower rate streams and each stream is transmitted from a different transmit antenna in the same frequency channel. If these signals arrive at the receiver antenna array with sufficiently different spatial signatures, the receiver can separate these streams into parallel channels (Fig. 2.8 [11]). Spatial multiplexing is used to
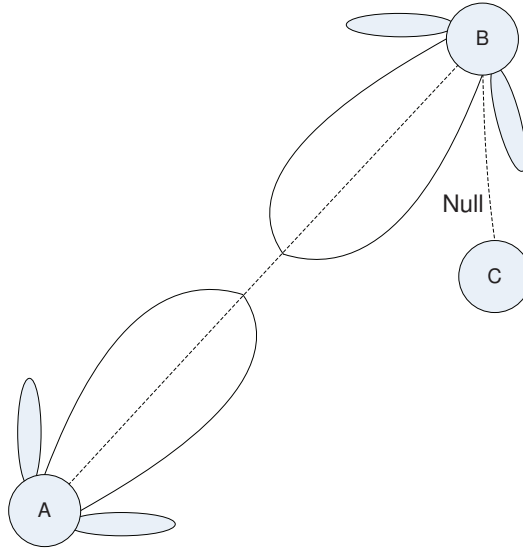
Figure 2.6: Beamforming to improve the signal-to-noise ratio and to reduce interference [11].

Transmitter
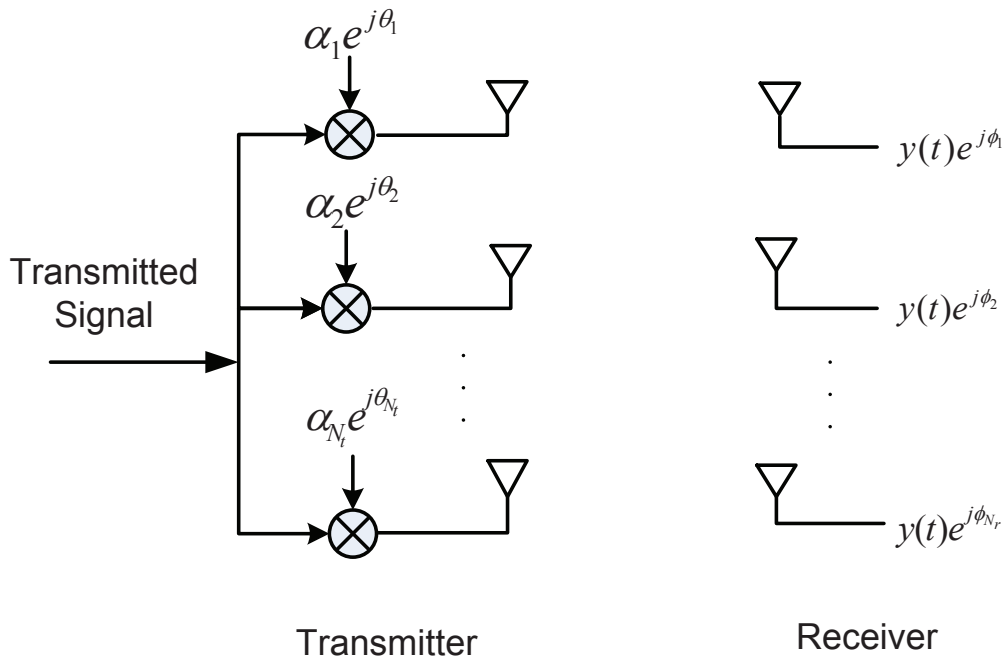
Receiver

Figure 2.7: Beamforming using multiple antennas [11]. In the figure, $\alpha_{\hat{i}}e^{j\theta_{\hat{i}}}$ denote the scaling factor for $\hat{i} \in N_t$, and $y(t)e^{j\phi_{\hat{j}}}$ represents phase shifted version of the received symbol vector for $\hat{j} \in N_r$.

support higher data rate applications. The maximum number of spatial streams is limited by the lesser in the number of antennas at the transmitter or receiver [11].
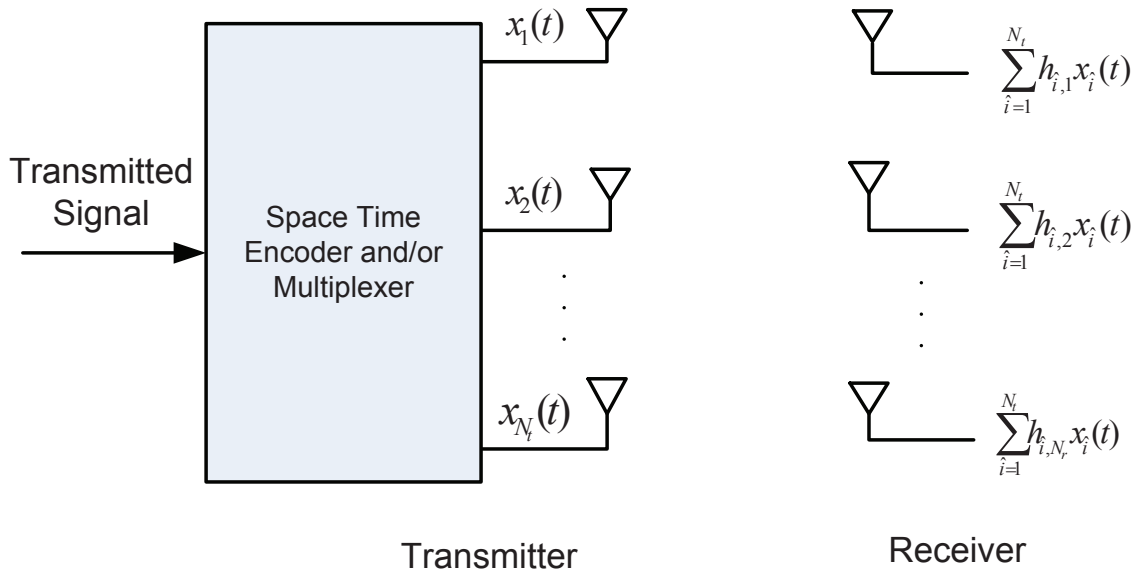
Figure 2.8: Space-time coding in MIMO system [11]. $\mathbf{x}_{\hat{i}}(t)$, and $h_{\hat{i},\hat{j}}$ in the figure represnt the transmit symbol vector and the channel gain between transmit and receive antennas for $\hat{i} \in N_t$ and $\hat{j} \in N_r$, respectively.

Spatial multiplexing can be used with or without transmit channel knowledge [45]. Spatial multiplexing can also be used for simultaneous transmission to multiple receivers, known as space-division multiple access. By scheduling receivers with different spatial signatures, good separability can be assured [11].

• **Space-time Coding** In space-time coding, a single stream (unlike multiple streams in spatial multiplexing) is transmitted, but the signal is coded using space-time coding as shown in Fig. 2.8. The signal is emitted from each of the transmit antennas with full or near orthogonal coding. Space-time coding exploits the independent fading in the multiple antenna system to enhance signal diversity [11].

Although MIMO systems result in drastic increase in spectral efficiency, it comes with the price of complexity, and large number of RF chains. Recent works on MIMO systems indicate that deploying a subset of available antennas i.e., selecting antennas can provide high throughput performance [46]. In Chapter 5, we will employ an antenna selection algorithm in cognitive settings to improve throughput performance of cognitive networks.

24

2.6 Conclusions

In this chapter, we have briefly discussed challenges for cognitive ad-hoc networks, the cognition cycle, machine learning, ANN, game theory, and MIMO techniques. For the remaining chapters, we will be using these protocols and mathematical tools to address the cognitive radio design issues of heterogeneous cognitive networks.

Chapter 3

Performance Analysis of Interference Aware Cognitive Ad-hoc Networks

In this chapter, we analyze the performance of cognitive ad-hoc networks using CSMA/CA MAC protocol for media access purpose. For the designed cognitive network, cognitive communication is limited by the interference imposed on primary users. We determine the probability of accessing the channel under Rayleigh fading condition for this opportunistic network. We then use this probability to determine the embedded Markov model in the cognitive nodes. Finally, we use this Markov model to determine the average channel access delay, throughput and service rate of cognitive nodes.

3.1 Introduction

MAC layer plays an important role for cognitive ad-hoc networks [32]. In [47], the authors survey the advantages, design consideration, and challenges of proposed MAC protocols for cognitive networks. In the literature, IEEE 802.11-like MAC protocols have been proposed in [47,48] and references therein. In coexistence with the primary user, the performance of the cognitive network becomes very important. For instance in [48], the authors proposed distributed multi channel MAC protocol for cognitive networks. In [49],

channel access delay for nodes is optimized over sensing time for cognitive networks. Stationary state probability is an important performance metric for coexistence condition. It can be used to determine the blocking probability, service probability, queue size, for performance evaluation. For heterogeneous networks, to determine the stationary state probability vector, Continuous Time Markov Chain (CTMC) is used in [50]. CTMC is also used in [51] to derive the blocking and forced termination probability of cognitive users for concurrent communication with the primary user. Conversely in [52], two-dimensional Markov chain model is used to determine the blocking probability, forced termination probability and service completion probability of multi radio cognitive users subject to primary users interference constraint. Using the state transition information, an analytical formulation of the saturation throughput of CSMA/CA networks with multiple access for multiple secondary users is presented in [53]. In [54], periodic memoryless access to the primary user channels is considered as partially observable Markov decision process and shown that close to optimal performance can be achieved for tight collision constraint. Nevertheless, in [55], the optimum number of cognitive users is determined when cognitive nodes contend with primary users for channel access. For this purpose, the authors in [55] determine the throughput of the channel and optimize it over the number of cognitive users.

Apart from the above mentioned studies, the authors in [56] and [57] used Markov model to determine performance metrics such as access delay, throughput, offered load for IEEE 802.11 MAC for both saturated and unsaturated traffic cases. For primary users' interference limited cognitive communication, the channel access delay, throughput and service rate is affected by the spectrum sensing time, contention delay, RTS (Request to send) and CTS (Clear to send) exchange period, and channel unavailability period due to primary users' interference limitations. The effect of primary users' interference constraint for performance evaluation is not determined in the literature. From this point of view, in this chapter our main contributions are

- We determine the channel access probability of MIMO cognitive ad-hoc networks.

- We model the transition of state in a tagged node using an embedded Markov model.

- This Markov model is used to determine the average channel access delay, throughput and service rate of nodes for interference limited communications.

The rest of the chapter is organized is as follows. The system model is presented in Section 3.2. Probability of channel availability, average of channel access delay, service rate and normalized throughput analysis and simulation results are presented in Sections 3.3, 3.4, 3.5, 3.6, respectively. Finally, conclusions are drawn in Section 3.7.

3.2 System Model

As indicated in Chapter 1, we consider $\hat{T}$ pairs of cognitive ad-hoc nodes coexist with licensed primary users in the same geographical area. Cognitive and primary users access the adjacent channels but due to spill over energy [22], cognitive communication may cause interference on primary users. We assume all cognitive nodes are within the radio range of each other. Cognitive source-destination pairs use N_t transmit and N_r receive antennas and achieve multiplexing gain. On the other hand, in the MAC sub-layer of the data link layer, nodes use CSMA/CA protocol with RTS/CTS mechanism. During the Distributed coordination function Inter Frame Space (DIFS) period, of the MAC protocol nodes perform channel sensing to determine the transmission opportunity [48]. Following this, nodes move to the back-off stage of the MAC protocol, if interference imposed on the primary users is below the specified threshold of primary users. Otherwise, cognitive nodes wait T_f amount of time before sensing the channel again. To model the transitions of these states for a packet in a node, a discrete-time Markov renewal process is established as illustrated in Fig. 3.1. The states in the figure can be divided into three categories: 1) channel access state $(F_i, i = 0, 1, 2, 3....., K)$ 2) back-off state
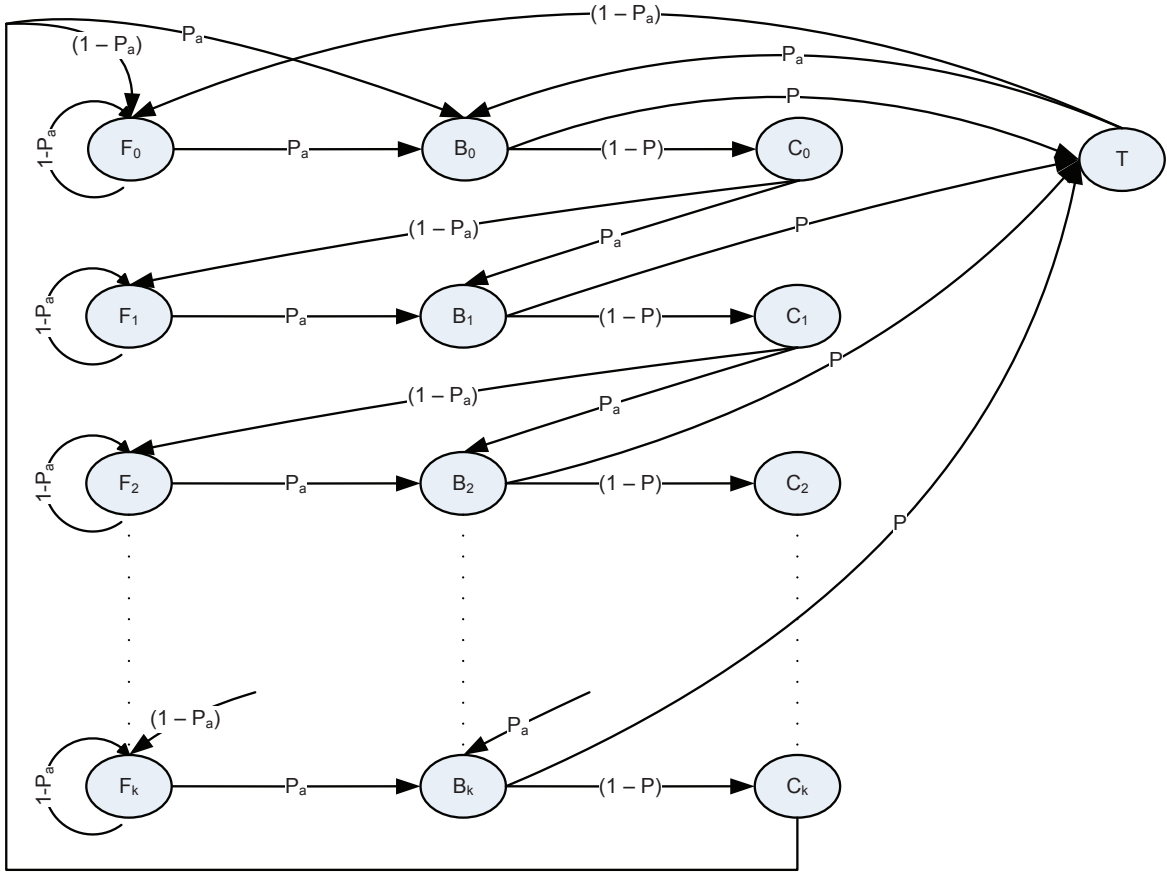
Figure 3.1: Embedded Markov model for the state transition process in each node.

$(B_i, i = 0, 1, 2, ..., K)$ 3) collision state $(C_i, i = 0, 1, 2, ..., K)$ and 4) transmission state (T).

As illustrated in the figure, if the channel is accessible, nodes start back off process after the state F_i. From the back-off state, the packet moves to the transmission state, if the request is successful, else moves to the collision state for unsuccessful requests. After each collision state, the packet is moved to higher level of back-off states. This process continues until the packet is dropped after K retransmission or collision events.

3.3   Probability of Channel Availability

To develop the mathematical model for the probability of channel availability, we define the interference signal $\boldsymbol{y}_{pl}^i$ at any primary user l due to spill over energy [22] by the cognitive communication using adjacent channels $i \in \hat{C}$ as,

$$\boldsymbol{y}_{pl}^i = \boldsymbol{G}_i \boldsymbol{x} \tag{3.1}$$

where $\boldsymbol{G}_i$ stands for an $1 \times N_t$ channel vector representing the corresponding channels between a primary user and cognitive node $i \in \hat{T}$, $\boldsymbol{x}$ denotes $N_t \times 1$ cognitive user transmit symbol vector.

From (3.1), the instantaneous interference power at the lth primary user can be written as

$$I_i^l = E((\boldsymbol{y}_{pl}^i)^H \boldsymbol{y}_{pl}^i) = \sigma \boldsymbol{G}_i.(\boldsymbol{G}_i)^H, \tag{3.2}$$

where $\sigma = E[\boldsymbol{x}^H \boldsymbol{x}]/N_t$. We also consider all cognitive users have uniform interference effect on primary users.

If Maximum Ratio Combining (MRC) is employed at primary nodes, from (3.1), we notice that the effective interference signal power at the primary user i is $\sigma \sum_{j=1}^{N_t} G_{ij}^2$. If we consider Rayleigh fading channel between cognitive and primary users, the effective interference power after combining is chi-square distributed with $2N_t$ degrees of freedom. That is, probability density function (pdf), of the interference power can be written as [11],

$$p_{\sigma_{eff}}(u) = \frac{u^{N_t-1} \exp^{-u/\sigma}}{\sigma^{N_t}(N_t - 1)!} \ u > 0. \tag{3.3}$$

For cognitive power σ and primary users interference threshold I_{th}, the probability

of channel availability can be written as,

$$
\begin{aligned}
P_a &= Probability(\sigma < I_{th}), \\
&= \int_o^{I_{th}} \frac{u^{N_t-1} \exp^{-u/\sigma}}{\sigma^{N_t}(N_t-1)!} du, \\
&= 1 - \exp^{-\frac{I_{th}}{\sigma}} \left(\sum_{i=1}^{N_t} \frac{(I_{th}/\sigma)^{i-1}}{(i-1)!} \right).
\end{aligned}
\tag{3.4}
$$

3.3.1 Model validation

To validate the probability of channel availability model in (3.4), we compare the theoretical and simulation results in Fig. 3.2. For simulation, we consider a channel is available if the interference is below the specified threshold. We record the number of instants when the channel is available over 10000 channel realizations, and determine the probability of channel availability results as indicated in the figure. The results indicate that channel availability improves with the increase in number of cognitive transmit antennas. This happens as the total power is kept constant and channel diversity appears. It is worthwhile to mention that for low SNRs [0 dB - 10 dB], 1, 2 and 3 antenna cases have higher channel availability, as the channel effect is the dominant force. Fig. 3.3 shows the effect of primary users interference on channel availability. The results demonstrate that the channel availability improves as primary users interference threshold increases. It is also clear from the results that the simulation and analytical results are very close which validates the model in (3.4).

3.4 Average Channel Access Delay

According to the system model described above, the conditional collision probability $\hat{\rho}$, and probability of successful transmission P for a tagged node can be expressed in
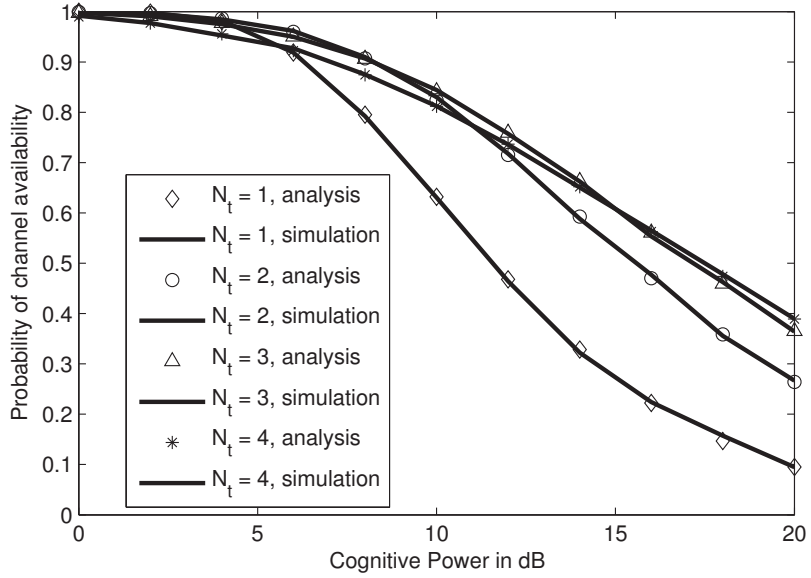
Figure 3.2: Probability of channel availability for cognitive transmit power per antenna at -20 dBm primary users' interference constraint.
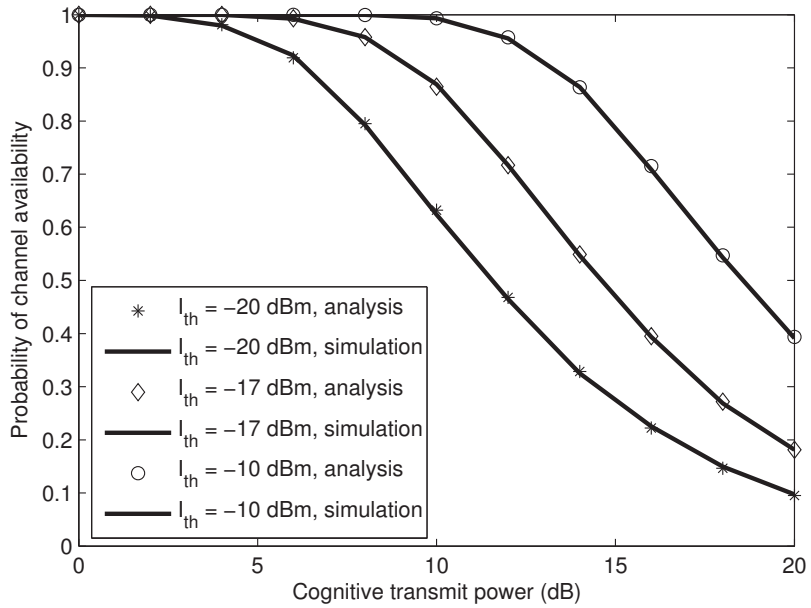
Figure 3.3: Probability of channel availability as a function of interference constraint.

terms of the transmission probability τ as,

$$\hat{\rho} = 1 - (1 - \tau)^{\hat{T}-1}, \tag{3.5}$$

$$P = (1 - \tau)^{\hat{T}-1}. \tag{3.6}$$

Also, τ can be written in terms of the collision probability for short retransmission limit [58] as,

$$\tau = \frac{2(1 - 2\hat{\rho})(1 - \hat{\rho}^{m+1})}{w(1 - (2\hat{\rho})^{m+1})(1 - \hat{\rho}) + (1 - 2\hat{\rho})(1 - \hat{\rho}^{m+1}) + w2^m \hat{\rho}^{m+1}(1 - 2\hat{\rho})(1 - \hat{\rho}^{K-m})}, \tag{3.7}$$

where m and K represent the maximum number of back-off states and maximum number of retransmission events, respectively. w denotes the minimum value of contention window size. One can notice that the value of $\hat{\rho}$ and τ can be determined from (3.5) and (3.7) using numerical techniques.

Holding time in Fig. 3.1 in state T and in state C are fixed for MAC protocol and can be determined as,

$$T_s = t_{DIFS} + t_{RTS} + t_{SIFS} + t_{CTS} + t_{SIFS} + t_{Packet} + t_{SIFS} + t_{ACK},$$

$$T_c = t_{DIFS} + t_{RTS} + t_{SIFS} + t_{EIFS}. \tag{3.8}$$

where t_{Packet} denotes the packet transmission time and the nominal values of other parameters in (3.8) for IEEE 802.11 protocol are given in Table 3.1. On the other hand, holding times in state F and B are dependent on the channel behavior.

Holding time in the back-off state depends on the time wasted due to packet collision, successful packet transmission by other nodes and waiting time of the back-off process for channel acquisition. The probability of successful transmission in the channel P_s, the collision probability in the channel P_c, and the probability of the channel being idle P_i can be expressed as,

$$P_s = \hat{T}\tau(1 - \tau)^{\hat{T}-1}, \tag{3.9}$$

$$P_c = 1 - (1 - \tau)^{\hat{T}} - \hat{T}\tau(1 - \tau)^{\hat{T}-1}, \tag{3.10}$$

$$P_i = (1 - \tau)^{\hat{T}}. \tag{3.11}$$

Using these probabilities, the average time required for two successive back-off timer decrementing instants d is given by,

$$d = T_s P_s + T_c P_c + P_i t_{slot}, \tag{3.12}$$

where t_{slot} represents the duration of a time slot. For short retry limit, the contention window size w_i can be written as,

$$w_i = \begin{cases} 2^i w, & \text{if } 0 \leq i < m \\ 2^m w. & \text{if } m \leq i \leq K \end{cases} \tag{3.13}$$

where w denotes the minimum value of contention window size and i represents the number of retransmission events.

At each back-off state, the value of back-off timer is set uniformly between 0 and $w_i - 1$. Also, the average value of back-off counter is given by,

$$E\{w_i\} = \begin{cases} \frac{2^i w - 1}{2} & \text{if } 0 \leq i < m, \\ \frac{2^m w - 1}{2} & \text{if } m \leq i \leq K. \end{cases} \tag{3.14}$$

Now, from (3.12) and (3.14), one can find the holding time Y_i in back-off state b_i for interference constraint as,

$$\begin{aligned} Y_i &= w_i d + (1 - P_a) w_i d + (1 - P_a)^2 w_i d + ... \\ &= \frac{w_i d}{P_a}. \end{aligned} \tag{3.15}$$

As w_i is not dependent on P_a and d, average holding time $E\{Y_i\}$ in back-off state b_i, can

be written as,

$$E\{Y_i\} = \frac{E\{w_i\}d}{P_a}. \tag{3.16}$$

Average holding time G_f in the channel access state F_i for interference constraint is given by,

$$
\begin{aligned}
G_f &= T_f + (1 - P_a)T_f + (1 - P_a)^2 T_f + (1 - P_a)^3 T_f.... \\
&= \frac{T_f}{P_a}. \tag{3.17}
\end{aligned}
$$

The total channel access delay, D starts from state F_0 until the service completion in state T. It can happen through single stage as, $F_0 \rightarrow B_0 \rightarrow T$ or multiple stages as, $F_0 \rightarrow B_0 \rightarrow C_0 \rightarrow F_1 \rightarrow B_1 \rightarrow C_1 \rightarrow F_2 \rightarrow B_2 \rightarrow T$ (Fig. 3.1). Access delay D_0 for stage $i = 0$ starts at F_0 to B_0 and ends at T with probability P as,

$$
\begin{aligned}
D_0 &= P_a(E\{Y_0\} + T_s) + (1 - P_a)(E\{Y_0\} + T_s + G_f) \\
&= E\{Y_0\} + T_s + \frac{1 - P_a}{P_a} T_f. \tag{3.18}
\end{aligned}
$$

In sequel, access delay at any stage D_i starts from state F_0 for $i = 0$ and after packet collision event C_{i-1} for $i = 1, .., K$ until the service completion in state T, given by

$$
D_i = \begin{cases}
\frac{1-P_a}{P_a} T_f + E\{Y_i\} + T_s, & \text{with prob. } P \\
\frac{1-P_a}{P_a} T_f + E\{Y_i\} + T_c + D_{i+1}. & \text{with prob. } 1 - P
\end{cases} \tag{3.19}
$$

It is worthwhile to note that the packet is dropped from the queue after the collision event at state $i = K$ and the node starts from state $i = 0$ with a new packet. Using (3.19) the average channel access delay for primary users' interference constraint can be determined

as,

$$E(D) = \frac{1 - P_a}{P_a} T_f + E\{Y_0\} + PT_s + (1 - P)(T_c + D_1)$$

$$= \underbrace{(1 - (1 - P)^{K+1}) T_s}_{\text{Packet transmission time}} + \underbrace{\frac{(1 - (1 - P)^K)(1 - P)}{P} T_c}_{\text{Collision time}}$$

$$+ \underbrace{\sum_{i=0}^{K-1} E\{Y_i\}(1 - P)^i + (1 - P)^K PE\{Y_K\} +}_{\text{Back-off time}}$$

$$\underbrace{T_f \frac{1 - P_a}{P_a} \sum_{i=0}^{K-1} (1 - P)^i + T_f \frac{1 - P_a}{P_a} (1 - P)^K P}_{\text{Channel access time}} \quad (3.20)$$

where $E(.)$ is the expectation operator.

3.4.1 Performance evaluation

Here, we carry out numerical analysis to evaluate the performance of the above mentioned system. We build an IEEE 802.11 [59] compatible ad-hoc network using the simulation parameters listed in Table 3.1. We use these parameters to build an event driven simulation program for the cognitive network introduced in section 3.2. It is to be noted that in the following performance results, each data point represents an average over 10,000 events.

First we present results for the average channel access delay for cognitive nodes. In Fig. 3.4 we plot the average channel access delay results as a function of the number of cognitive nodes for different cognitive transmit power. The results show that the access delay increases with the increase in cognitive transmit power and number of cognitive nodes. This happens as the channel becomes unavailable with higher probability due to the increase in transmit power as observed in Fig. 3.2. On the other hand, the access delay increases with the number of cognitive nodes for two reasons: 1) waiting time for transmission opportunity and 2) the number of packet collision incident increases with

Table 3.1: Simulation setting

Parameter	Value
No. of channels	1
Data type	Best effort
Packet Payload	8184 bits
MAC header	272 bits
MAC protocol	CSMA/CA
PHY header	127 bits
ACK	112 bits+PHY header
RTS	160 bits+PHY header
CTS	112 bits+PHY header
Slot time	50 μs
DIFS	128 μs
SIFS	28 μs
Bit rate	2 Mb/s
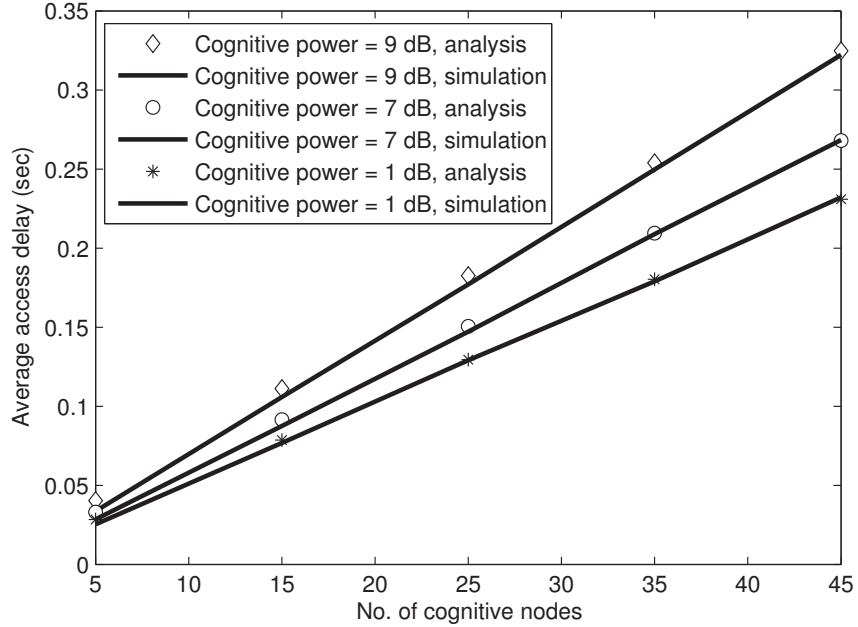
Figure 3.4: Average channel access delay for $N_t = N_r = 1$ at -20dBm interference constrain.

the number of nodes in the network.

We investigate the effect of the interference constraint in Fig. 3.5. Reported results indicate that the access delay performance improves with the increase in interference threshold. We confirm this gain using the channel availability probability in Fig. 3.3. As
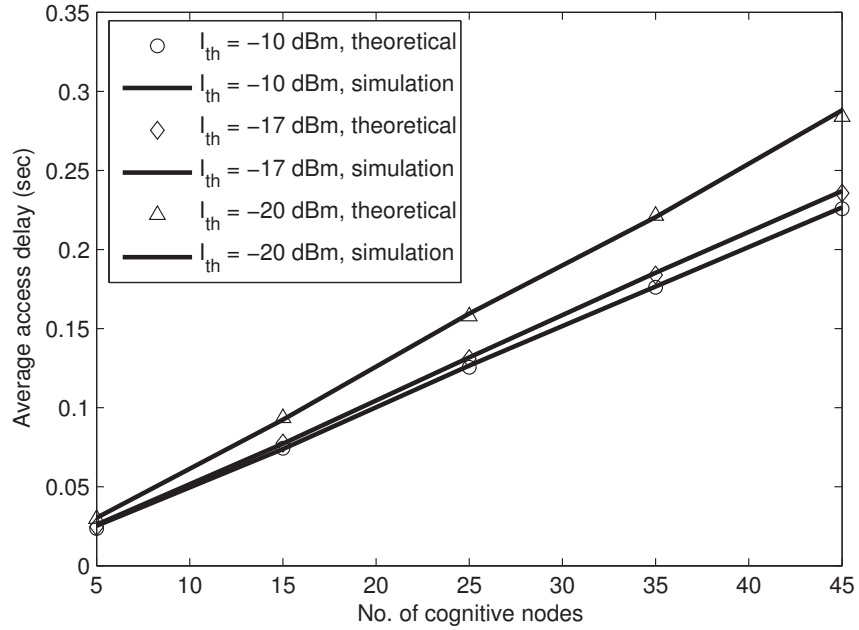
Figure 3.5: Average channel access delay for $N_t = N_r = 1$ and at 8 dB cognitive power.

seen from these results, the channel availability improves with the increase in interference threshold. That is, the waiting time for transmission opportunity (i.e., channel access delay) reduces with the increase in interference threshold.

In Fig. 3.6 we show the advantages of the multiple antenna system for cognitive nodes. We notice that the average access delay decreases as more antennas are employed. This performance gain is contributed by higher data rate and probability of channel availability (Fig. 3.3) due to the usage of multiple antennas.

We plot the average access delay results for different T_f (channel unavailability time due to fading) time duration in Fig. 3.7. From (3.19), it is evident that the channel access delay varies with the slot time duration. This phenomena is also observed in both simulation and analytical results.
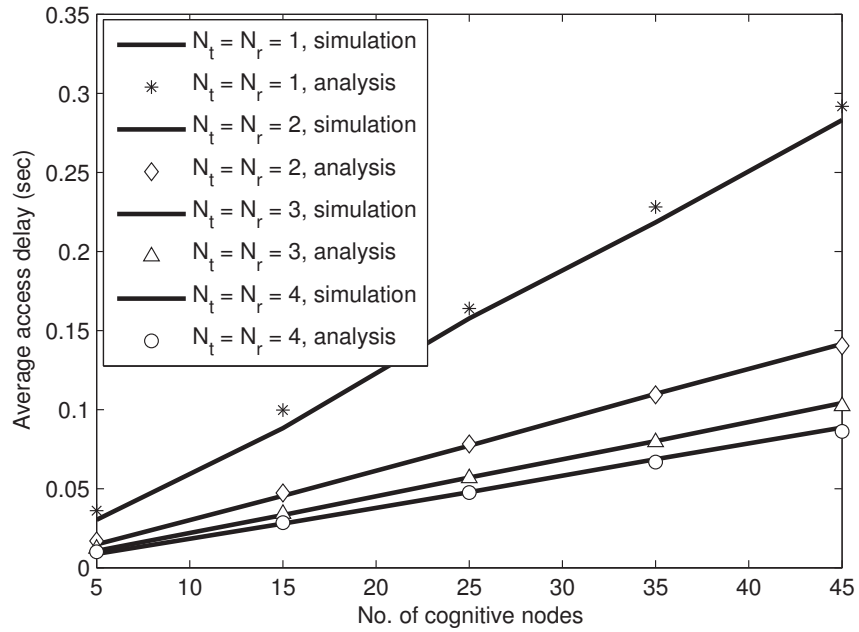
Figure 3.6: Average channel access delay at 8 dB cognitive power and -20 dBm interference constrain.
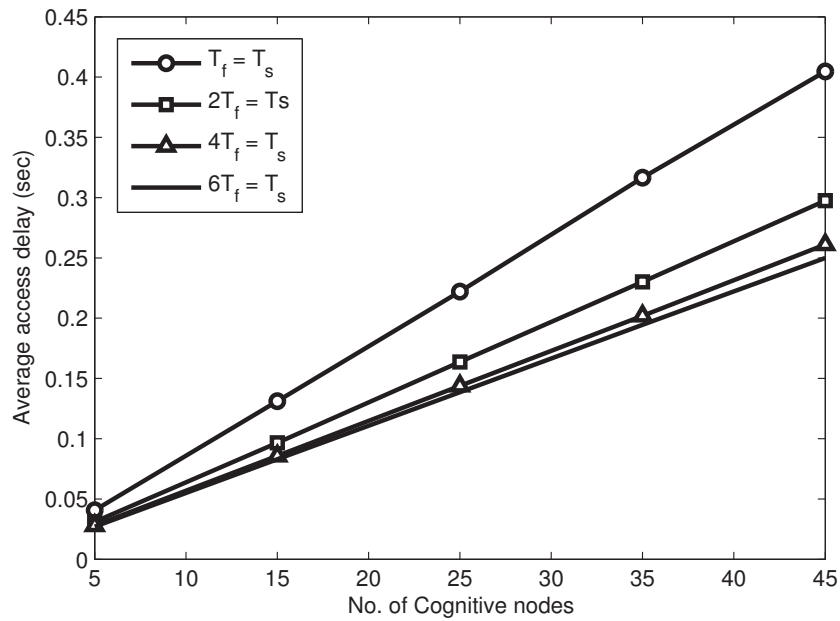
Figure 3.7: Effect of fading on access delay for $N_t = N_r = 1$, -20 dBm interference limit and at 8 dB cognitive power.

3.5 Average Service Rate

According to Fig. 3.1, steady state probabilities of the states are given by,

$$\pi_{C_i} = (1 - P)\pi_{B_i}, \quad \text{for } i = 0, 1, ..., K \tag{3.21}$$

$$\pi_{F_i} = \begin{cases} \frac{1-P_a}{P_a}(\pi_T + \pi_{C_K}) & \text{for } i = 0 \\ \frac{1-P_a}{P_a}\pi_{C_{i-1}}, & \text{for } i = 1, ..., K \end{cases} \tag{3.22}$$

and

$$\pi_{B_i} = \begin{cases} P_a(\pi_T + \pi_{C_K} + \pi_{F_i}) & \text{for } i = 0 \\ P_a(\pi_{F_i} + \pi_{C_{i-1}}), & \text{for } i = 1, ..., K. \end{cases} \tag{3.23}$$

Using (3.22), for $i = 1, ..., K$, (3.23) can be written as,

$$\pi_{B_i} = (1 - P_a)\pi_{C_{i-1}} + P_a\pi_{C_{i-1}}$$

$$= \pi_{C_{i-1}}$$

$$= (1 - P)\pi_{B_{i-1}}. \tag{3.24}$$

Accordingly, from (3.24), π_{B_K} and π_{C_K} can be written as,

$$\pi_{B_K} = (1 - P)^K \pi_{B_0}$$

$$\pi_{C_K} = (1 - P)^{K+1} \pi_{B_0}, \tag{3.25}$$

and

$$\pi_{B_i} = (1 - P)^i \pi_{B_0} \quad \text{for } i = 1, ..., K \tag{3.26}$$

Now for $i = 0$, π_{B_0} can be determined using (3.22), (3.23) and (3.25) as,

$$\pi_{B_0} = \frac{P_a}{1 - P_a} \pi_{F_0} \tag{3.27}$$

$$= \pi_{C_K} + \pi_T$$

$$= (1 - P)^{K+1} \pi_{B_0} + \pi_T$$

$$= \frac{1}{1 - (1 - P)^{K+1}} \pi_T. \tag{3.28}$$

Using (3.25) to (3.28), and the analysis of limiting state probabilities of the Markov renewal process in [60], the service probability or service rate can be determined as,

$$\bar{\pi}_T = 1 / \left[1 + \frac{\hat{\tau}_f}{\hat{\tau}_T} \left\{ \frac{1 - P_a}{P_a} \frac{1}{P} \right\} + \frac{\hat{\tau}_c}{\hat{\tau}_T} \frac{1}{1 - (1-P)^{K+1}} \left\{ \frac{1 - (1-P)^{K+2}}{P} - 1 \right\} \right.$$
$$\left. + \frac{\hat{d}}{P_a(1 - (1-P)^{K+1})} \left\{ \sum_{i=0}^{m} (1-P)^i \frac{1 + w_i}{2} + \sum_{i=m+1}^{K} (1-P)^i \frac{1 + w_m}{2} \right\} \right], \tag{3.29}$$

where $\hat{\tau}_f$, $\hat{\tau}_c$, $\hat{\tau}_T$ and $\hat{d}$ denote holding time in states F, C, T and B expressed in terms of slot times, respectively. $\hat{d}$ is given by [57],

$$\hat{d} = \frac{1}{\hat{\tau}_T} + (1 - P) \frac{\hat{\tau}_c}{\hat{\tau}_T} - \left(1 - \frac{\hat{\tau}_C}{\hat{\tau}_T} \right) P \log P. \tag{3.30}$$

3.5.1 Performance evaluation

In this subsection we use network parameters in Table 3.1 to examine the service probability analysis presented in (3.29). Fig. 3.8 reveals that the service probability decreases with the increase in number of cognitive nodes and cognitive transmit power. The service probability performance degrades for two reasons: 1) packet collision increases with the number of nodes in the network, and 2) nodes get less opportunity for transmission at high transmit power due to channel unavailability.
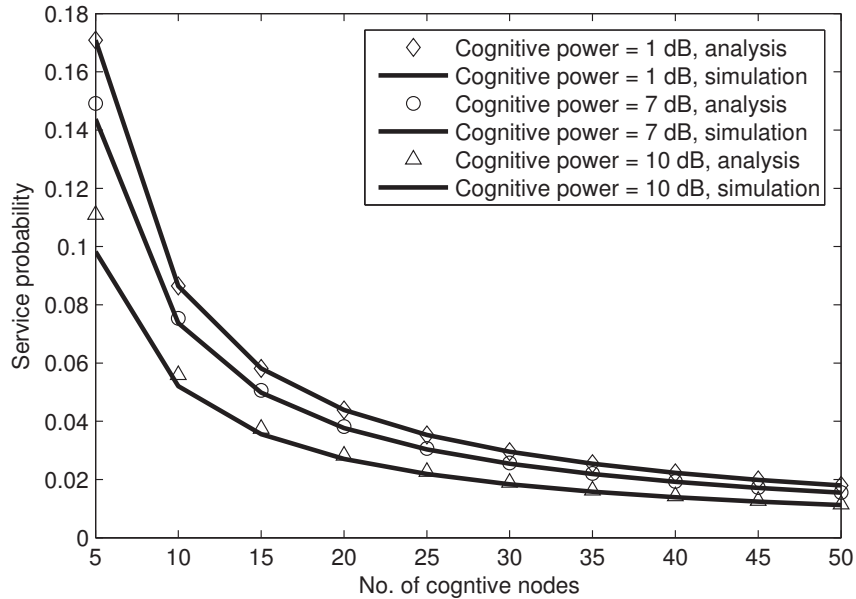
Figure 3.8: Service probability of cognitive nodes for $N_t = N_r = 1$ at -20dBm interference constrain.

We show the effect of primary users' interference threshold on the service probability in Fig. 3.9. As noticed in Fig. 3.3, channel availability probability increases with the increase in the primary users' interference threshold. As a result, the service probability performance improves with the increase in the primary users' interference threshold.

In Fig. 3.10, we plot the service probability curves when cognitive transmit and receive node pairs use multiple antennas. Unlike the access delay case, the service probability is not affected by the usage of multiple antennas, as nodes periodically access the channel and channel access period is constant for all nodes.

Now we present the effect of T_f time slot duration on service probability in Fig. 3.11. As evident, indicate that the performance improves with the decrease in the duration of T_f time. In this case, we provide argument similar to the access delay case. That is, the performance improves as nodes receive more time for data transmission purpose.
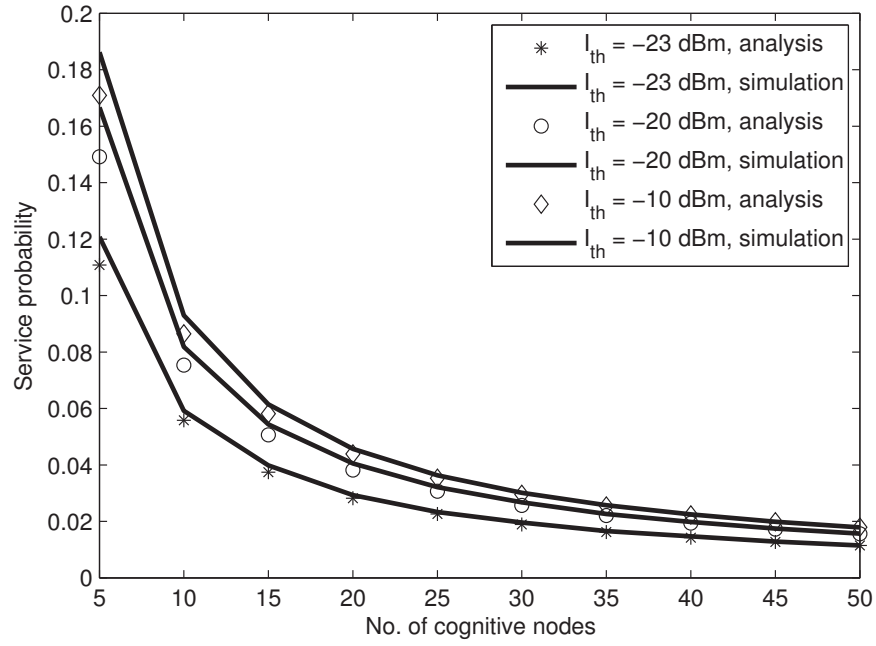
Figure 3.9: Service probability of cognitive nodes for $N_t = N_r = 1$ and at 8 dB cognitive power.
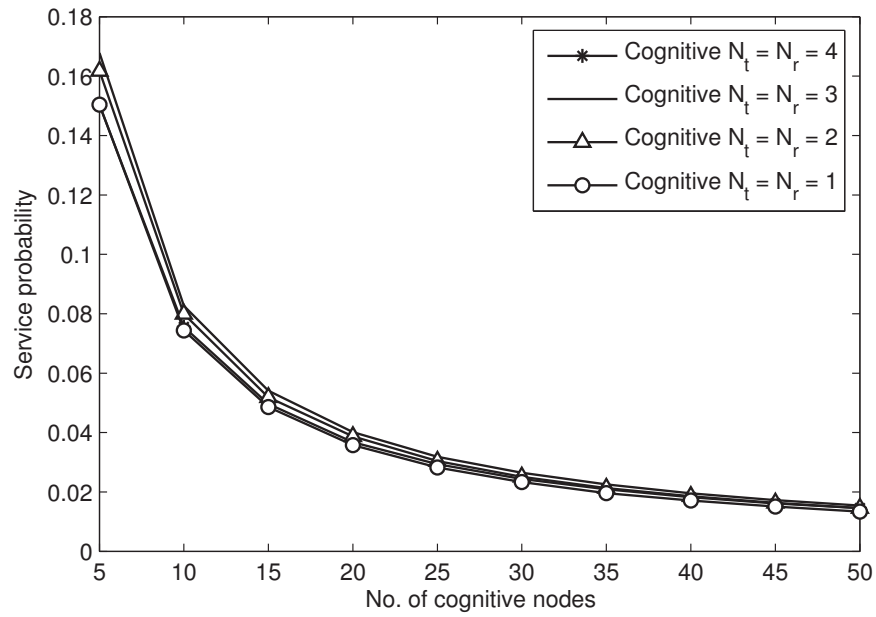
Figure 3.10: Service probability of cognitive nodes for 8 dB cognitive power and -20 dBm interference constrain.
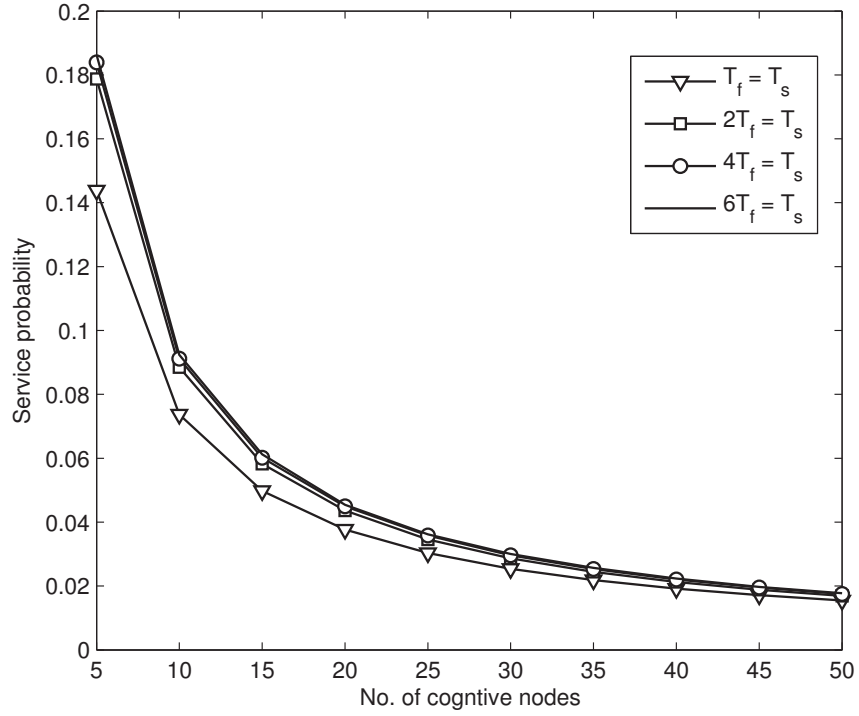
Figure 3.11: Service probability of cognitive nodes for $N_t = N_r = 1$, -20 dBm interference limit and at 8 dB cognitive power.

3.6   Normalized Throughput

At this point, we determine the normalized throughput for the network. Similar to the analysis in [56] and [59], we define the normalized throughput as,

$$\eta = \frac{Payload\ information\ transmitted\ in\ a\ slot\ time}{Length\ of\ a\ slot\ time}. \tag{3.31}$$

Using (3.16), (3.12) and with the help of [59], the normalized throughput can be written as,

$$\eta = \frac{P_a P_s t_{packet}}{d}. \tag{3.32}$$

3.6.1 Performance evaluation

Now we present some performance results for the normalized throughput analysis. As before, we use the parameters listed in Table 3.1 to simulate an IEEE 802.11 compatible network. We plot the normalized throughput results in Fig. 3.12. One can notice that similar to the access delay (Fig. 3.2) case, the normalized throughput improves with the decrease in cognitive transmit power.

In Fig. 3.13, we examine the effect of interference threshold on cognitive users' normalized throughput. Both simulation and analytical results show that the throughput improves with the increase in interference limit. Also the channel availability improves for cognitive nodes with the increase in interference limit. As a result, nodes suffer from less outage time which helps to improve the average throughput.

We investigate the variation in throughput due to usage of multiple antennas for cognitive nodes in Fig. 3.14. Our simulation and analytical results show that throughput being normalized, is not affected by the usage of multiple antennas. Now, we show the
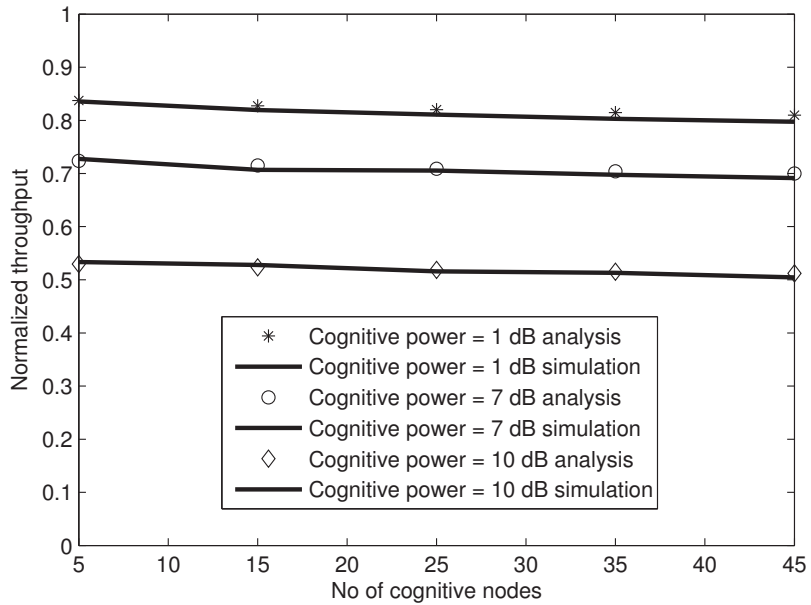
Figure 3.12: Normalized throughput of cognitive nodes for $N_t = N_r = 1$ at -20dBm interference constrain.
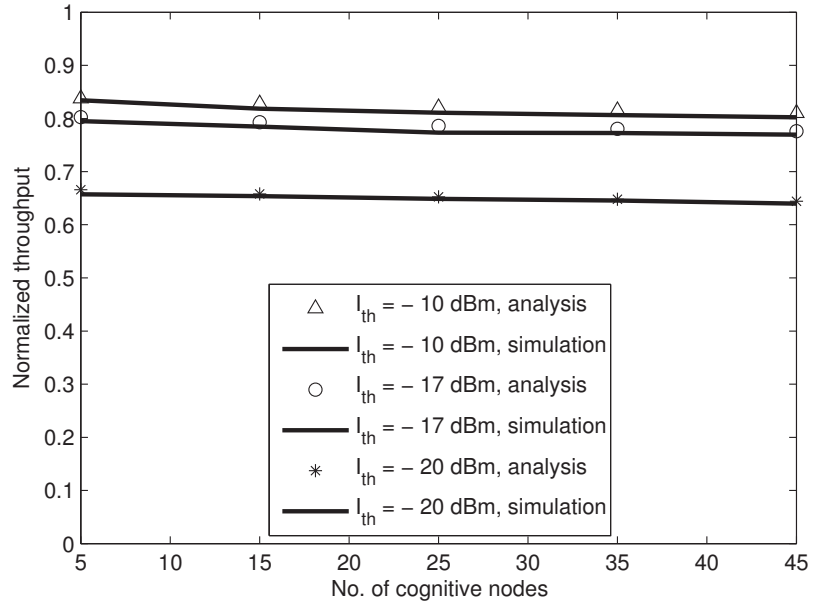
Figure 3.13: Normalized throughput of cognitive nodes for $N_t = N_r = 1$ and at 8 dB cognitive power.
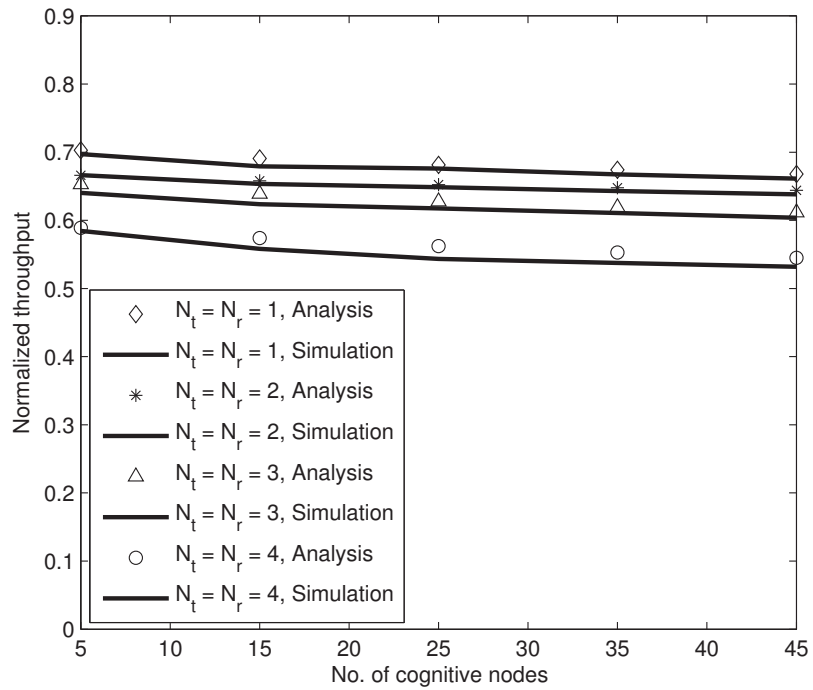
Figure 3.14: Normalized throughput of cognitive nodes for 8 dB cognitive power and -20 dBm interference constraint.
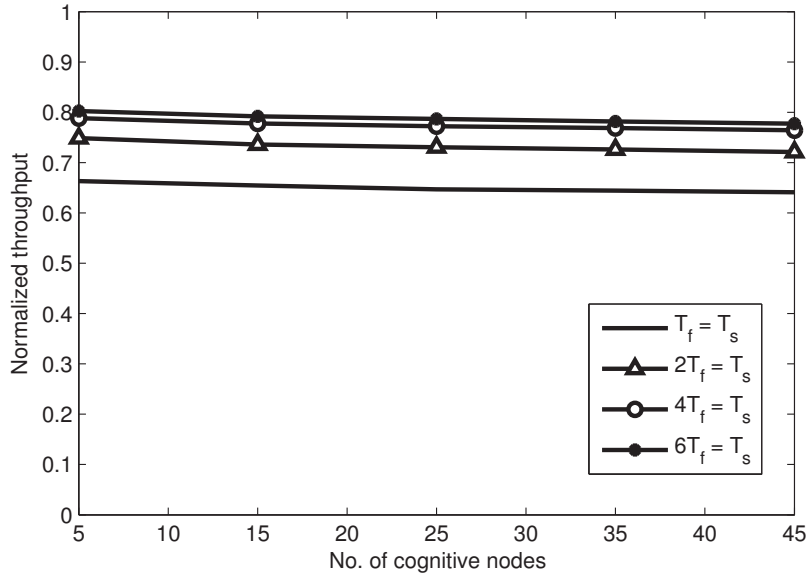
Figure 3.15: Normalized throughput of cognitive nodes for $N_t = N_r = 1$, -20 dBm interference limit and at 8 dB cognitive power.

effect of T_f slot time duration on throughput results in Fig. 3.15. One can notice that throughput improves as channel unavailability duration due fading duration decrease. Similar effect of fading duration is also noticed for access delay case in Fig. 3.7.

3.7 Conclusions

We determined the average access delay, service probability, and throughput for interference limited cognitive networks. We also presented analytical results for channel availability of cognitive networks with respect to transmit power. In this study, we have considered short retransmission limit. As a result, packets are dropped after a fixed amount of retransmission events. Conversely, access delay results without retransmission limit case reported in [57], indicate an exponential increase in delay. However, exponential decrease in service time indicates less loss in performance for higher number of nodes in the network, which is beneficial for large networks. Nevertheless, our analysis indicates that network performance depends on transmit power, packet length and number of an-

tennas used. For this reason, optimization techniques can be applied to achieve a desired performance gain for certain operating environment. Similarly, a designed network can be analyzed to determine its operating parameters. However, in this chapter we have considered all cognitive nodes operate in a single channel. In Chapter 4, we consider a multi-channel environment for cognitive nodes.

Chapter 4

Channel Selection for Heterogeneous Nodes in Cognitive Networks

In the previous chapter, we have considered all cognitive nodes operating in a channel and determine performance matrices of interference aware ad-hoc networks. In practice, cognitive radios are envisioned to operate over multiple channels. In this chapter, we extend our study to design an cognitive ad-hoc network over multiple channels.

We propose algorithms to address the channel allocation and fairness issues of multi-band multi-user cognitive ad-hoc networks. Nodes in the network have unequal channel access probability and thus heterogeneous. Also, nodes have no prior information about the offered bandwidth or number of users in the multiple access system. In that, nodes use reinforcement learning algorithm to predict future channel selection probability from the past experience and reach an equilibrium state. Proof of convergence of this multi party stochastic game is provided. Finally, numerical results are presented for performance evaluation of the proposed channel allocation algorithms. We further extend this study as we consider cooperative communication context. Cognitive nodes use modified MAC protocol to achieve cooperative communication. In the process, nodes achieve diversity gain and exchange channel selection information to further improve the network

performance.

4.1 Introduction

Cognitive radios are envisioned to dynamically adapt operating parameters according to the surrounding environment. For adaptation purpose in ad-hoc networks, cognitive nodes encounter challenges such as, lack of cooperation between nodes, resource management, unstable user statistics, etc. In that sense, game theory is a mathematical tool to model these challenges in the ad-hoc network [41]. Also, in the repeated game, players can learn from past experiences to determine future actions [61]. In some recent works, learning algorithms are used in repeated game for channel selection in cognitive networks. In [12], co-operative Q learning is used to assign channels for cognitive nodes. Q learning is also used in [13] to assign channels for two cognitive nodes from a set of two channels. On the other hand, in [14] the authors used stochastic learning automata based algorithm for channel selection for cognitive nodes. No-external-regret learning is used in [15], to address the channel selection problem for cognitive ad-hoc networks. In [16], the authors considered 'user satisfaction' as selection criteria to address the joint channel and power allocation problem for cognitive ad-hoc networks. Machine learning is also used in [62] to address the channel allocation problem for heterogeneous (unequal bandwidth or interference limit on primary users) cognitive networks. It is worth noting that, the channel allocation problem for heterogeneous cognitive networks was first studied in [63] and in our previous study [24], we were the first to consider fairness issues in channel selection. To our best knowledge, channel selection for heterogeneous cognitive nodes i.e., with unequal packet arrival rate is not considered to date. From this point of view, in this chapter our main contributions are

- We evaluate the performance of user satisfaction based Q learning channel selection algorithm for ad-hoc cognitive networks in heterogeneous environment.

- The proposed algorithm considers application layer packet arrival rate for channel selection in data link layer of OSI model.

- We prove the convergence of the algorithm.

- We propose cooperative Q learning to reduce the convergence time of the algorithm.

The rest of the chapter is organized is as follows. The system model is presented in Section 4.2. Cooperative Q learning algorithm is presented in Section 4.3. Simulation settings and results of the proposed algorithm are presented in Section 4.4. Finally, conclusions are drawn in Section 4.5.

4.2 System Model

We consider $\hat{T}$ pairs of cognitive nodes coexist with licensed primary users in the same geographical area. We assume cognitive nodes belong to an ad-hoc network, where nodes can listen to all the nodes of the network. For wireless resource allocation purposes, we consider cognitive nodes use $\hat{C}$ unused frequency bands of the primary user and can access single channel at a particular time. We also assume that, no central controller exists for cognitive nodes and IEEE 802.11 algorithm [59] is used for channel sharing purposes. In this multiple access designed network, there are more than one free frequency slot available, as a result at any given time, more than one node pairs may communicate. We investigate the effect of the channel transmission rate (R_{tr}) on the performance of the network. This happens as channels differ in bandwidths. It is noted that random channel assignment will cause large difference in user satisfaction among cognitive nodes. To overcome the channel transmission rate effect, we propose Q learning based channel selection algorithm for the cognitive nodes. In that, cognitive nodes apply the learning based channel selection strategy in the non-cooperative repeated game model of the ad-hoc network. We mathematically define the non-cooperative game as $\{\hat{T}, \{S_i\}_{i \in \hat{T}}, \{U_i\}_{i \in \hat{T}}\}$, where $\hat{T}$ is

the set of cognitive nodes (decision makers), S_i is the set of strategies $\{s_a, s_b...s_{\hat{C}}\}$, for node i, for $\hat{C}$ available channels. Player i uses the utility function $U_i : S_i \to \mathbb{R}$ to select the strategy s_a from the set S_i for the current strategy profile of its opponents: S_{-i}. At some point of the game, nodes may select a strategy profile $S = [s_1, s_2....s_{\hat{T}}]$ such that no players would deviate anymore. This point is known as the Nash equilibrium point and this only happens iff (4.1) exists.

$$U_i(S) \geq U_i(\acute{s}_a, s_{-a}), \forall i \in \hat{T}, \acute{s}_a \in S_i. \tag{4.1}$$

We employ the function in [64] to calculate the utility of strategies that accounts for the channel data rate R_{tr}^a of channel a and packet arrival rate λ of node $i \in \hat{T}$ of the selfish cognitive nodes in the non-cooperative game,

$$U_i(s_a, s_{-a}) = \beta + \gamma \log(\frac{R_{tr}^a}{\lambda} - \delta), \tag{4.2}$$

where $\log(.)$ stands for natural logarithm function. Numerical constants β, γ, and δ in the utility function are user defined. If cognitive nodes use only the utility to select channels, it will cause large number of channel switching events i.e., operation overhead. To minimize the number of channel switching, we apply learning algorithm. We consider three learning algorithms for channel allocation purposes namely, Q-learning, learning automata and No-external-regret learning. Learning automata based channel selection is analyzed in [14], and in the following paragraphs we will describe the No-external-regret and the Q learning algorithms.

4.2.1 No-external-regret learning

First we consider the No-external-regret learning algorithm [65], and use the exponential updating scheme. In this algorithm, cognitive nodes preserve channel utilities for a certain amount of time and compute the future channel selection probability using

---
Algorithm 1 Channel selection using No-external-regret learning
---
1: Begin with random channel allocation.
2: **while** channel $< \hat{C}$ **do**
3:      Calculate channel utility from the received packet date rate.
4:      Compute $U_i^t(s_a) = \sum_{t=1}^{t} U_i(s_a)$.
5:      channel=channel+1
6: **end while**
7: Compute probability using (4.3).
8: Choose the channel $\max_{(s_a)}(p_i^{t+1}), \forall a \in \hat{C}$ and set the channel to transmit packet.
9: Repeat step (2) to (9) for every packet.
10: End of session
---

these past utility information as,

$$p_i^{t+1}(s_a) = \frac{(1+\alpha)^{U_i^t(s_a)}}{\sum_{\acute{s}_a \in S_i}(1+\alpha)^{U_i^t(\acute{s}_a)}}, \tag{4.3}$$

where $U_i^t(s_a) = \sum_{j=1}^{t} U_i^j(s_a)$ and $U_i^t(\acute{s}_a) = \sum_{j=1}^{t} U_i^j(\acute{s}_a)$ denote the cumulative utilities over time t, $p_i^{t+1}(s_a)$ represents the probability assigned to strategy s_a at time $t+1$, for $\alpha > 0$, where α denote the learning rate. Algorithm 1 summarizes this channel selection algorithm.

4.2.2   Q learning

In the Q learning, cognitive nodes maintain a Q table [66]. Entries of the table are updated based on quality of actions i.e., rewards it achieves in a state as,

$$Q_{t+1}(s,a) = Q_t(s,a) + \alpha \left[E \left(U(s_a, s_{-a}) - Q_t(s,a) \right] \right], \tag{4.4}$$

where $Q_{t+1}(s,a)$ and $Q_t(s,a)$ represent Q entries at time $(t+1)$ and t, respectively for selecting action a from state s. $E\left[U(s_a, s_{-a})\right]$ denote the average reward and α is the learning rate.

In our study, the Q learning algorithm selects a channel that has maximum Q value based on ϵ greedy exploration. ϵ greedy exploration works as nodes select a random

Algorithm 2 Channel selection using Q learning

1: Initialize $Q(s,a) = 0$
2: Begin with random channel allocation.
3: Transmit packet using multiple access scheme in channel $a \in \hat{C}$.
4: **while** channel $< \hat{C}$ **do**
5:       Calculate channel utility from the received packet date rate.
6:       Calculate average reward $E\left(U(s_a, s_{-a})\right) = \left(U_t(s_a, s_{-a}) + U_{t-1}(s_a, s_{-a})\right)/2$
7:       Update $Q(s,a)$ values using (4.4)
8:       channel=channel+1
9: **end while**
10: Assign channel using ϵ greedy exploration
11: Update ϵ value
12: Repeat step (4) to (11) for every packet.
13: End of session
---

channel with probability ϵ and select a channel based on Q table with probability $(1 - \epsilon)$. Nodes start the exploration with a very high ϵ value and update ϵ after each successful packet transmission as,

$$\epsilon = \epsilon - \frac{\epsilon}{Update\ parameter}. \tag{4.5}$$

From (4.5), we can write the probability of selecting a channel as in (4.6). Algorithm 2 summarizes this channel selection algorithm.

$$p_{t+1}\left(s_a\right) = \begin{cases} 1 - \epsilon + \left(\frac{\epsilon}{Update\ parameter}\right) & \text{if } Q_t(s,a) \text{ is} \\ & \text{the highest,} \\ \frac{\epsilon}{Update\ parameter} & \text{Otherwise.} \end{cases} \tag{4.6}$$

4.2.3   Learning automata

Now we consider learning automata algorithm. In this algorithm nodes select a channel, $a \in \hat{C}$ based on the action probability table. After this step nodes update entries of the action probability table based on rewards achieved by executing the action. The

---
Algorithm 3 Channel selection using Learning automata

1: Initialize $q(s, a) = 0$
2: Begin with random channel allocation.
3: Transmit packet using multiple access scheme in channel $a \in \hat{C}$.
4: **while** channel $< \hat{C}$ **do**
5:       Calculate channel utility from the received packet date rate.
6:       Calculate average reward $E\left(U(s_a, s_{-a})\right) = \left(U_t(s_a, s_{-a}) + U_{t-1}(s_a, s_{-a})\right)/2$
7:       Update $q(s, a)$ values using (4.7)
8:       channel=channel+1
9: **end while**
10: Repeat step (3) to (9) for every packet.
11: End of session
---

action probability table is updated [67] as,

$$
\begin{aligned}
q_{t+1}(s, a) &= q_t(s, a) + \alpha \tilde{U}(s_b, s_{-a})[1 - q_t(s, a)], \quad \text{for } a = b \\
q_{t+1}(s, a) &= q_t(s, a) - \alpha \tilde{U}(s_b, s_{-a}) q_t(s, a), \quad\quad\quad \text{for } a \neq b
\end{aligned}
\tag{4.7}
$$

where $q_{t+1}(s, a)$ and $q_t(s, a)$ represent action probabilities at time $(t+1)$ and t, respectively for selecting action a from state s, $\tilde{U}(s_a, s_{-a})$ denotes the normalized utility determined as,

$$
\tilde{U}(s_a, s_{-a}) = \frac{U(s_a, s_{-a})}{\max_{a \in \hat{C}} E\left(U(s_a, s_{-a})\right)}
\tag{4.8}
$$

Algorithm 3 summarizes this channel selection algorithm [67].

4.2.4 Proof of convergence

In this subsection, we prove that these multi party learning algorithms converge to a Nash equilibrium point. Let us define potential function as,

$$
\hat{P} = \sum_{i=1}^{\hat{C}} \sum_{j=1}^{\theta\{\hat{C}_i\}} U_j\left(\theta\{\hat{C}_i\}\right),
\tag{4.9}
$$

where $\theta\{\hat{C}_i\}$ denote the cardinality of channel $\hat{C}_i$ i.e., indicates the number of nodes in channel $i \in \hat{C}$. As the nodes use CSMA/CA scheme to access the channel, at given time

only a single node can win the transmission opportunity in a channel. Also, nodes switch channels after the end of a packet transmission i.e., at a given time only a single node makes a channel switch. From the above mentioned algorithms we also notice that a cognitive node makes a channel switch iff,

$$\Delta U_i \left[\theta\{\hat{C}_i\} \right] = U_i \left[\theta\{\hat{C}_{j+1}\} \right] - U \left[\theta\{\hat{C}_k\} \right], \quad \text{if } U_i \left[\theta\{\hat{C}_{j+1}\} \right] > U \left[\theta\{\hat{C}_k\} \right] \qquad (4.10)$$

This unilateral move also increases the value of the potential function as,

$$
\begin{aligned}
\Delta \hat{P} &= \sum_{i=1}^{\theta\{\hat{C}_{j+1}\}} U_i \left[\theta\{\hat{C}_{j+1}\} \right] + \sum_{i=1}^{\theta\{\hat{C}_{k-1}\}} U_i \left[\theta\{\hat{C}_{k-1}\} \right] \\
&\quad - \left\{ \sum_{i=1}^{\theta\{\hat{C}_j\}} U_i \left[\theta\{\hat{C}_j\} \right] + \sum_{i=1}^{\theta\{\hat{C}_k\}} U_i \left[\theta\{\hat{C}_k\} \right] \right\} \\
&= U_i \left[\theta\{\hat{C}_{j+1}\} \right] - U_i \left[\theta\{\hat{C}_k\} \right] \\
&= \Delta U_i \left[\theta\{\hat{C}_i\} \right].
\end{aligned}
\qquad (4.11)
$$

From (4.11) one can notice that $\hat{P}$ is an exact potential game and therefore, has at least a pure strategy Nash equilibrium [68]. Hence, if the nodes are homogeneous i.e., all nodes have same bandwidth requirement, the potential game may have multiple Nash equilibrium. All the Nash equilibrium points in such scenario will result in same system throughput [14]. Conversely, for heterogeneous environment this multi party game will converge to a unique Nash equilibrium point.

At this point, we will determine the effect of this Nash equilibrium on the learning algorithms. For No-external-regret learning, as $\Delta U = 0$ happens at the Nash equilibrium, we can write,

$$
\begin{aligned}
U_i^t(s_a) &= U_i^{t+1}(s_a), \\
U_i^t(\acute{s}_a) &= U_i^{t+1}(\acute{s}_a).
\end{aligned}
\qquad (4.12)
$$

From (4.3) and (4.12), it is easy to conclude that after Nash equilibrium, nodes converge to an equilibrium condition and no further channel switching events occur for No-external-regret learning as,

$$p_i^{t+1}(s_a) = p_i^{t+2}(s_a). \tag{4.13}$$

Also, for learning automata (4.7) and (4.12) indicate that after the Nash equilibrium no further channel switching happens as,

$$q_{t+1}(s, a) = q_t(s, a). \tag{4.14}$$

Now, for Q learning from (4.4), we can form differential equation [69] for Q entries of the Q table as,

$$\frac{Q_{t+1}(s, a) - Q_t(s, a)}{\Delta t} = \alpha \left[E \left(U(s_a, s_{-a}) \right) - Q_t(s, a) \right],$$
$$\frac{dQ}{dt} = \alpha \left[E \left[U(s_a, s_{-a}) \right] - Q_t(s, a) \right]. \tag{4.15}$$

Integration of this differential equation represents Q values [69] at time t as,

$$Q_t = K e^{-\alpha t} + E \left[U(s_a, s_{-a}) \right], \tag{4.16}$$

where K is a constant of integration. From (4.16), Q values at time $t \to \infty$ can be written as,

$$\lim_{t \to \infty} Q_t = E \left[U(s_a, s_{-a}) \right]. \tag{4.17}$$

From (4.13), (4.14) and (4.17), one can notice that Q learning, learning automata, and No-external-regret learning algorithms converge.

Utility at time t for any node $i \in N$ can be written using (4.2), (4.3) and (4.6) as,

$$U_i^t = U_i^t(s_a, s_{-a})p_t(s_a) + \sum_{b=1, b \neq a}^{\hat{C}} U_i^t(s_b, s_{-b})p_t(s_{-a}). \tag{4.18}$$

57

Also, from (4.3) and (4.6), one can notice that $\lim_{t \to \infty} p_t = 1$. Therefore, nodes converge to a pure strategy Nash equilibrium after the convergence of this stochastic learning event.

4.2.5 Complexity analysis

The above mentioned algorithms have very low time and memory complexity. Each iteration of the No-external-regret channel selection algorithm at any node $i \in \hat{T}$ has a time complexity $O(max\{|U_i||\hat{C}|^2, |\hat{C}|^3\})$ [24]. Conversely, each iteration of the Q learning and learning automata has time complexity of $O\left(|S|^2|\hat{C}|\right)$ [35]. Also, examining the algorithms, one can notice that memory space complexity of No-external-regret learning is $O(|U_i||\hat{C}|^2)$ [24] and Q-learning and learning automata is $O(2|\hat{C}|)$ [35].

4.3 Cooperative Q Learning

In this section, we consider that cognitive nodes exchange channel information to facilitate Q learning. As seen in the previous section, nodes rely on its own packet exchange information for Q learning. Also, in our previous chapter we noticed that nodes periodically access the channel. As a result, the learning rate for any node in the network is long. Here, we consider that nodes embed the average channel reward information with the ACK message. This follows with, all other nodes in the channel updating the Q table using this average channel reward information. This small change in the MAC protocol will cost very small amount of extra time to transmit the ACK packet. Also, for the sake of simplicity we consider received ACK packets are error free. This modified Q learning algorithm is presented in Algorithm 4.

Algorithm 4 Channel selection using cooperative Q learning

1: Initialize $Q(s, a) = 0$
2: Begin with random channel allocation.
3: Transmit packet using multiple access scheme in channel $a \in \hat{C}$.
4: **while** channel $< \hat{C}$ **do**
5:     **if** packet received $==$ yes **then**
6:         Calculate channel utility from the received packet date rate
7:     **else**
8:         Get channel utility from ACK packets
9:     **end if**
10:     Calculate average reward $E\left(U(s_a, s_{-}a)\right) = \left(U_t(s_a, s_{-a}) + U_{t-1}(s_a, s_{-a})\right)/2$
11:     Update $Q(s, a)$ values using (4.4)
12:     channel=channel+1
13: **end while**
14: Assign channel using ϵ greedy exploration
15: Update ϵ value
16: Repeat step (4) to (11) for every packet
17: End of session

4.4   Results

Here, we carry out numerical analysis to evaluate the performance of the above mentioned algorithms. We build an IEEE 802.11 [59] compatible ad-hoc network using the simulation parameters listed in Table 4.1. We use these parameters to build an event driven simulation program for the cognitive network introduced in section 4.2.

First we present average data rate results for the channel selection algorithms. In addition to the Q learning, No-external-regret learning and learning automata based algorithms mentioned in section 4.2, we consider as a benchmark random channel selection for performance comparison. In random selection, cognitive nodes select a channel from the pool of available channels with equal probability and use the selected channel for the entire period of communication. Fig. 4.1 indicates that the Q learning channel selection algorithm offers the best performance. In the multi party non-cooperative game multiple Nash equilibrium points may exist. In Q learning, nodes use an exploration phase in addition to the exploitation phase to reach the best equilibrium condition. Conversely, in No-external-regret and learning automata algorithms due to the absence of the exploration

Table 4.1: Simulation setting

Parameter	Value
No. of cognitive nodes	50
No. of channels	3
Bandwidth, Channel 1, 2 & 3	2 MHz, 4 MHz & 6 MHz
Data type	Best effort
Packet Payload	8184 bits
Packet arrival rate, λ	Uniform (1,5)
MAC header	272 bits
MAC protocol	CSMA/CA
$\beta, \gamma, \& \delta$ of utility function	0.16, 0.8 & 400
α	0.02
Update parameter	100
PHY header	127 bits
ACK	112 bits+PHY header
RTS	160 bits+PHY header
CTS	112 bits+PHY header
Slot time	50 μs
DIFS	128 μs
SIFS	28 μs
Bit rate, channel 1, 2 & 3	2 Mb/s, 4 Mb/s, 6 Mb/s
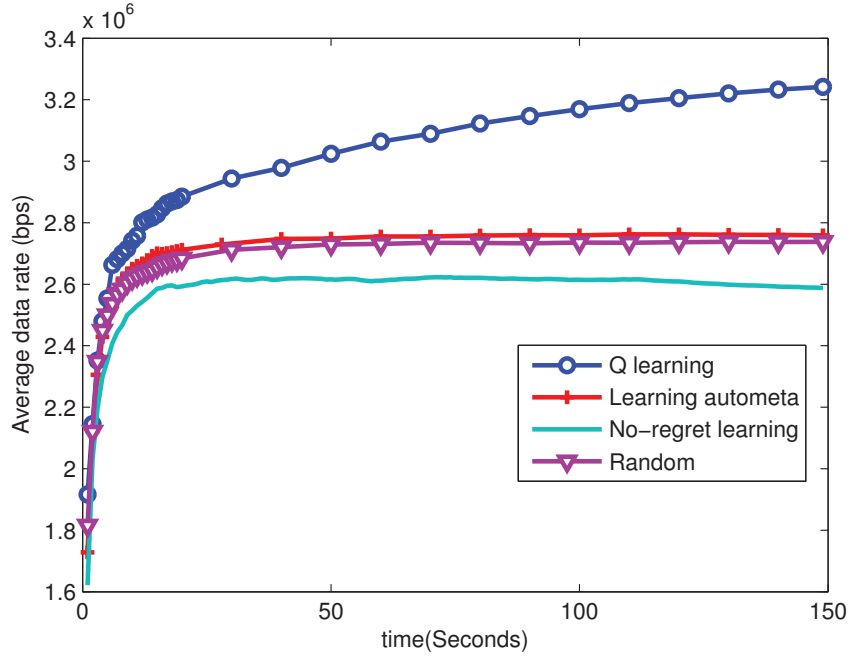
Figure 4.1: Average data rate of the cognitive nodes for different learning algorithms.

phase, channel selection performance is affected by the instantaneous performance of the channel instead of the long run performance. In Fig. 4.2 we plot the variance in user utility for cognitive nodes. Similar to the average data rate performance, we also notice the best performance for the Q learning based channel selection. We plot the number of channel selection events in Fig. 4.3. As shown, the Q learning has higher number of switching events compared to the No-external-regret and the learning automata based algorithms. This happens as the Q learning has an exploration phase. Nevertheless, over the time, all algorithms converge to a stable state. In the stable state, nodes have very few switching events.

Now, we present average data rate results for cooperative Q learning algorithm. In Fig. 4.4 one can notice that cooperative Q learning has better performance at the beginning. However, both cooperative and non-cooperative cases have equal data as time elapses. We confirm this behavior with the help of number of channel switching results in Fig. 4.5. As seen, cooperative Q learning algorithm has very fast convergence time compared to the non-cooperative case. However, as time elapses non-cooperative Q
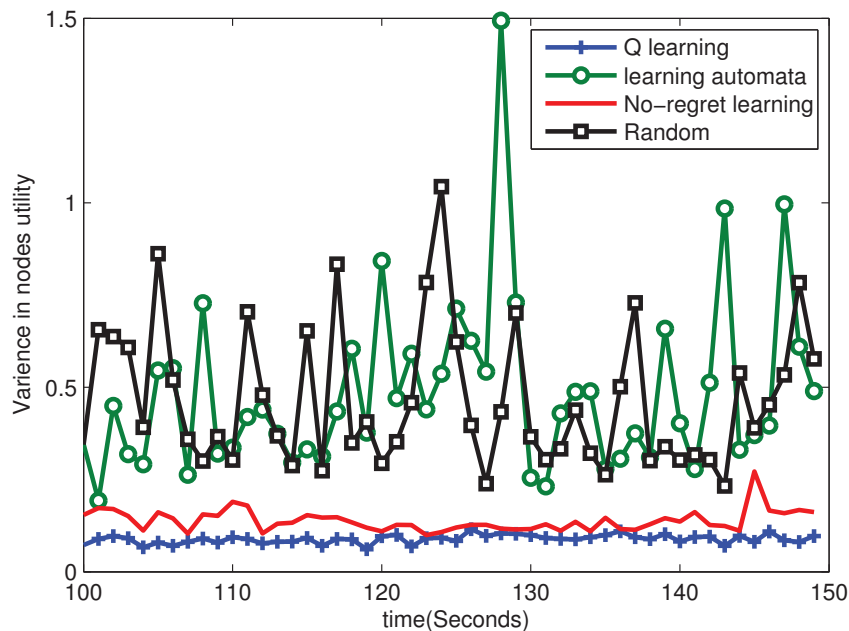
Figure 4.2: Variance in user satisfaction level for learning algorithms.
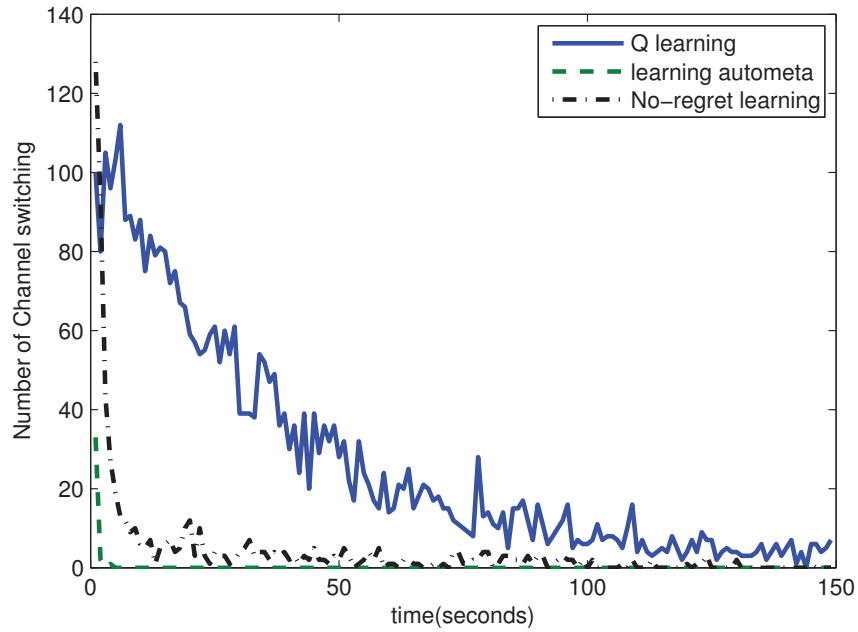
Figure 4.3: Number of channel switching events for different learning algorithms.
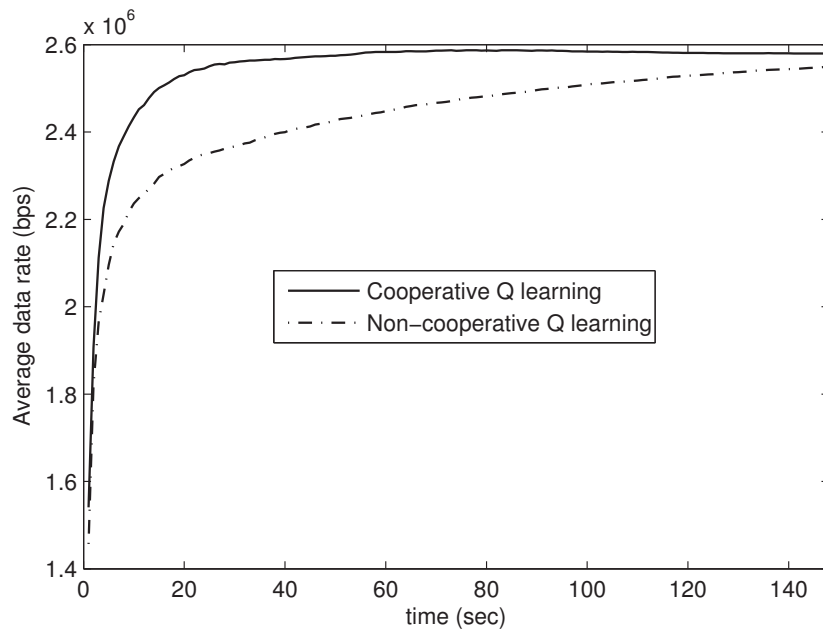
Figure 4.4: Average data rate of the cognitive nodes for cooperative Q learning algorithm.

learning converges, as a result data rate for non-cooperative learning also increases and become equal to the cooperative Q learning case. In Fig. 4.6, we plot the variance in user utility for cooperative Q learning and Q learning algorithms. As noticed, both algorithms
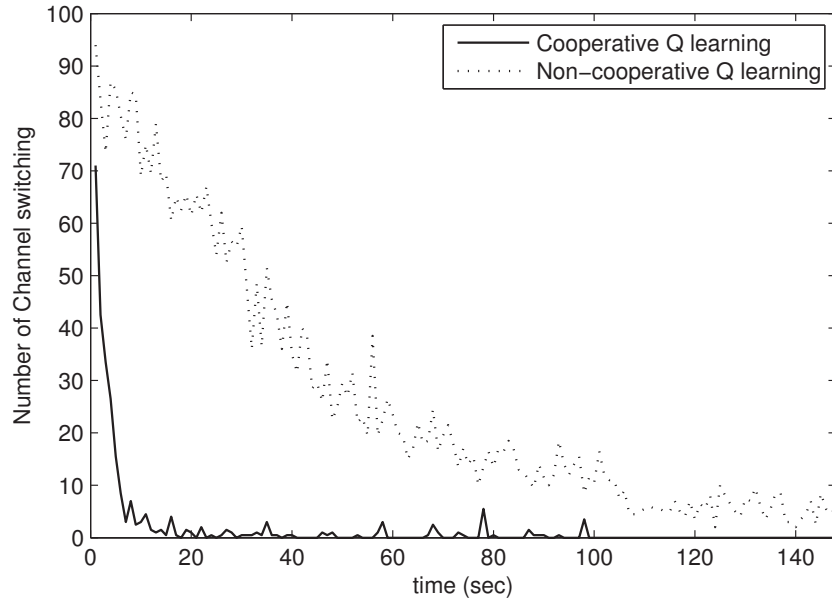
Figure 4.5: Number of channel switching events for cooperative Q learning algorithm.
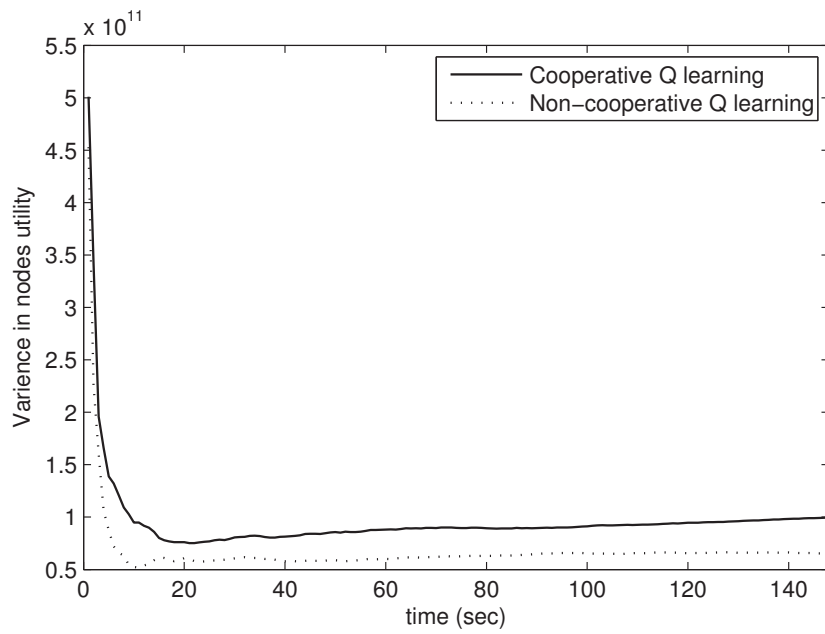
Figure 4.6: Variance in user satisfaction level for cooperative Q learning algorithm.

have equal performance i.e., fairness is achieved for both algorithms.

4.5 Conclusions

We investigated the performance of learning based channel selection approaches for cognitive ad-hoc networks. We presented proof of convergence for the algorithms for multi-band cognitive ad-hod networks with heterogeneous nodes. It was shown that learning based channel selection algorithms converge to a Nash equilibrium point for nodes having unequal arrival packet rate in multi-party multi-agent stochastic game. We also showed that Q learning based algorithm can improve the average data rate of the network, and can reduce the user satisfaction variance i.e., improve fairness among cognitive nodes. We further show that convergence time and data rate improves for cooperative learning. However, in the following chapter we considered MIMO systems for cognitive communication and hence apply channel allocation algorithm for performance improvement.

Chapter 5

Cross-Layer Antenna Selection and Beamforming for MIMO Cognitive Radios

It is noticed that channel selection algorithms are able to improve the performance of cognitive networks. To further improve the performance, we extend our study to include MIMO techniques and explore the possibilities to improve spectrum utilization.

We propose spectrum efficiency improvement algorithms of multi-band multiuser MIMO cognitive ad-hoc networks. To improve the transmission efficiency of the MIMO system, a cross-layer antenna selection algorithm is proposed. Cross-layer antenna selection algorithm works as the data link layer efficiency information is used for antenna selection purpose to achieve very high efficiency at the data link layer. Conversely in cognitive communication, power at which cognitive nodes can transmit is limited by the primary users' interference limit. As a result, achievable efficiency at cognitive nodes depend on the interference limit set by the primary user. For that, beamforming techniques can be employed to suppress co-channel interference in radio devices. In a cognitive setting, beamforming can be beneficial as it can be applied to cancel interference among

co-located primary users and cognitive users. Here, we propose an antenna selection algorithm combined with zero-forcing beamforming to improve the throughput of cognitive MIMO radios. In that, we maximize an objective function for the system throughput where precoding is applied on the transmitted spatial multiplexed signals. Numerical results show the advantages offered by the proposed algorithm under different scenarios.

Using the transmission efficiency results, user data rate of the cognitive ad-hoc network is determined. Objective function for the average data rate of the multi-band multiuser cognitive MIMO ad-hoc network is also defined. For the average data rate objective function, primary users interference is considered as performance constraint. Furthermore, using the user data rate results, a learning-based channel allocation algorithm is proposed.

5.1   Introduction

During the past decade, extensive research has been conducted to improve the spectrum utilization in wireless applications. Among these activities, MIMO technology has shown to improve the spectrum efficiency and the reliability of the channel. Despite these efforts, spectrum crisis situations still exist due to the fixed spectrum allocation policy where users are assigned portions of the spectrum permanently. Due to the unprecedented growth of wireless users, some portions of the assigned spectrum become heavily congested, while leaving other parts unutilized. To solve this problem, and to efficiently utilize the available spectrum, cognitive radios have been proposed. It is envisioned that cognitive radios will share the spectrum along with existing primary users in a dynamic and an opportunistic manner [9].

By sensing the environment, cognitive radios may determine opportunity in time, frequency or space domain. For instance, inside a time-division multiple-access (TDMA) based primary network, cognitive nodes can use the unused time slots as an opportunity

[70,71]. Also, cognitive radios can use the unused frequency spaces of the primary network [4]. However, in addition to time, frequency and space domain, MIMO systems add another degree of freedom to cognitive radios. For instance, cognitive users equipped with MIMO can use beamforming to reduce interference on primary users and thus, operate concurrently. In some recent works [72–74] this type of interference reduction technique is formulated as non-convex optimization problem. Although, theoretically achievable information rate is determined in [72, 73], and [74], it is very difficult to determine the wight vector as the problem is non-convex. Another approach is presented in [75], to completely cancel interference between primary and cognitive nodes using pre-coding and post-coding techniques. In addition, a closed form expression for achievable capacity limit is also presented by the authors.

Apart from the opportunity detection phase, utilizing the detected spectrum is one of the key challenges for cognitive networks. One of the prominent techniques to improve spectrum utilization is through MIMO techniques. As cognitive radios are able to access very small amount of wireless resources, this high spectrum efficiency renders MIMO systems extremely valuable for cognitive devices. However, spectrum efficiency of MIMO systems can be further improved by using antenna selection schemes [10]. Moreover, it is also shown that a cross-layer antenna selection scheme can reap a very high transmission efficiency in a 'point-to-point' MIMO system [46]. On the other hand, in [76] the authors exploit the spatial and temporal domains of MIMO cooperative cognitive networks to achieve high transmission efficiency.

Motivated by the works in [22, 75], and [46], we propose a cross-layer MIMO transmit-antenna selection algorithm and beamforming to reach high transmission efficiency as well as concurrent operation with the primary user for cognitive MIMO systems. Cross-layer antenna selection is beneficial as packet error rate (PER) is considered at the link-layer which identifies usable channels. Thus, with low number of RF chains, high efficiency is achievable with low decoding complexity. On the other hand when beamforming

67

is employed with cross-layer antenna selection, interference imposed on the primary user can be mitigated. As a result, cognitive users are able to communicate below the primary user interference level. Different from [76], we employ a cross-layer design where efficiency is considered for selecting less number of antennas per user.

From the above mentioned context this chapter is organized as follows. Section 5.2 introduces the analysis and performance evaluation results of the cross-layer antenna selection algorithm for primary users' interference limited cognitive communication. This is followed by the theoretical analysis and performance evaluation results for the cross-layer antenna selection and beamforming algorithm in Section 5.3. Further, antenna selection algorithm is combined with the channel selection algorithm described in Chapter 4 to propose cross-layer antenna selection and channel allocation algorithm in Section 5.4 Finally, conclusions are presented in Section 5.5.

5.2 Cross-Layer Antenna Selection

In Chapter 3, we have presented access probability analysis for cognitive ad hoc networks. In this part of the work, we propose MIMO cross-layer transmit-antenna selection algorithms to improve the spectrum utilization in a cognitive setting.

5.2.1 System model

For the system model presented in Chapter 1, we make the following assumptions. The ad-hoc network contains $\hat{T}$ pairs of cognitive users and any node can listen to all other nodes in the network. For wireless resource allocation purposes, we consider cognitive nodes that can make use of $\hat{C}$ unused frequency bands of the primary users. Also, the number of available channels for cognitive radios is less than the number of cognitive users, i.e., $\hat{C} < \hat{T}$. As a result, a channel may be shared by more than one cognitive user using multiple access techniques. If a channel is selected by many users, the overall

data rate per node will reduce due to collisions and users will then be forced to search for a different channel. To reduce the number of channel switchings, nodes employ a learning-based channel selection algorithm. On the other hand, to improve the wireless resource utilization, cognitive source-destination pairs use N_t transmit and N_r receive antennas. Nodes also use Decision Feedback Detection (DFD) to cancel interference and improve detection. In the Logical Link Control (LLC) sub-layer, nodes use Go-Back-N (GBN) protocol, and CSMA/CA protocol in the MAC sub-layer of the data link layer as shown in Fig. 5.1. Nodes exchange information between physical layer and data link layer for cross-layer antenna selection and channel allocation purposes. In the following subsections, we address these algorithms in detail.

The primary users' interference limited cross-layer antenna selection algorithm works as follows. At first, a cognitive source node determines the combination of maximum possible usable antennas for a given transmit power and primary users' interference constraint. Then, source nodes consult with respective receivers on the optimum combination of $K \leq N_t$ transmit antennas. During this phase, a cognitive receiver searches for the subset p, from all possible combination set $P = \{\{1\}, \{2\}..\{N_t\}, \{1,2\}, \{1, N_t\}, ..., \{1, 2...N_t\}\}$,
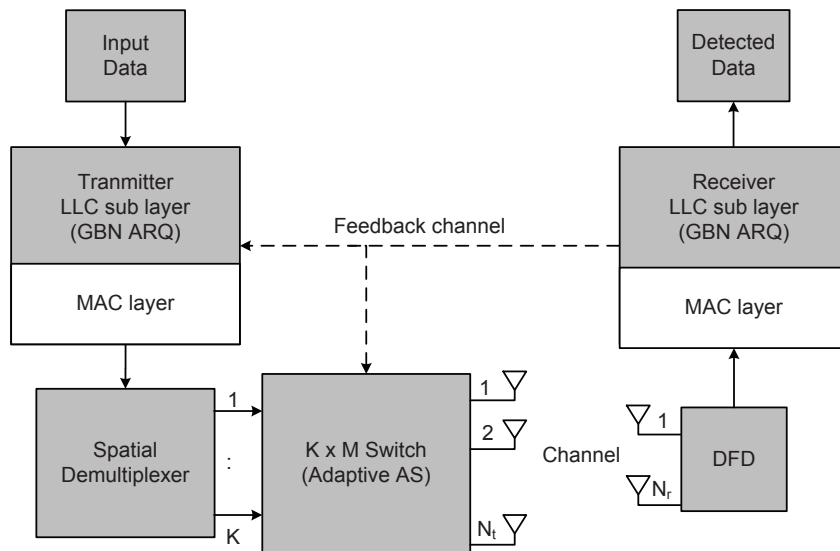
Figure 5.1: Communication system model for cognitive nodes.

that achieves the maximum transmission efficiency at the LLC sub layer. This information of the optimum subset p of transmit antennas is relayed back to the cognitive transmitter through a feedback channel. At the transmitter side, cognitive nodes use this subset p to divide the incoming data into K parallel streams for spatial multiplexing and subsequent transmission from the K-selected antennas.

5.2.2 Performance analysis for perfect channel estimation

To develop the mathematical model for the transmission efficiency, we express the received signal $\boldsymbol{y}_c \in C^{N_r \times 1}$ at cognitive receivers as

$$\boldsymbol{y}_c = \boldsymbol{H}_p \boldsymbol{\Pi} \boldsymbol{x} + \boldsymbol{n} \tag{5.1}$$

where $\boldsymbol{H}_p$ is an $N_r \times K$ channel sub-matrix, $\boldsymbol{\Pi} \in \mathbb{R}^{K \times K}$ represents channel dependent permutation matrix for greedy QR detection ordering [77], $\boldsymbol{x}$ denotes $N_t \times 1$ cognitive user transmit symbol vector, and $\boldsymbol{n} \in CN(0, N_o I_{N_r})$ is the complex Gaussian noise vector with zero mean and variance N_o, where $\boldsymbol{I}_{N_r}$ is an identity matrix of size N_r.

We consider all cognitive users have uniform interference effect on primary users. For this reason we drop the subscript l in (3.2) for our further analysis. If the transmission probability of cognitive node is τ_i, then the total interference level at the primary user for $\hat{T}$ cognitive users can be written as,

$$I_{total} = \sum_{i=1}^{\hat{T}} \tau_i I_i. \tag{5.2}$$

We assume CSI between cognitive source and destination pairs is available at the cognitive receiver. Also, cognitive receivers use Zero-Forcing (ZF) algorithm to suppress the interference between the K spatially-multiplexed layers [10]. If no error propagation occurs among the detected layers at the DFD, the MIMO channel between cognitive nodes

decouple into K parallel Single-Input and Single-Output (SISO) virtual sub-channels [78]. Given this, the output signal-to-noise ratio (SNR) for the jth sub-channel can be written as,

$$\rho_j = r_{jj}^2 \rho_o, \tag{5.3}$$

where $\rho_o = E[\boldsymbol{x}^H \boldsymbol{x}]/KN_o$ is the average received SNR per receive antenna, and r_{jj}^2 is the diagonal elements of the matrix $\boldsymbol{R}_p$ calculated using $\boldsymbol{H}_p \boldsymbol{\Pi} = \boldsymbol{Q}_p \boldsymbol{R}_p$.

Considering Binary-Phase-Shift-Keying (BPSK) transmission, the bit-error rate (BER) of the jth layer provided that all previous layers are correctly detected, can be written as

$$BER_j = Q(\sqrt{2r_{jj}^2 \rho_o}), \ for \ j = 1, 2, ..., K, \tag{5.4}$$

where $Q(.)$ is the Gaussian Q-function. Since each L-symbol data packet is divided into K-parallel streams before transmission, the packet error rate is given by

$$PER(\boldsymbol{H}_p, \rho) = 1 - \left[\prod_{j=1}^{K} (1 - BER_j) \right]^{L/K}. \tag{5.5}$$

Having obtained the PER in (5.5), one can evaluate the transmission efficiency (i.e., normalized throughput), defined as the ratio of effective information transfer rate to the information or bit rate of the channel. For GBN protocol with window size W, the instantaneous transmission efficiency [79] at the receiver side of node i can be expressed as,

$$\eta_i(\boldsymbol{H}_p, \rho) = \frac{K}{N_t} \frac{1 - PER(\boldsymbol{H}_p)}{1 + (W - 1)PER(\boldsymbol{H}_p)}. \tag{5.6}$$

5.2.3   Performance analysis for imperfect channel estimation

Here we investigate the effect of imperfect CSI. For this purpose, we assume a time frame consisting of L_t training or pilot symbols and L_d data symbols. Radio devices can estimate the channel $\boldsymbol{H_p}$ using a priori knowledge of these training symbols in maximum-

likelihood estimation method to yield,

$$\hat{\boldsymbol{H}}_{\boldsymbol{p}} = \boldsymbol{H}_{\boldsymbol{p}} + \Delta \boldsymbol{H}_{\boldsymbol{p}}, \tag{5.7}$$

where $\Delta \boldsymbol{H}_{\boldsymbol{p}}$ represents the error matrix for channel estimation. Hence, one can rewrite the received signal vector at the cognitive user as,

$$\boldsymbol{y}_c = \boldsymbol{H}_p \hat{\boldsymbol{\Pi}} \boldsymbol{x} + \boldsymbol{n}. \tag{5.8}$$

Using (5.7) in (5.8) we obtain,

$$\tilde{\boldsymbol{y}}_c = \hat{\boldsymbol{Q}}^H \boldsymbol{H}_p \hat{\boldsymbol{\Pi}} \boldsymbol{x} + \boldsymbol{n}$$
$$= \hat{\boldsymbol{R}} \boldsymbol{x} - \boldsymbol{Q}^H \Delta \boldsymbol{H}_p \hat{\boldsymbol{\Pi}} \boldsymbol{x} + \tilde{\boldsymbol{n}}, \tag{5.9}$$

where $\hat{\boldsymbol{H}}_{\boldsymbol{p}} \hat{\boldsymbol{\Pi}} = \hat{\boldsymbol{Q}} \hat{\boldsymbol{R}}$ and $\tilde{\boldsymbol{n}} = \boldsymbol{Q}^H \boldsymbol{n}$.

Given the channel estimation technique, one can evaluate the received SNR for the jth sub channel [46] as,

$$\hat{\rho}_j = \frac{\hat{r}_{ii}^2 \lambda}{\lambda \sum_{j=1}^{K} |\Omega_{ij}|^2 + N_o}, \tag{5.10}$$

where $\boldsymbol{\Omega} = \boldsymbol{Q}^H \Delta \boldsymbol{H}_p \hat{\boldsymbol{\Pi}}$, $\lambda = E[\boldsymbol{x}^H \boldsymbol{x}]/K$, and $E[\tilde{\boldsymbol{n}}^H \tilde{\boldsymbol{n}}] = E[\boldsymbol{n}^H \boldsymbol{Q} \boldsymbol{Q}^H \boldsymbol{n}] = E[\boldsymbol{n}^H \boldsymbol{n}] = N_o$. Now, using this SNR in (5.4) - (5.6), one can evaluate the instantaneous transmission efficiency for the imperfect CSI case.

Algorithm 5 summarizes this antenna selection algorithm. For the cross-layer antenna selection algorithm, cognitive source nodes select the antenna combination that provides maximum transmission efficiency at the LLC sub-layer for a given interference threshold at the primary user, that is

$$H_p = \arg \max_{H_p} \eta_i(\boldsymbol{H}_p, \rho), \quad s.t. \ I_{total} \leq I_{th}. \tag{5.11}$$

72

Algorithm 5 Cross-layer Antenna Selection Algorithm

1: Packet Transmission Initiation.
2: Measure I_{total} using primary users' pilot signals.
3: Use step 1 measurement results to calculate the maximum number of usable antennas during DIFS period of the IEEE 802.11 standard.
4: Send RTS signal using antennas identified in step 2.
5: Calculate H_p at the receiver side using (5.11).
6: Add the sub-matrix p with the CTS signal of the receiver.
7: Transmit CTS.
8: Use the sub-matrix p to divide and transmit data.
9: End of packet transmission.

Note that for the optimization criteria we consider the transmission efficiency over throughput, as it clearly indicates the sources of inefficiency while it can also be used to evaluate the achievable throughput of the network.

5.2.4 Analysis

The transmission efficiency for interference limited cognitive communication can be determined, using the probability of channel availability P_a ((3.4), Chapter 3) as,

$$\eta_i(\boldsymbol{H}_p, \rho) = P_a \frac{1 - PER(\boldsymbol{H}_p)}{1 + (W-1)PER(\boldsymbol{H}_p)}. \tag{5.12}$$

It is worth noting that (5.12) represents the transmission efficiency without antenna selection. To determine the transmission efficiency for the cross-layer antenna selection case, we develop a 2 dimensional matrix z containing probability of channel availability in the first column and corresponding transmission efficiency in the second column for a certain 'cognitive-to-cognitive' channel. After this step, we sort the efficiency matrix z according to descending order of efficiency. If the length of the sorted matrix is L,

theoretical transmission efficiency is given by,

$$\eta_{max}(\rho) = P_a(j)\eta_i(\boldsymbol{H}_j, \rho) + (1 - P_a(j))P_a(j+1)\eta_i(\boldsymbol{H}_{j+1}, \rho)$$

$$+ (1 - P_a(j))(1 - P_a(j+1))P_a(j+2)\eta_i(\boldsymbol{H}_{j+2}, \rho).......... \qquad (5.13)$$

where $P_a(j)$ represents the probability of channel availability for antenna combinations corresponding to index $j = 1, 2, ..., L$.

5.2.5 Complexity analysis

Each iteration of the antenna selection algorithm through exhaustive search method has complexity $O(2^{N_t})$. This time complexity is a result of the exhaustive search of the antenna selection algorithm where it runs over all combination of $\{\binom{N_t}{K}, \ for \ K = 1, 2...N_t\}$ that results in time complexity $O(2^{N_t})$. On the other hand, the antenna selection algorithm has to store $O(2^{N_t})$ elements, resulting in memory space complexity $O(2^{N_t})$.

5.2.6 Performance evaluation

In this section, we evaluate the performance of the above mentioned algorithm. For this purpose, we build an IEEE 802.11 [59] compliable ad-hoc network. All nodes are equipped with four antennas (4×4 MIMO). The ad-hoc network contains 40 cognitive source-destination pairs. We consider cognitive nodes with perfect CSI. We also assume nodes use primary users pilot symbols [10] or blind channel estimation methods [80] to estimate the CSI of 'primary-to-cognitive' channels. At this point, we consider nodes experience flat fading in all frequency channels and choose the elements of 'Cognitive-to-Cognitive' channel matrix $\mathbf{H}_p$ to be zero mean and unit variance independent and identically distributed (i.i.d.) circularly symmetric Gaussian random variables. In the system model, cognitive and primary users use side by side bands, resulting in spill over energy among adjacent frequency bands. To model this spill over energy, we consider the

Table 5.1: Simulation setting

Parameter	Value
ARQ protocol	GBN
ARQ window size	4 Packets
No. of transmit antennas	4
No. of receive antennas	4

elements of 'Cognitive-to-Primary' channel matrix $\mathbf{G}$, as zero mean and 10^{-3} variance complex Gaussian variables [22]. The remaining simulation parameters are listed in Table 5.1. We use these parameters to build a simulation program for the cognitive network introduced in subsection 5.2.1.

First we present the performance results for the antenna selection algorithm. For performance comparison purposes, we consider three cases, viz., Without Antenna Selection (WAS), Maximum Antenna Selection (MAS) and Cross-Layer Antenna Selection (CLAS). In the WAS strategy, cognitive nodes transmit using all the available antennas, provided that the interference imposed by primary users is below the prespecified threshold. If the interference constraint is not satisfied, cognitive users turn off all their antennas. On the contrary, cognitive users in the MAS algorithm use physical layer measurements to determine the maximum possible usable antennas given the interference threshold on the primary user is satisfied. In our CLAS algorithm, nodes select the antennas that maximize the LLC transmission efficiency defined by (5.11).

We plot the transmission efficiency results and percentage of antenna usage in Figs. 5.2 and 5.3, respectively. Fig. 5.2 also contains theoretical transmission efficiency results for WAS and CLAS algorithms obtained using (5.12) and (5.13), respectively. At relatively low SNRs ([0-12] dB), the CLAS algorithm offers the largest transmission efficiency where both MAS and WAS have lower but similar transmission efficiency. This is due to the fact that, at low SNRs, the channel between cognitive users has more dominant effect on the BER performance than the imposed interference threshold at the primary user. In the CLAS algorithm, since the performance of the wireless links differ widely at low SNRs,

75

Figure 5.2: Transmission efficiency for cognitive nodes with different antenna selection algorithms, primary user interference constraint ≤ -10 dBm.
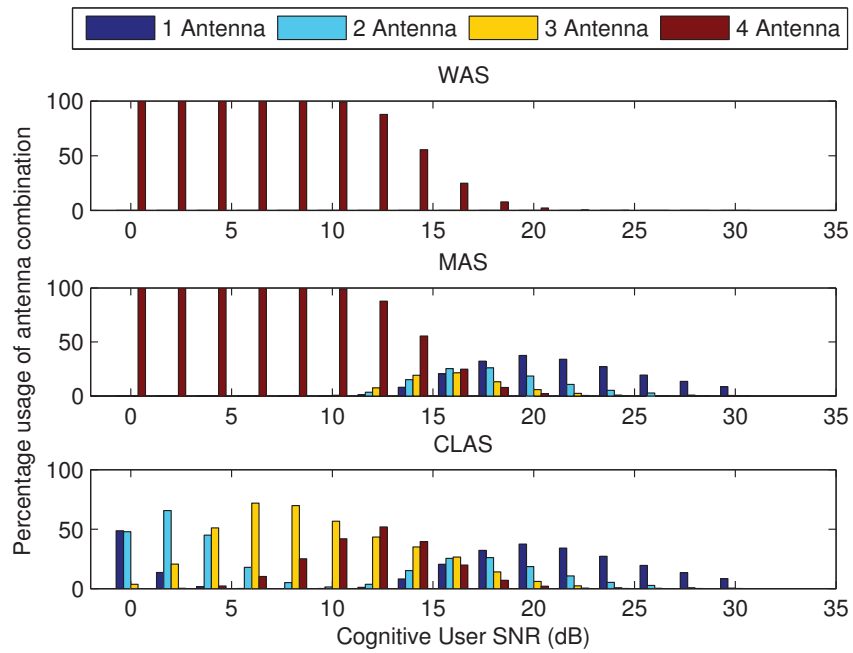
Figure 5.3: Percentage of antenna usage for primary user interference constraint ≤ -10 dBm.

the antenna selection algorithm shows significant transmission efficiency gains. On the other hand, as MAS and WAS algorithms do not consider channel reliability for antenna selection, data packets need to be retransmitted until it is successfully received. This argument ties well with the percentage of antenna usage results in Fig. 5.3. As seen, one antenna usage is dominant at very low SNRs ([0-3] dB) while multiple antennas (2 and 3 antennas) combination usage becomes dominant at moderate SNRs ([3-12] dB) for the CLAS. On the contrary, at low SNRs, both WAS and MAS select four antenna combination most of the time.

At high SNRs ([12-30] dB), the results in Fig. 5.2 indicate that the transmission efficiency of the MAS algorithm improves and converges with the CLAS. Also, all three algorithms reach a maximum value after which, the performance is controlled by the more dominant interference threshold where any increase in SNR results in lower transmission efficiency. This agrees with the results in Fig. 5.3 where one can notice that when the SNR increases, nodes increasingly become unable to use more antennas due to the interference constraint. It is also noticed that both CLAS and MAS perform equally, as the channel has less effect at high SNRs.

We plot the achievable transmission efficiency curves in Fig. 5.4 as a function of the primary users' interference threshold, where the transmit power is set to 12 dB. At low values of interference thresholds ([-40 to -20] dBm), the number of usable/selected antennas is very small to limit the effect of interference on primary users. As a result, the CLAS algorithm has fewer choices for antenna selection and hence similar transmission efficiency for both CLAS and MAS algorithms. For the same reasons, the performance of the WAS is very poor in this case. At high interference thresholds, the CLAS has higher degrees of freedom to leverage large transmission efficiency gains.

At this point, we evaluate the effect of CSI and error propagation among sub-streams of the zero forcing algorithm on the system throughput. First, we present results for imperfect CSI. To generate the error matrix for channel estimation, we select an
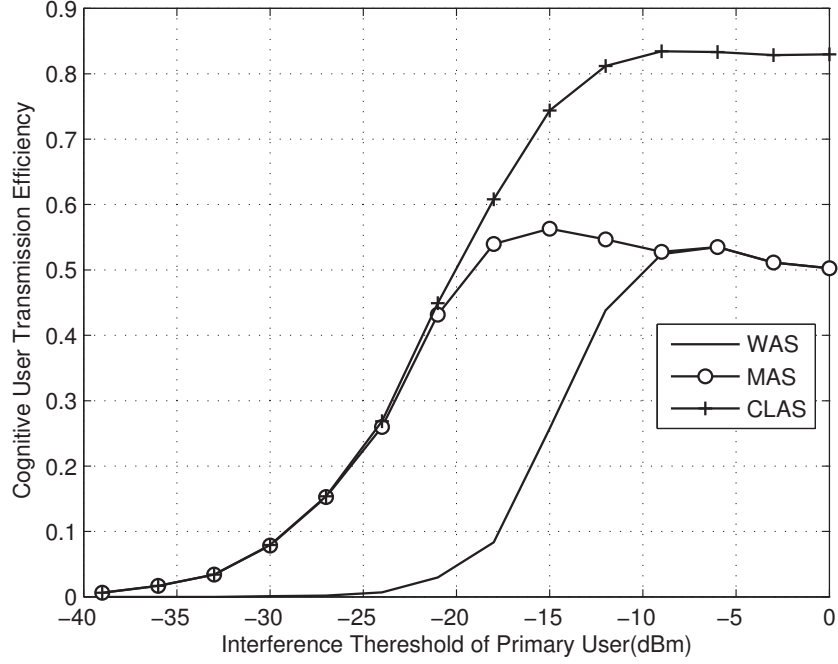
Figure 5.4: Achievable cognitive user transmission efficiency for different interference constraints and 12 dB cognitive user transmit power.

orthogonal pilot sequence from a constant energy constellation across all the transmit antennas [11]. For instance, training sequence $\boldsymbol{x_p}$ for BPSK modulation of training length $N_p = 4$, and for 4 transmit antennas can be written as,

$$\boldsymbol{x_p} = \frac{1}{\sqrt{4}} \begin{bmatrix} 1 & 1 & 1 & 1 \\ -1 & 1 & -1 & 1 \\ -1 & 1 & 1 & -1 \\ -1 & -1 & 1 & 1 \end{bmatrix} \tag{5.14}$$

For Maximum Likelihood (ML) channel estimation, error matrix $\Delta \boldsymbol{H}_p$ is given [11] by,

$$\Delta \boldsymbol{H}_p = \frac{N_t}{N_p \sqrt{\rho}} \boldsymbol{x}_p^H N_o \tag{5.15}$$

The throughput curves in Fig. 5.5, reveal that some performance degradation occurs due
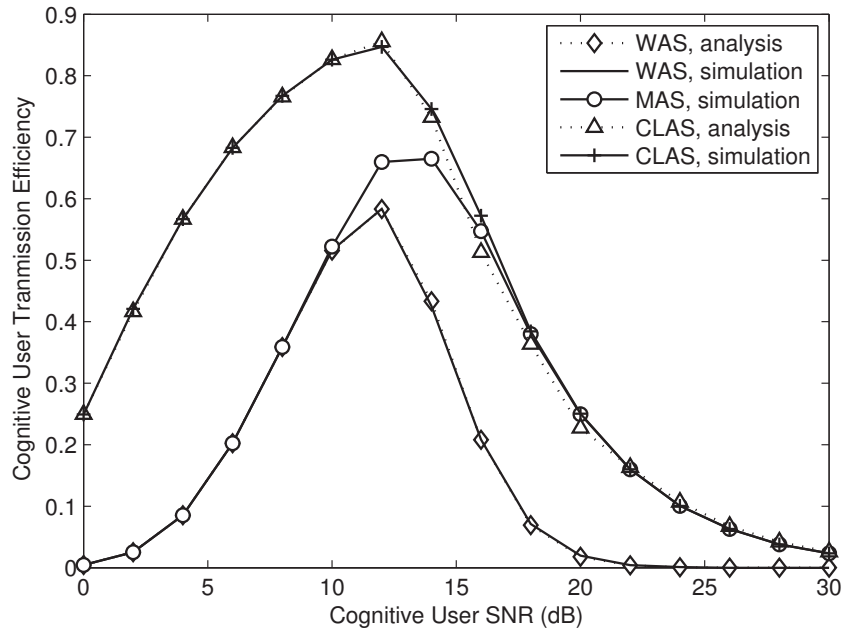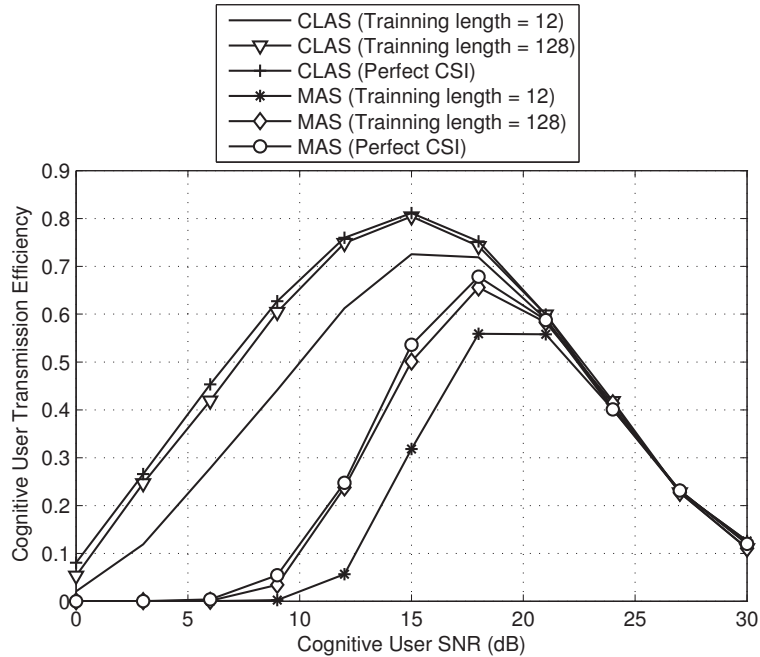
Figure 5.5: Transmission efficiency for cognitive nodes with different antenna selection algorithms, primary user interference constraint $\leq$ -10 dBm at imperfect CSI .

to imperfect CSI. With the increase of number of training symbols, the performance of the proposed algorithm shows results close to the perfect CSI case. Another important remark is that, in all cases, the proposed cross-layer design is shown to outperform other conventional schemes.

To evaluate the effect of error propagation of the spatially-layered system on the throughput performance, we consider the error propagation model and analytical results presented in [81] and [82]. The corresponding throughput results are shown in Fig. 5.6. Similar to the imperfect CSI case, one can notice that all systems are equally affected by the error propagation in the detected layers. In all systems, we have noticed throughput degradation relative to the ideal case of no error propagation. However, as can be seen, the proposed CLAS still outperforms both the MAS and the case of no antenna selection.
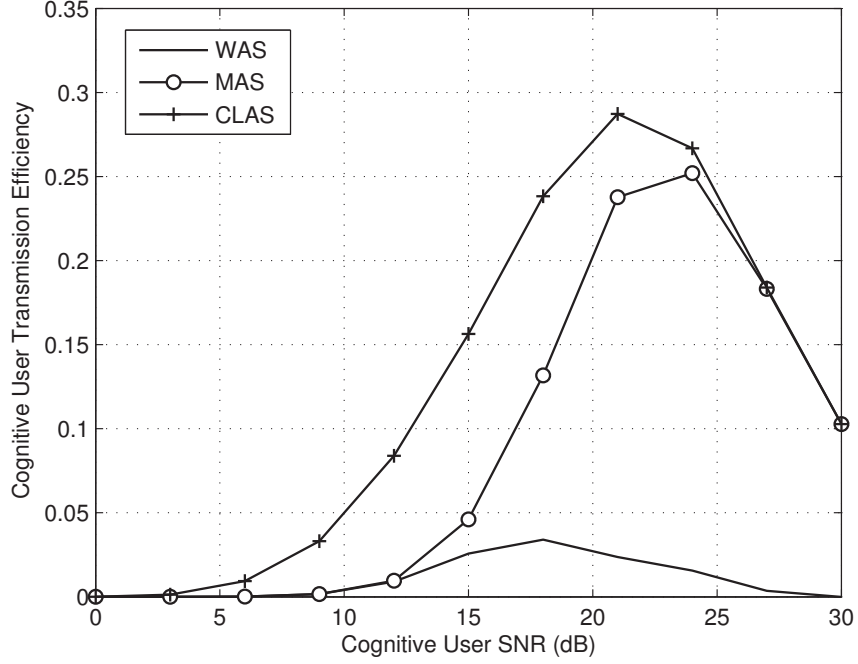
Figure 5.6: Transmission efficiency for cognitive nodes with different antenna selection algorithms, primary user interference constraint $\leq$ -10 dBm for error propagation between sub-streams.

5.3 Cross-Layer Antenna Selection and Beamforming

In this section, we apply the antenna selection approach presented above to propose a cross-layer based MIMO transmit antenna selection and beamforming algorithm to achieve large throughput gains by allowing concurrent communications of primary and cognitive users.

We consider a scenario similar to [75], where cognitive users opportunistically use the wireless resources of a licensed primary user. In addition, we assume cognitive nodes use GBN protocol for the LLC sub-layers. At the physical layer, cognitive nodes use data demultiplexer to divide the incoming data into M parallel streams (Fig. 5.7). These data streams (layers) are fed to M RF chains. Assuming that CSI is available at the transmitter through a feedback channel, cognitive nodes perform antenna selection and precoding. For the antenna selection, cognitive nodes search for M antennas from N_t available trans-
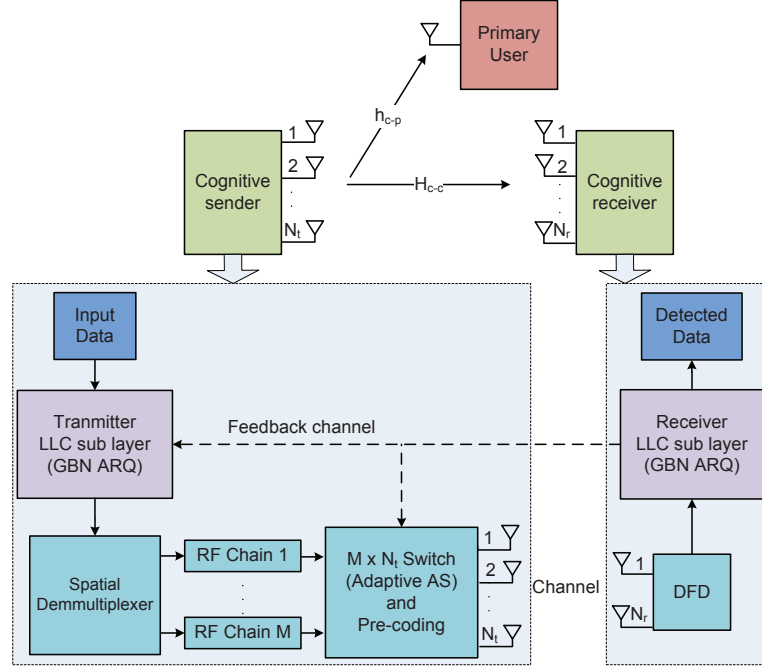
Figure 5.7: Communication system model for cross-layer antenna selection and beamforming algorithm.

mit antennas for maximum LLC layer throughput. That is given an antenna set P, the optimal subset $p \in P$ of size $M \leq N_t$ is selected for maximum throughput. Having selected the optimal antennas, in the precoding stage, cognitive nodes use the CSI of 'cognitive-to-primary' link to determine the beamforming vector. That is, the proposed cross-layer antenna selection and beamforming (CLBF) algorithm works as precoded symbols are transmitted using the selected antennas. On the other hand, cognitive receivers are equipped with $N_r(N_t \leq N_r)$ receive antennas, and DFD to extract the transmitted data streams.

5.3.1 Performance analysis for perfect channel estimation

In this subsection, we consider perfect CSI is available at the cognitive receiver. Thus for the above mentioned system, cognitive nodes determine a zero forcing beamforming precoding matrix $\mathbf{A} \in C^{M \times M}$, such that the primary user experiences zero interference

due to 'Cognitive-to-Cognitive' communication, i.e.,

$$\boldsymbol{G}_i\mathbf{A} = 0 \;\; s.t. \|\mathbf{A}\|_2 = 1. \tag{5.16}$$

Using (5.16) and introducing $\boldsymbol{x}_c = \boldsymbol{A}\boldsymbol{x}$, from (3.2) and (5.1) we obtain,

$$\boldsymbol{y}_c = \boldsymbol{H_p}\boldsymbol{x}_c + \boldsymbol{n} = \boldsymbol{H_p}\boldsymbol{A}\boldsymbol{x} + \boldsymbol{n}, \tag{5.17}$$

$$y_{pl}^i = \boldsymbol{G}_i\boldsymbol{x}_c = \boldsymbol{G}_i\boldsymbol{A}\boldsymbol{x} = 0,$$
$$I = {y_{pl}^i}^H y_{pl}^i = 0. \tag{5.18}$$

By introducing $\boldsymbol{H_p}\boldsymbol{A} = \widetilde{\boldsymbol{H}}$, (5.17) can be transformed as,

$$\boldsymbol{y}_c = \widetilde{\boldsymbol{H}}\boldsymbol{x} + \boldsymbol{n}. \tag{5.19}$$

The received SNR, ρ, for the selected antenna combinations can be written as [75],

$$\rho = \frac{\psi}{\lambda}, \tag{5.20}$$

where $\psi = d_{11}\sigma$, λ denotes the first element of the covariance of the noise $\mathbf{n}$, σ is the cognitive transmit power, and d_{11} is the non-trivial diagonal element of the matrix $\mathbf{D}$ with $\mathbf{D}$ being calculated using singular value decomposition as, $\widetilde{\boldsymbol{H}} = \boldsymbol{U}\boldsymbol{D}\boldsymbol{V}^H$ (where $\mathbf{U}$ and $\mathbf{V}$ are unitary matrices).

If BPSK modulation is considered, the BER of the jth data stream for selected antenna combinations can be written as,

$$BER_j = Q(\sqrt{2\rho}). \tag{5.21}$$

Since each L-bit data packet is divided into M parallel streams before transmission, packet

Algorithm 6 Cross-Layer Antenna Selection and Beamforming
_____
1: Session Initiation
2: Determine $\mathbf{G}_i$ using primary users' pilot signals.
3: Measure I_{total} using $\mathbf{G}_i$.
4: Determine H_p using (5.23).
5: Use step 2 measurement to determine the matrix A.
6: Determine the beamforming symbol vector $\mathbf{x}_c = A\mathbf{x}$
7: Transmit $\mathbf{x}_c$.
8: End of session
_____

error rate is given by

$$PER(\boldsymbol{H}_p, \rho) = 1 - \left[\prod_{j=1}^{M} (1 - SER_j) \right]^{L/M}. \qquad (5.22)$$

Using the obtained PER, the transmission efficiency (i.e., normalized throughput) for GBN protocol with window size W can be written as (5.6).

Finally, the cross-layer based antenna selection and beamforming algorithm works as cognitive source node first selects the antenna combination to achieve maximum throughput at the LLC sub-layer, then precoding is applied to the transmitted symbols for zero forcing the interference at the primary user, as presented in (5.23). Algorithm 6 summarizes this procedure.

$$H_p = \arg\max_{H_p} \eta(\boldsymbol{H}_p, \rho) \qquad (5.23)$$

5.3.2   Performance analysis for delayed and imperfect CSI

Here we derive an expression for the instantaneous transmission efficiency for imperfect CSI. In the following analysis, we have considered two cases, (a) delayed CSI and (b) erroneous or imperfect CSI. First, we present the case of delayed CSI. Given the channel $\boldsymbol{H_p}$, we denote the delayed channel estimate at the receiver by $\hat{\boldsymbol{H}}_{\boldsymbol{p}}$. For this purpose, we use the channel estimation analysis presented in [45] to relate the delayed CSI and the

actual CSI at the cognitive receiver by,

$$\hat{\boldsymbol{H}}_{\boldsymbol{p}} = \beta \boldsymbol{H}_{\boldsymbol{p}} + \sqrt{1 - \beta^2} \boldsymbol{Z}. \tag{5.24}$$

where $\beta = J_o(2\pi f_d T \Delta)$, $J_o(.)$ represents zero-order Bessel function, f_d is the Doppler frequency, T is frame duration, Δ is the feedback delay in frames, and the elements of $\boldsymbol{Z} \in C^{N_r \times M}$ represent zero-mean unit-variance Gaussian random variables. Hence, one can rewrite the received signal vector at the cognitive user in (5.17) as,

$$\boldsymbol{y}_c = \boldsymbol{H}_{\boldsymbol{p}} \boldsymbol{x}_{\boldsymbol{c}} + \boldsymbol{n} = \left[\frac{1}{\beta} \hat{\boldsymbol{H}} - \frac{\sqrt{1 - \beta^2}}{\beta} \boldsymbol{Z} \right] \boldsymbol{x}_{\boldsymbol{c}} + \boldsymbol{n}. \tag{5.25}$$

Using the singular-value-decomposition of $\hat{\boldsymbol{H}} = \boldsymbol{U} \hat{\boldsymbol{D}} \boldsymbol{V}^H$, (5.25) can be written as,

$$
\begin{aligned}
\widetilde{\boldsymbol{y}}_c &= \tfrac{1}{\beta} \hat{\boldsymbol{D}} \boldsymbol{V}^H \boldsymbol{x}_{\boldsymbol{c}} - \tfrac{\sqrt{1-\beta^2}}{\beta} \boldsymbol{U}^H \boldsymbol{Z} \boldsymbol{x}_{\boldsymbol{c}} + \boldsymbol{U}^H \boldsymbol{n} \\
&= \tfrac{1}{\beta} \hat{\boldsymbol{D}} \hat{\boldsymbol{x}}_{\boldsymbol{c}} - \tfrac{\sqrt{1-\beta^2}}{\beta} \boldsymbol{\Omega} \boldsymbol{x}_{\boldsymbol{c}} + \widetilde{\boldsymbol{n}},
\end{aligned}
\tag{5.26}
$$

where $\boldsymbol{\Omega} = \boldsymbol{U}^H \boldsymbol{Z}$. Since $E[\hat{\boldsymbol{x}}_{\boldsymbol{c}}^H \hat{\boldsymbol{x}}_{\boldsymbol{c}}] = E[\boldsymbol{x}_{\boldsymbol{c}}^H \boldsymbol{V} \boldsymbol{V}^H \boldsymbol{x}_{\boldsymbol{c}}] = E[\boldsymbol{x}_{\boldsymbol{c}}^H \boldsymbol{x}_{\boldsymbol{c}}] = E[\boldsymbol{x}^H \boldsymbol{A}^H \boldsymbol{A} \boldsymbol{x}] = \sigma$ and $E[\widetilde{\boldsymbol{n}}^H \widetilde{\boldsymbol{n}}] = E[\boldsymbol{n}^H \boldsymbol{U} \boldsymbol{U}^H \boldsymbol{n}] = E[\boldsymbol{n}^H \boldsymbol{n}] = N_o$, the received SNR can defined as,

$$\rho = \frac{\frac{1}{\beta^2} d_{11}^2 \sigma}{\sigma \frac{1-\beta^2}{\beta^2} \sum_{j=1}^{2} |\Omega_{1j}|^2 + N_o}. \tag{5.27}$$

Similar to the perfect CSI case and considering BPSK modulation, using (5.6), (5.21), (5.22), and (5.27), the instantaneous transmission efficiency is given by,

$$\eta(\boldsymbol{H}_p, \rho) = \frac{\left[1 - Q(\sqrt{2\rho})\right]^{L/M}}{1 + (W - 1) \left(1 - \left[1 - Q(\sqrt{2\rho})\right]^{L/M}\right)}. \tag{5.28}$$

Now, we investigate the effect of imperfect CSI. For this purpose, we assume a time frame consisting of L_t training or pilot symbols and L_d data symbols. Radio devices can

estimate the channel $\boldsymbol{H_p}$ using a priori knowledge of these training symbols in maximum-likelihood estimation method to yield,

$$\hat{\boldsymbol{H}} = \boldsymbol{H_p} + \Delta\boldsymbol{H_p}, \tag{5.29}$$

where $\Delta\boldsymbol{H_p}$ represents the error matrix for channel estimation. Given the channel estimation technique, one can evaluate the received SNR as,

$$\rho = \frac{d_{11}^2 \sigma}{\sigma \sum_{j=1}^{2} |\Omega_{1j}|^2 + N_o}, \tag{5.30}$$

where $\Omega = U^H \Delta\boldsymbol{H_p}$, and d_{11} is the non-trivial diagonal element of the matrix $\mathbf{D}$ with $\mathbf{D}$ being calculated using singular-value-decomposition, $\hat{\boldsymbol{H}}_{\boldsymbol{p}} = \boldsymbol{UDV^H}$. Using the SNR, one can evaluate the instantaneous transmission efficiency for imperfect channel estimation.

Recall that, the cross-layer based antenna-selection and beamforming algorithm first selects the antenna combination to achieve maximum throughput at the LLC sub-layer. Then precoding is applied to the transmitted symbols for zero-forcing the interference at the primary user, as presented in (5.31)

$$H_p = \arg\max_{H_p} \eta(\boldsymbol{H}_p, \rho). \tag{5.31}$$

It is important to mention that in the cross-layer antenna selection algorithm, antenna combination is selected from the available antennas that achieve maximum transmission efficiency at the LLC sub-layer. For this purpose, a search process considers all possible antenna combinations. Conversely, in the cross-layer antenna selection and beamforming, the search process considers only the combinations that can be applied to beamform the transmitted symbols. That is beamforming is employed here to cancel interference between cognitive and primary users.

5.3.3 Complexity analysis

In is worth noting that the complexity of the proposed algorithm grows with the number of transmit antennas. We calculate the complexity of the algorithm by the required number of floating point addition and multiplication operations. One can notice that, determining the beamforming matrix [75] requires only six addition and multiplication operations, and the antenna search algorithm requires $\binom{N_t}{M}$ operations for the combined algorithm. Thus, the total complexity of the cross-layer antenna selection and beamforming algorithm is equivalent to $O(\binom{N_t}{M} 6)$.

5.3.4 Performance evaluation

We carry out numerical analysis for performance evaluation of the above mentioned algorithm. For this purpose, we consider cognitive users operate in the adjacent frequency band of the primary user. We assume cognitive nodes have perfect channel state information (CSI) of 'Cognitive-to-Cognitive' and 'primary-to-cognitive' links. We also assume, channel remains static for the entire period of a packet transmission and change independently form one packet to another. This let us choose the elements of 'Cognitive-to-Cognitive' channel matrix $\mathbf{H}$ as Rayleigh variable with zero mean and unit variance. However, to model the elements of the 'Cognitive-to-Primary' channel matrix we choose Rayleigh variable with zero mean and 10^{-3} variance. Although, we do not consider the 'Primary-to-Cognitive' channel for the sake of simplicity, our study can be easily extended to this case. Other simulation parameters are listed in Table 5.2.

We plot the normalized throughput curves in Fig. 5.8 where we consider five scenarios, (a) no antenna selection, (b) Beamforming in a 2×2 MIMO system (BF), (c) cross-layer antenna selection (CLAS), (d) proposed CLBF in 2×2 system (M=2 antennas selected from $N_t = 4$ antennas), and (e) proposed CLBF in 2×2 system (M=2 antennas selected from $N_t = 6$). The performance of these algorithms are evaluated under the condition that cognitive communication limited by the primary user interference constraint

Table 5.2: Simulation settings

Parameter	Value
Packet Payload	1024 bytes
Frame duration	2 ms
ARQ protocol	GBN
ARQ window size	4 Packets
PER threshold	10^{-6}
No. of RF chain, M	2

Figure 5.8: Throughput performance of cognitive users with a primary user interference constraint $\leq$ -20 dBm and ARQ window size = 4.

$\leq$ -20 dBm. For the no antenna selection case, cognitive nodes are able to communicate, if the resultant primary user interference is lower than the specified interference threshold. In CLBF, cognitive nodes first select the antenna combinations for maximum LLC layer normalized throughput, then apply beamforming over the selected antennas.

Fig. 5.8 indicates that the CLBF algorithm outperforms CLAS, BF and no antenna selection algorithms. As one can see , the use of antenna selection combined with beam-forming offers larger throughput gains as the number of available antennas increases. The

extra throughput gain achieved is due to the ability of the proposed algorithm to remedy the interference effects at the primary users while maximizing the throughput of the cognitive network. Different from the CLBF and BF algorithms, the performance with CLAS and no antenna selection is shown to deteriorate as the SNR goes high due to the interference constraint set at the primary user.

In Fig. 5.9, we examine the effect of delayed CSI on the throughput performance. Our simulation results reveals that performance degradation occurs due to delayed CSI where degradation is more evident in the BF case than the CLBF case. Also as seen, in all cases, the proposed cross-layer design is shown to outperform the beamforming scheme.

In Fig. 5.10 we examine the effect of imperfect channel-state information on the transmission efficiency. Similar to the delayed CSI case, imperfect CSI causes small degradation in the transmission efficiency using small number of training symbols. Furthermore,

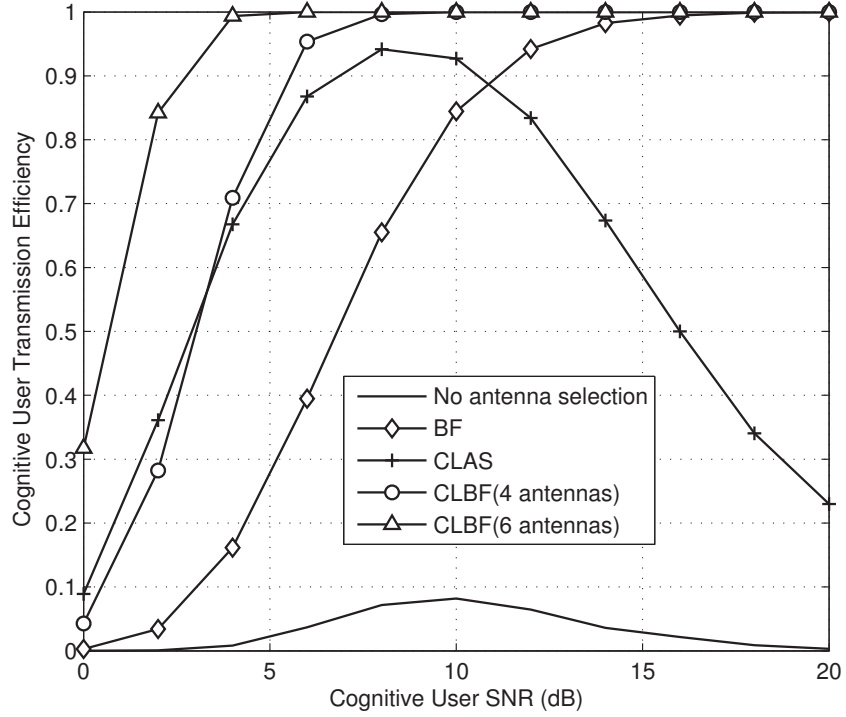Figure 5.9: Effect of channel estimation delay on the throughput performance of cognitive users with primary user interference constraint $\leq$ -20 dBm and ARQ window size = 4.
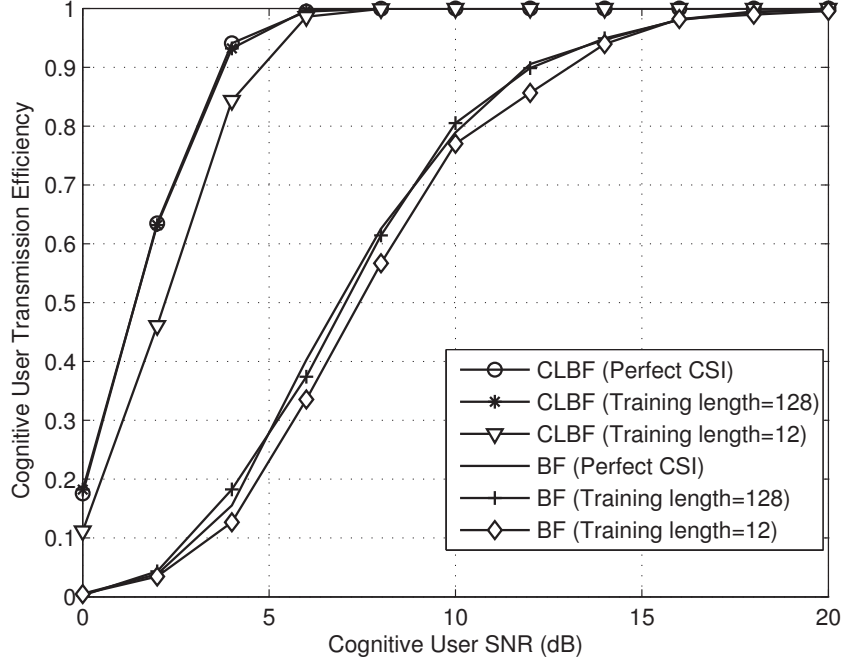
Figure 5.10: Effect of imperfect channel estimation errors on the throughput performance of cognitive users with primary user interference constraint $\leq$ -20 dBm and ARQ window size = 4.

in all cases, the proposed cross-layer design is shown to outperform the beamforming scheme.

To further explore the effect of number of antenna combination, we examine the throughput performance as a function of available antennas N_t. The results are shown in Fig 5.11 where we compare the performance of the cross-layer antenna selection (CLAS) without beamforming with the proposed CLBF. Note that the CLAS, similar to the no antenna selection case, is limited by the interference threshold at the primary user. As shown, one can leverage large throughput gains by increasing the number of available antennas in the CLBF algorithm. On the contrary, the CLAS achievable throughput is limited by the primary user interference constraint.

In Fig. 5.12, we plot the achievable efficiency curves of cognitive users as a function of the interference constraint at the primary user for a cognitive SNR = 8 dB. The results reveal the differences between three scenarios; no antenna selection, BF, and proposed
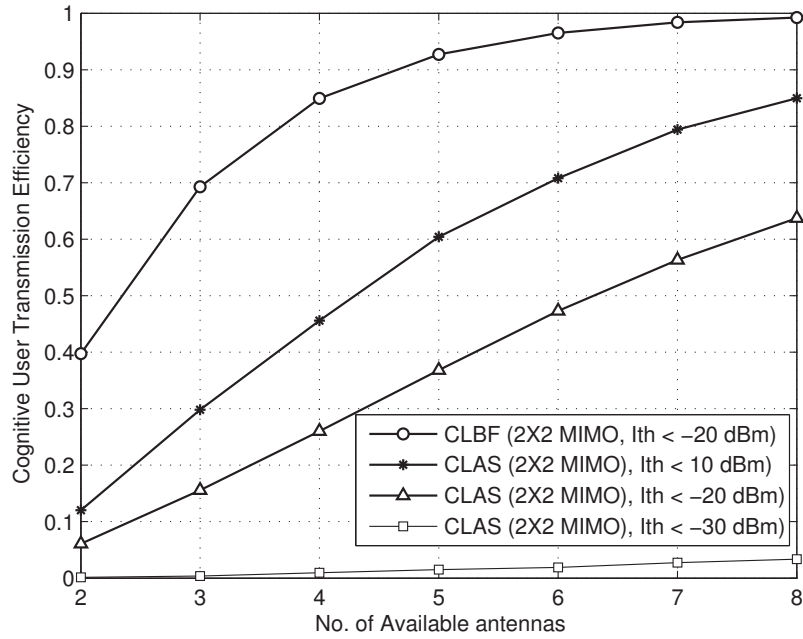
Figure 5.11: Throughput as a function of number of antenna combinations for a 2×2 MIMO system at SNR=8 dB and ARQ window size = 4.
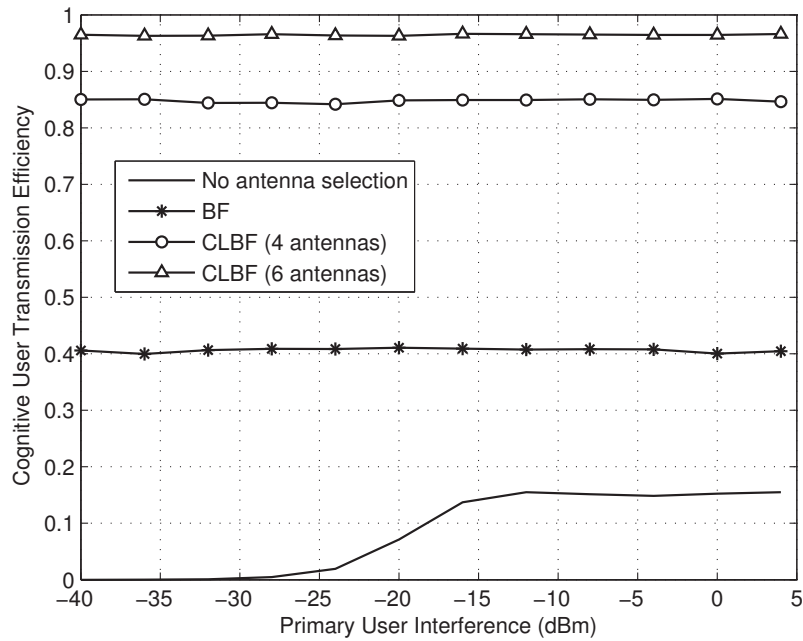
Figure 5.12: Effect of primary user interference threshold for cognitive user SNR=8 dB and ARQ window size = 4.

CLBF where the CLBF and BF are shown to be interference resistant with the former offering larger throughput gain.

We have simulated the system to investigate the effect of window size. The results are shown in Fig. 5.13. We simulate the system for three window sizes, $w = 4$, $w = 16$ and $w = 64$. From (5.6), one can notice that the transmission efficiency is inversely proportional to the window size. This phenomenon is also revealed in the simulation results. In the figure, simulation results indicate that, for low SNRs the efficiency decreases with the increase in window size. Conversely at high SNRs as the packet-error rate becomes zero, the widow size has no effect on the efficiency.

5.4 Combined Antenna/Channel Selection

We use the transmission efficiency results of the previous subsections to determine the achievable data rate for cognitive nodes. To determine the achievable data rate, we

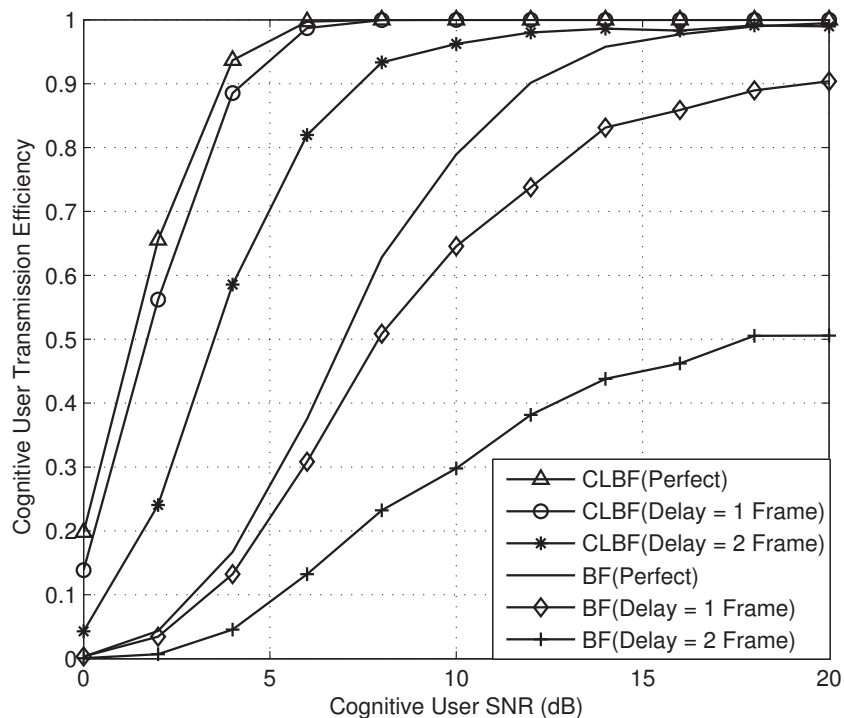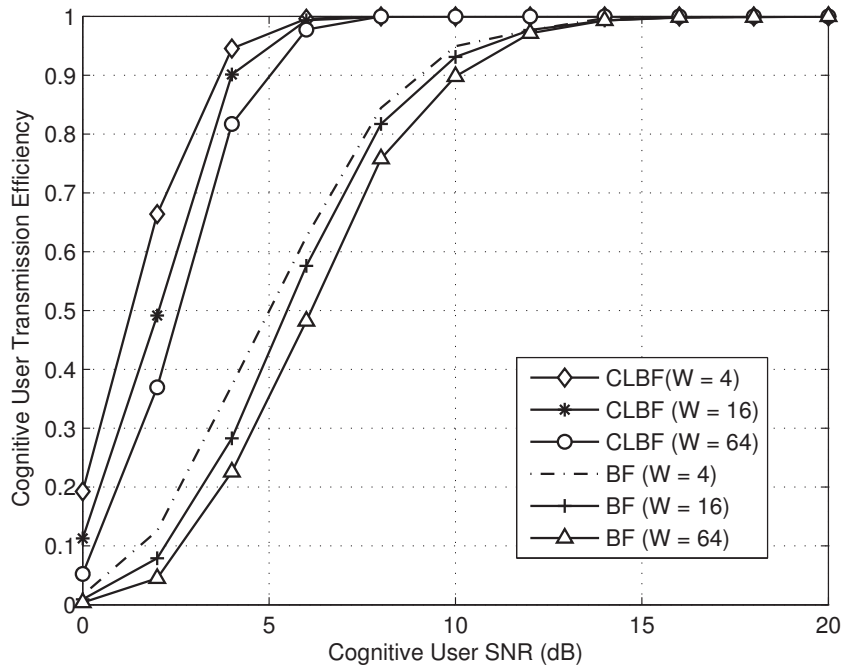Figure 5.13: Effect of the window size on the throughput performance of cognitive users at a primary user interference constraint $\leq$ -20 dBm.

first determine the LLC layer transmission efficiency $\eta_i(\boldsymbol{H}_p, \rho)$. Then, we multiply the transmission efficiency by the bit rate KR_{tr}. Note that R_{tr} is the bit rate per transmit antenna and K is the number of applied transmit antennas. We express the achievable data rate, χ_i, at the LLC sub layer of any cognitive node $i \in M$ as

$$\chi_i = KR_{tr}\eta_i(\boldsymbol{H}_p, \rho). \tag{5.32}$$

From (5.3)-(5.5), we notice that, in order to maximize the transmission efficiency, the SNR needs to be increased. However, the interference at the primary users also increases with the increase in SNR. For this reason, we express the average data rate of cognitive nodes (limited by the interference threshold I_{th} of primary users) as

$$f(\rho) = \frac{\sum\limits_{i=1}^{M} \chi_i}{M} \qquad s.t. \ I_{total} \leq I_{th}. \tag{5.33}$$

Nodes in a MBMMCAN may deploy antenna selection along with channel selection scheme for throughput improvement. For the combined cross layer antenna/channel selection scheme, nodes apply the algorithms in steps. During the session initiation period, nodes transmit using antenna selection algorithm in a randomly selected channel and record channel performance parameters. Over the course of time, nodes switch the operating channel to learn about all available channels. In particular, nodes apply the learning algorithm to calculate the channel switching probability in (4.3), (4.7) or (4.6). Given this, nodes apply the antenna selection algorithm for the chosen frequency slot (channel). When a session ends, nodes erase all learned data and repeat the whole process for the next session.

5.4.1 Results

From the previous results, it becomes clear that combining the cross-layer antenna selection with the learning-based channel selection can further improve the transmission efficiency of the cognitive network. To demonstrate this, we employ the combined channel and antenna selection algorithm in the multi-band multiuser MIMO cognitive ad-hoc network. We apply four different combinations of strategies for performance evaluation, namely, (1) learning-based channel allocation and CLAS, (2) random channel allocation and CLAS, (3) learning-based channel allocation and WAS, and (4) random channel allocation and WAS. The reported average data rate results in Fig. 5.14 show that the CLAS algorithm along with learning-based channel selection policy achieves the highest average network data rate. This is simply due to the fact that in learning-based algorithm, nodes have less channel switching events (i.e., less overhead) and hence better throughput.
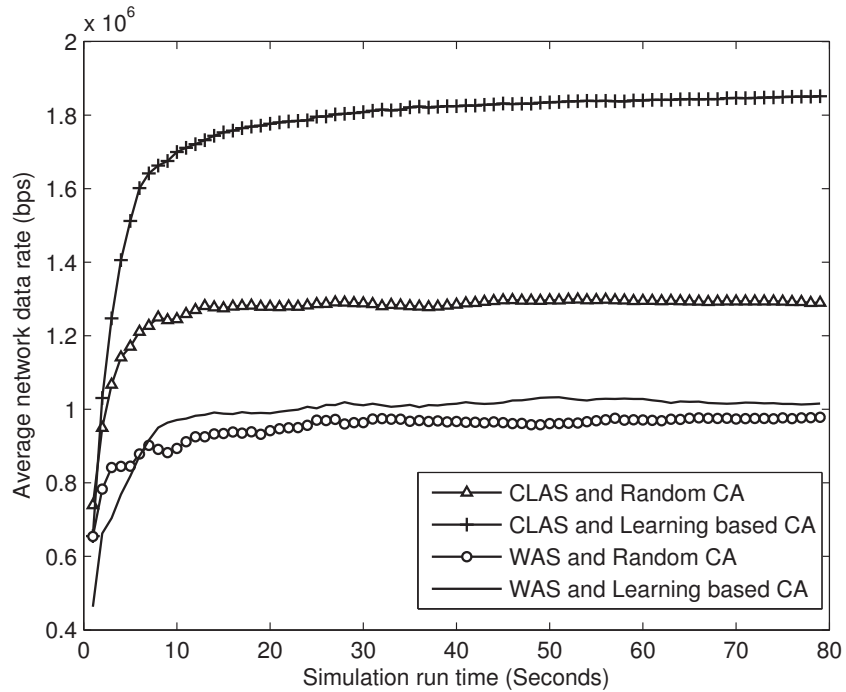
Figure 5.14: Average data rate of the cognitive nodes for different antenna selection algorithms at 12 dB transmit power and interference threshold $\leq$ -10dBm with unequal frequency slots.

93

Apart from the equal interference case presented before, we also study the effect of random interference on the network performance. To generate these results we consider σ in (3.2) to be uniformly distributed over the range 0 to 12 dB. Given this, we apply the combined channel and antenna selection algorithm in the multi-band multiuser MIMO cognitive ad-hoc network. For performance comparison, we consider the four combinations of antenna selection and channel selection algorithms introduced in Fig. 5.14. As seen from Fig. 5.15, the reported average data rate results for the random interference case show that the CLAS algorithm along with learning-based channel selection policy achieves the highest average network data rate. This is simply due to the fact that in learning-based algorithm, nodes have less channel switching events (i.e., less overhead) and hence better throughput. However, it is worthwhile to notice that the performance comparison of the antenna selection and the channel selection algorithms show similar trend for both equal (Fig. 5.14) and random interference (Fig. 5.15) cases.
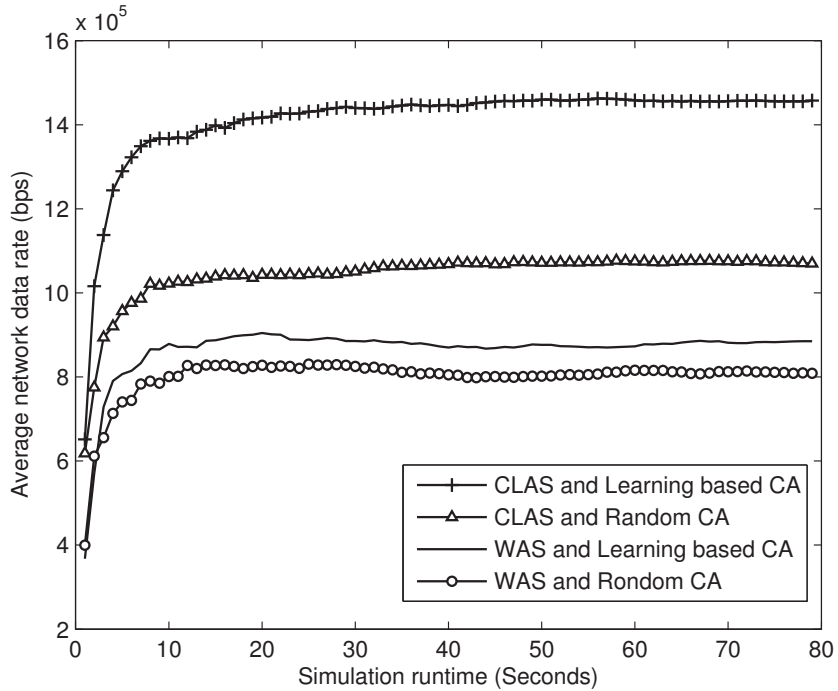
Figure 5.15: Average data rate of the cognitive nodes for different antenna selection and channel selection algorithms for interference threshold $\leq$ -20dBm with unequal frequency slots and random interference at primary users.

94

5.5   Conclusions

We investigated the performance of a cross-layer antenna selection and channel selection algorithms for cognitive networks. Our simulation results indicate that cross-layer antenna selection algorithm improves the transmission efficiency significantly compared to the conventional systems. Furthermore, we proposed an antenna selection algorithm applied with beamforming to gain high throughput in cognitive radio networks. The proposed algorithm allows cognitive users to access the channel with no interference effect on primary users using beamforming. Our proposed cross-layer algorithm is shown to offer high throughput using low number of RF chains. The simulation results also show that the effect of imperfect channel-state information and delayed estimates is not significant where the system still able to outperform other schemes.Our results also indicate that when the cross layer antenna selection algorithm is combined with the learning-based channel selection, the average data rate of the cognitive network improves significantly.

Chapter 6

Blind Primary User Identification in MIMO Cognitive Networks

In our previous chapters, we assume that cognitive nodes have perfect knowledge of primary users information. In this chapter, we investigate ANN techniques for primary users' signal detection purpose.

As indicated in Chapter 2, early detection of primary users presence is one of the most important tasks for cognitive communication. Also, in cognitive settings nodes may receive signals from primary users and from other cognitive users simultaneously. For such scenario, we propose primary user signal detection using modulation class identification method. We consider multiple transmit and multiple receive antennas for cognitive nodes. We employ ANN for the modulation identification purpose. The proposed algorithm works as higher order moments and cumulants are calculated from the received signal samples at each of the receiving branches of cognitive nodes. After this step, these features are fed to the ANN to determine the presence of primary users. Final identification decision is drawn using the decision from all receiving branches. We present numerical results of our algorithm and compare these results with the theoretical results of the energy detection algorithm [23].

6.1   Introduction

Spectrum sensing is one of the key elements for cognitive radio operation [1]. Cognitive radio devices should be aware of spatial and temporal contents of the operating environment. That is cognitive radio devices use sensing techniques to learn and map the spectrum parameters such as interference limit, spectrum opportunity in time, frequency and space domain. Spectrum sensing methods studied in the literature are mainly focused on primary users' transmitter detection. In these methods, sensing process involves digital signal processing operations on the received primary users' data. Some of the methods used require a priori information of the primary users' data [83, 84] while other methods can detect blindly [84]. In the following paragraphs we will briefly describe the pros and cones of these methods.

In the matched filter detection method, a known signal is correlated with an unknown signal, to detect the presence of the known signal signature in the unknown signal [83]. Matched filter detection method requires less time to achieve high processing gain. For CR devices, this detection method has limited usage for two reasons [83]. First, this method requires prior knowledge of the primary users data. Another limitation of this method indicates the need of multiple receivers for all signal types it detects. For these reasons, matched filter detection method has limited usage in cognitive settings.

Cyclostationary feature detection is another coherent detection method. In telecommunications, modulation, sampling, multiplexing, and coding operations, or other methods applied to aid channel estimation create periodicity i.e., cyclostationary properties in the radio signal. In the cyclostationary feature-detection method, primary user signal is identified by exploiting the cyclostationary features of the received signal [84]. It is possible, as noise is a stationary signal with no correlation, conversely modulated signals are cyclostationary signals with spectral correlation due to the embedded redundancy of signal periodicity. This method is robust as it does not need any knowledge of the noise power. But, similar to matched filter detection methods, cyclostationary detection meth-

ods also need prior knowledge of primary users signal and it has high implementation complexity [83, 84].

On the other hand, energy detection is a non-coherent detection method capable of performing optimally, as no prior knowledge is needed about the primary user signal. In energy detection method, RF energy of the received signal strength is measured to indicate whether the channel is idle or not. Wide-band spectrum can be sensed in this method simply from the power spectral density of the received signal. Besides these advantages, energy detection methods also have some limitations [84]. First, at low SNRs this method cannot accurately determine the noise variance which causes noise uncertainty and thus exhibits poor detection capability. The second drawback of energy detection is that it cannot distinguish between interference and signal from other cognitive users sharing the same channel. The third drawback is that it requires high sensing time for a given probability of detection.

In this study, spectrum sensing using automatic modulation classification (AMC) algorithm is adopted. AMC is a valuable tool for both civilian and military applications. Rapid development of software defined radio and cognitive radio devices makes it more promising, especially their deployment in applications such as spectrum management, interference identification, and signal surveillance. On the same lines, AMC is advantageous, as it can identify modulation types of the received signal without any a prior knowledge. As a result, we find significant amount of research and development of AMC algorithms for SISO systems [85]. In general, the developed AMC algorithms can be categorized into two classes, decision theoretic approaches [86, 87] and pattern recognition approaches [88–91]. In the decision theoretic approach, prior knowledge of the probability functions are used to classify the modulation type of received signal using hypothesis testing [86, 87]. Conversely, pattern recognition approaches, as some basic characteristics [88–91] of the received signal are extracted to classify the signal into certain class. In this study, we will use ANN for the pattern recognition approach. We choose ANN for

its robustness and easier implementation facilities. An ANN consists of three blocks, feature extraction, network training and performance evaluation. Features of the signal are extracted using some signal processing methods such as spectral based features set [88], higher order statistics (HOS) [89], constellation shape [90], and wavelet transforms [91]. Here, we consider HOS to extract features. ANN exhibits additional benefits for classification, as it does not need to be preprogrammed with thresholds for classification. For this reason, ANN is important for signal detection in cognitive settings. For instance, in [20, 21] the authors used ANN classifier to detect primary user signal.

In cognitive settings 'cognitive-to-cognitive' signal can be interfered by the primary user or by another cognitive user communication. In this scenario, early detection of interference source has not been studied. For this reason, we propose to employ ANN to identify the primary users' presence by identifying the modulation type of the primary user. Our study is different from the studies in [20] and [21], as our approach detects primary user signal while cognitive users are communicating. This is very helpful for cognitive users, as nodes can perform sensing while communicating. This will minimize unwanted interference on primary users' communication from cognitive spectrum access.

The rest of the chapter is organized is as follows. The system model is presented in Section 6.2. The proposed modulation classification algorithm is discussed in Section 6.3. Simulation model and results of the proposed algorithm are presented in Section 6.4 and Section 6.5 respectively. Finally, conclusions are drawn in Section 6.6.

6.2   System Model

Similar to previous chapters, we consider a cognitive ad-hoc network coexists with licensed primary users in the same geographical area. Cognitive users use Dynamic Spectrum Access (DSA) techniques to opportunistically utilize primary users' frequency bands. We assume any node of the cognitive ad-hoc network can listen to all other nodes in the

network. In this network, primary users can resume transmission while cognitive pairs are communicating. In such event, communicating cognitive node pairs have to vacate the occupied frequency band as soon as possible. We also assume that cognitive nodes are equipped with N_t antennas for transmission and N_r antennas for reception while primary user use SISO systems. The proposed cognitive receiver side of the system adopts modulation identification structure as shown in Fig. 6.1. In the next section we will introduce the proposed modulation classification algorithm that will successfully identify the received signal type for the cognitive node pairs.

Unlike the previous chapter here we consider cognitive nodes receive signal from both cognitive users and and primary users. To develop the mathematical model for the modulation classification algorithm, we express the received signal $\boldsymbol{y}_c \in C'^{N_r \times 1}$ at cognitive receivers as,

$$\boldsymbol{y}_c = \boldsymbol{h}_c \boldsymbol{x}_c + \boldsymbol{h}_p x_p + \boldsymbol{n}, \tag{6.1}$$

where $\boldsymbol{h}_c$ is $N_r \times N_t$ and $\boldsymbol{h}_p$ is $N_r \times 1$ matrices represent 'cognitive-to-cognitive' and 'primary-to-cognitive' channel gain respectively, $\boldsymbol{x}_c \in C^{N_t \times 1}$ and x_p are transmit symbol vector of cognitive and transmit symbol of the primary user respectively and $\boldsymbol{n} \in CN(0, \sigma^2 \boldsymbol{I}_{N_r})$ is the complex Gaussian noise vector with zero mean and variance σ^2, where $\boldsymbol{I}_{N_r}$ is the identity matrix of size N_r. We also assume source symbols of cogni-
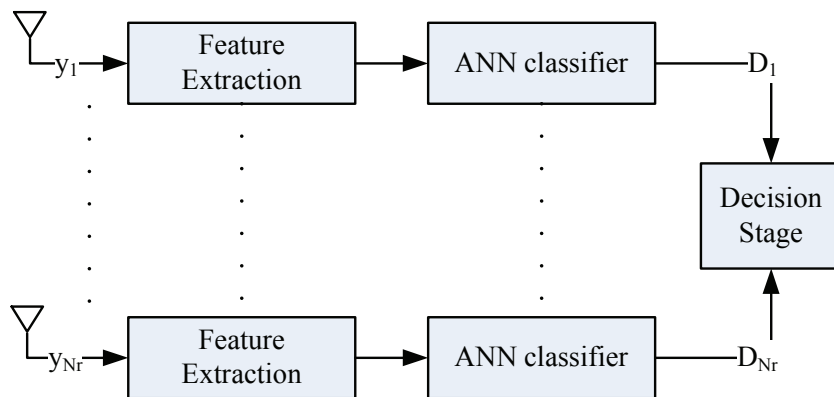
Figure 6.1: Communication system model for cognitive nodes.

100

tive and primary users are i.i.d, and mutually independent. The symbols are normalized to have zero-mean and unit energy and belong to any of the linear modulation schemes, Amplitude-shift Keying (ASK), Quadrature Amplitude Modulation (QAM) or Phase-shift keying (PSK).

6.3 Modulation Identification

In this section, we discuss artificial neural network based automatic modulation classification algorithm. The algorithm consists of three blocks, feature extraction, network training, and performance evaluation. In the following subsections we describe these features.

6.3.1 Feature extraction

Feature identification is one of the important aspects of modulation classification. As indicated in section 6.2, previous works [20, 21, 89] have shown that among the best candidates for signal identification are higher order moments and cumulants of the received signal. For N samples of any signal x, higher moment of order k is defined by

$$M_{km}(x) = E\left[x^{k-m}(x^*)^m\right].$$
(6.2)

The cumulant of order k of the zero-mean signal x is defined by

$$C_{km}(x) = Cum\left[\underbrace{x,...,x}_{(k-m)times}\ \underbrace{x^*,...,x^*}_{mtimes}\right].$$
(6.3)

Also, the relation between moments and cumulants can be expressed as,

$$Cum[x_1,....x_n] = \sum_{\phi}(\alpha-1)!\,(-1)^{\alpha-1}\prod_{v\in\phi}E\left(\prod_{i\in v}x_i\right),$$
(6.4)

where ϕ runs through the list of all partitions of $1, ..., n$, v runs through the list of all blocks of the partition ϕ, and α is the number of elements in the partition ϕ. For instance, the fourth-order cumulant of zero-mean signals x, y, z and w is given by

$$Cum\,[x, y, z, w] = E\,(xyzw) - E\,(xy)\,E\,(zw)$$
$$- E\,(xz)\,E\,(yw) - E\,(xw)\,E\,(yz)\,. \tag{6.5}$$

Based on (6.5), moments estimation leads to estimate of the cumulants. That is for a given zero mean signal $\boldsymbol{y}$ of (6.1) with N samples, one can estimate the moments and cumulants as,

$$\hat{M}_{km}\,(y) = E[y^{k-m}\,(n)\,(y^*)^m\,(n)], \tag{6.6}$$

$$\hat{C}_{20}\,(y) = E[y^2\,(n)], \tag{6.7}$$

$$\hat{C}_{21}\,(y) = E[|y\,(n)|^2], \tag{6.8}$$

$$\hat{C}_{40}\,(y) = E[y^4\,(n)] - 3E[y^2\,(n)], \tag{6.9}$$

$$\hat{C}_{41}\,(y) = E[y^3\,(n)\,y^*\,(n)] - 3E[y^2\,(n)]E[y\,(n)\,y^*\,(n)], \tag{6.10}$$

$$\hat{C}_{42}\,(y) = E[|y\,(n)|^4] - \left|E[y^2\,(n)]\right|^2 - (E[y\,(n)\,y^*\,(n)])^2\,, \tag{6.11}$$

$$\hat{C}_{60}\,(y) = E\left[y^6\,(n)\right] - 15E\left[y^4\,(n)\right]E\left[y^2\,(n)\right] + 30E\left[y^2\,(n)\right]\,, \tag{6.12}$$

$$\hat{C}_{61}\,(y) = E\left[y^5\,(n)\,y^*\,(n)\right] - 5E\left[y^4\,(n)\right]E\left[y\,(n)\,y^*\,(n)\right] - 10E\left[y^2\,(n)\right]E\left[y^3\,(n)\,y^*\,(n)\right]$$
$$+ 30E\left[y\,(n)\,y^*\,(n)\right]E\left[y^2\,(n)\right]^2\,, \tag{6.13}$$

$$\hat{C}_{62}(y) = E\left[y^5(n)(y^*(n))^2\right] - E\left[y^4(n)\right]E\left[(y^*(n))^2\right]$$

$$- 8E\left[y(n)y^*(n)\right]E\left[y^3(n)y^*(n)\right] - 6E\left[y^2(n)\right]E\left[y^2(n)(y^*(n))^2\right]$$

$$+ 6E\left[(y^*(n))^2\right]E\left[y^2(n)\right]^2 + 24E\left[y^2(n)\right]E\left[y(n)y^*(n)\right]^2, \tag{6.14}$$

$$\hat{C}_{63}(y) = E\left[y^3(n)(y^*(n))^3\right] - 6E\left[y^2(n)\right]E\left[y(n)(y^*(n))^3\right]$$

$$- 9E\left[y(n)y^*(n)\right]E\left[y^2(n)(y^*(n))^2\right] + 18E\left[y^2(n)\right]E\left[(y^*(n))^2\right]E\left[y(n)y^*(n)\right]$$

$$+ 12E\left[y(n)y^*(n)\right]^3. \tag{6.15}$$

To remove the scale problem, we normalize the signal y to have a unit energy, i.e., $C_{21} = 1$. However, practically higher order moments and cumulants are normalized as,

$$\tilde{M}_{km}(x) = \hat{M}_{km}(x)/M_{21}^{k/2}(x), \tag{6.16}$$

$$\tilde{C}_{km}(x) = \hat{C}_{km}(x)/C_{21}^{k/2}(x). \tag{6.17}$$

for $k = 2, 4, 6, ...$ and $m = 0, .., k/2$.

It is worthwhile to note that for modulation identification in SISO systems the authors in [92] used the cumulants up to the fourth order and the hierarchical classification algorithm. Their study proves that algorithm based on higher order cumulants and moments is naturally robust to constellation rotation, phase jitter and resistant to additive colored Gaussian noise. Note that in this thesis, we consider higher cumulants and moments up to order six as in (6.6)-(6.15).

6.3.2   Network training

Features extracted using the method in the previous subsection follow a certain pattern for different types of modulated signals. This can lead us to identify modulation types depending on the moments and cumulants i.e., patterns of the received signal. Here, we deploy ANN to identify this pattern, as it is one of the best tools for pattern

recognition problems. We consider a multilayer feed-forward ANN for this classification problem. Moments and cumulants are the inputs of this ANN and modulation types are outputs.

The training process of the network begins after selecting the number of hidden layers, the number of nodes in each layer and features subset selection process. In this study, we use resilient backpropagation learning algorithm (RPROP) [93] to train the initiated artificial neural network. After the training phase, a test phase is initiated, and the ANN classifier is evaluated through the probability of identification. In the next section, we will present the test phase results of our designed network.

6.3.3 Decision formulation

In our system model, the receiver is equipped with multiple antennas. At this point, modulation class detection can be done either from the received symbols of N_r branches or from the estimate of the received symbols N_t. Similar to [94], we call the first type as Direct Digital Modulation Identification (D-DMI) technique and use this for performance evaluation of our network.

Let us consider we have N_r decision vectors. The final decision is made in favor of certain modulation class if that class is identified in $\hat{M}$ classifiers out of N_r classifiers. We use $\left\lceil \frac{N_r}{2} \right\rceil$ as the value of $\hat{M}$. Other methods [95] such as logical OR, logical AND (LA), etc., can also be used for this purpose. For the system, all the ANN classifiers and N_r processed signals are identical, which results in identical probability of identification p_i in N_r decisions branches. We express the final probability for $\hat{M}$ out of N_r by

$$P = \sum_{k=\hat{M}}^{N_r} \binom{N_r}{k} p^k (1-p)^{N_r-k}. \tag{6.18}$$

Table 6.1: Theoretical values of higher order statistics for different modulation classes

Features \ Mod.	BPSK	QPSK	8PSK	QPSK + BPSK	QPSK + 8PSK
M41	1	0	0	2	0
M42	1	1	1	5	6
M60	-1	0	0	-13	0
M61	0	0	0	-4	-1
M62	1	0	0	7	-1
M63	0	0	0	22	-2
C60	-16	-1	0	-15	0
C61	-7	2	0	-1	0
C62	9	0	0	7	-2
C63	16	4	4	13	10

6.3.4 Complexity analysis

The complexity of moment and cumulant calculation in (6.2) is of order N. One can notice that estimating a moment of order k requires only about N complex additions and $k \times N$ complex multiplications. Also, from (6.4), cumulant calculation is of order N. That is, the features extraction process has a very low complexity $O(N)$. On the other hand, the complexity of the ANN classifier is low. This is due to the outputs of a layer in the ANN classifier are linear combinations of the inputs to this layer. Thus the computational cost of the classifier depends on the number of nodes at each layer. As the structure is static and predefined, and the number of nodes at each layer is small, the ANN classifier needs only a small number of operations to obtain the output which is inexpensive and has low complexity.

6.4 Simulation Model

In this section we will present test results of the above mentioned detection algorithm. To train the network, 1000 sets of 16 features (6.6)-(6.15) are considered, where each of these features are calculated using 512 samples of the received signal at cognitive nodes. We have listed theoretical values of these moments and cumulants in Table 6.1 for unit variance and noise free case. One can notice that, when one type of modulated symbols impose on another type of modulated symbols, the resultant signal achieves a distinct set of features. In our algorithm, ANN uses this property to detect the presence of primary user signal buried in cognitive users' signals.

Our designed neural network has 16 input nodes, which is equal to the number of features. However, the optimal number of hidden layers is not easy to determine. We performed extensive simulations and identified that the optimal ANN structure contains two hidden layers network (excluding the output and the input layers), where the first layer consists of 10 nodes and the second of 15 nodes. Also, we have considered the sigmoid function for the outputs of the layers [94].

After the training phase, the network is tested with 1000 features for performance evaluation. We consider the probability of identification as our performance metric,

$$p = \frac{N_c}{N_{toal}} \times 100, \tag{6.19}$$

where N_c is the number of events for which modulation is correctly detected and N_{total} denotes the total number of trails. For the MIMO case, we use this probability as identification probability for a single channel and determine the probability of identification from (6.18). It is worthwhile to mention that during the process of training, the network does not need any explicit information about primary users' signals. The process can be best described as learning phase, while the network trains itself to generate the predefined output.

6.5 Simulation Results

We consider 'cognitive-to-cognitive' pairs using QPSK modulation scheme. Cognitive nodes also receive signals from the primary user as indicated in (6.1). Our goal is to detect primary users' signals while cognitive node pairs are communicating. We also consider two sets of modulation classes for the primary user as, $Set1 = \{BPSK, 8PSK\}$ and $Set2 = \{BPSK, 8PSK, 16QAM, 64QAM, 4ASK, 8ASK\}$. We train the ANN to identify primary users' presence, as given by the hypotheses,

$$\boldsymbol{y}_c = \begin{cases} \boldsymbol{h}_c\boldsymbol{x}_c + \boldsymbol{h}_p\boldsymbol{x}_{p,BPSK} + \boldsymbol{n}, & \boldsymbol{x}_p \text{ if from BPSK modulation } \bar{H}_1 \\ \boldsymbol{h}_c\boldsymbol{x}_c + \boldsymbol{h}_p\boldsymbol{x}_{p,8PSK} + \boldsymbol{n}, & \boldsymbol{x}_p \text{ if from 8PSK modulation } \bar{H}_2 \end{cases} \qquad (6.20)$$

In Fig. 6.2 we compare detection probability results for the above mentioned classification sets, $Set1$ and $Set2$. We have detected two hypotheses for $Set1$ and six hypotheses for $Set2$. The figure demonstrates that the probability of identification decreases with the increase in the size of classification set.

To validate our results, we also include ANN results for single source and theoretical probability of identification results for the energy detection (ED) method [23]. By single source ANN, we indicate a scenario where two hypotheses in (6.21) are tested to identify $BPSK$ modulated primary users' signals from $QPSK$ cognitive signal and Gaussian noise. For hypothesis H_1, the received signal at cognitive nodes contains primary users' signals, the cognitive signal and noise. Conversely for hypothesis H_0, the received signal contains the cognitive signal and noise. We have determined the probability of identification for these two hypotheses using ANN and ED methods.

$$\boldsymbol{y}_c = \begin{cases} \boldsymbol{h}_c\boldsymbol{x}_c + \boldsymbol{h}_p\boldsymbol{x}_p + \boldsymbol{n}, & H_1 \\ \boldsymbol{h}_c\boldsymbol{x}_c + \boldsymbol{n}. & H_0 \end{cases} \qquad (6.21)$$

We investigate the effect of number of samples on the probability of identification
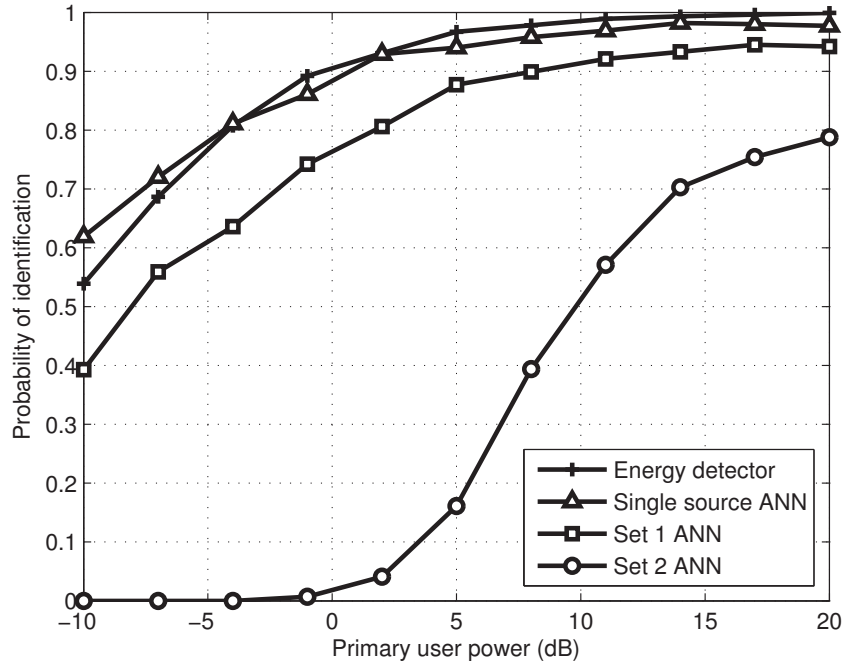
107

Figure 6.2: Comparison of detection probability for ANN and ED sensing at 5% false alarm rate and -5 dB cognitive power.

in Fig. 6.3. We notice that the identification probability improves with the increase in SNR and number of samples. An increase in number of samples and SNR enable the features be easily distinguished, which improves the identification probability. We also notice that $Set1$ has better identification probability than the identification probability of $Set2$.

At this point, we evaluate the effect of cognitive users' power and multiple receive antennas on the probability of identification. First we present the results showing the effect of cognitive users' transmit power. The probability of identification results in Fig. 6.4, reveals that some performance degradation occurs with the increase in cognitive users' power. This is due to the fact that with the increase in cognitive users' power, primary users' signal becomes corrupted and hence poor identification features. Further, the probability of identification results in Fig. 6.5 indicate that multiple receive antennas improve the identification performance significantly. We confirm this gain as multiple
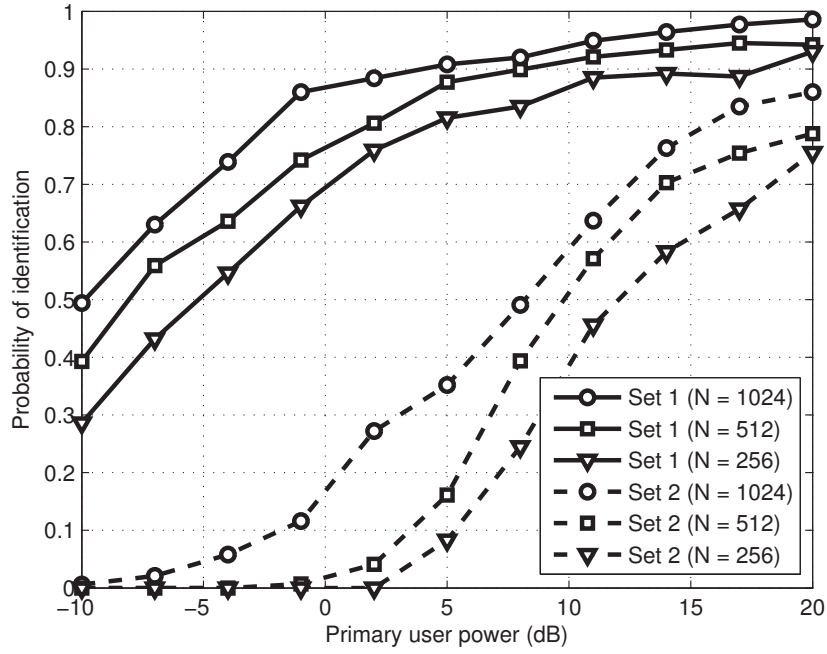
Figure 6.3: Effect of number of samples on probability of identification at 5% false alarm rate, -5dB cognitive user power and $N_r = 1$.
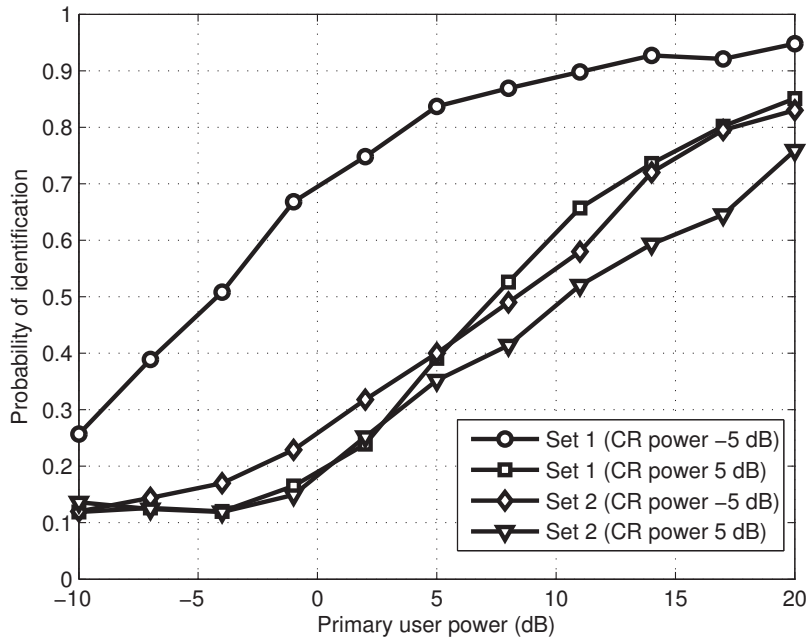
Figure 6.4: Effect of cognitive users power on identification probability at 5% false alarm rate.

109
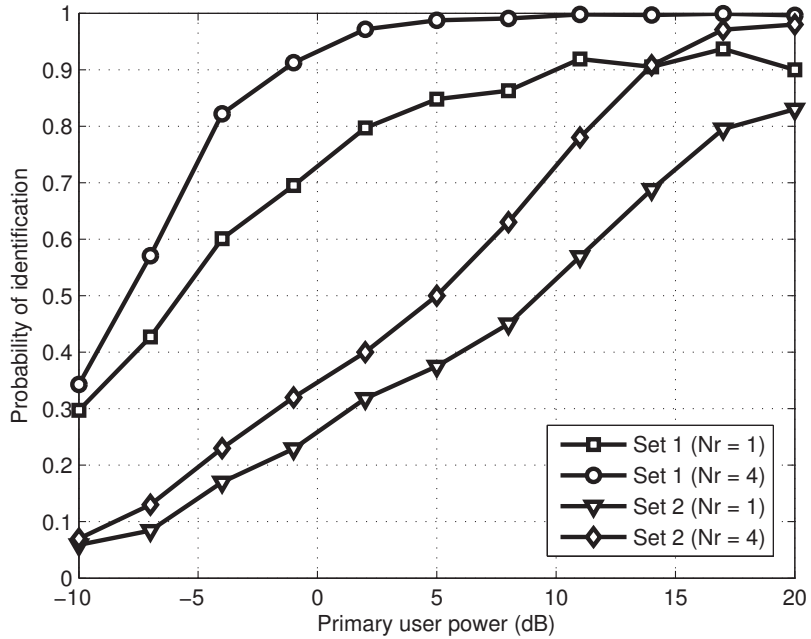
Figure 6.5: Effect of multiple antennas at the cognitive receiver on probability of identification at -5dB cognitive power and 5% false alarm rate.

antennas at the receiver add diversity to the system which improves the identification capability.

Now we investigate the effect of primary users' interference threshold on cognitive communication. For this purpose, we consider that cognitive nodes are able to transmit if interference caused by cognitive communication is below the interference threshold set at the primary user. From the probability of identification results of Fig. 6.6, it is shown that ANN identifies the presence of both cognitive node and primary nodes for cognitive SNRs below 0 dB. On the other hand, for cognitive SNRs above 0 dB, only the presence of the primary node is identified. This happens as cognitive nodes are not able to transmit at higher SNRs due to the interference constraint set by the primary node.
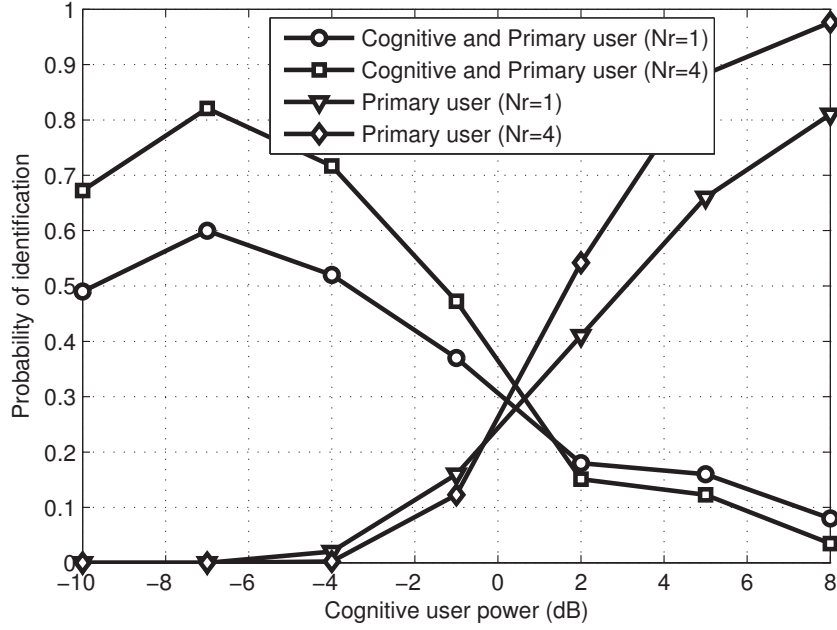
Figure 6.6: Effect of interference threshold at the primary node on probability of identification at -20dBm interference threshold, -5dB Primary user power and 5% false alarm rate for $Set1$.

6.6 Conclusions

We have presented an algorithm for primary user identification using modulation class detection. We also evaluated the effect of multiple receive antennas on identification probability. We presented simulation result for both intra-class and inter-class identifications. Our simulation results showed that neural networks can be adopted to identify primary users' presence with very high accuracy while cognitive users are communicating.

Chapter 7

Conclusions and Future Studies

7.1 Summery and Conclusions

In this section we briefly summarize major contributions and the accomplished work in this thesis.

In Chapters 1 and 2, we briefly reviewed cognitive networks, machine learning, ANN, the Game theory, and MIMO techniques. Challenges for cognitive networks are mentioned and available mathematical tools to address design challenges are addressed.

In Chapter 3, we presented analysis to determine the probability of channel availability for interference-limited cognitive networks. Using this probability and Markov model we determined the average access delay, throughput and service time for interference limited cognitive networks. These results and analyses can be applied in network design or analyze performance of existing networks. Nevertheless, in this chapter we considered all cognitive nodes operate in a single frequency band. For this purpose, we extended our study for a multi-band environment for cognitive nodes in Chapter 4.

We investigated the performance of learning based channel selection approaches for multi-band multi user cognitive ad-hoc networks in Chapter 4. We presented proof of convergence for the algorithms for multi-band cognitive ad-hod networks with heterogeneous

nodes. It was shown that learning based channel selection algorithms converge to a Nash equilibrium point for nodes having unequal arrival packet rate in multi-party multi-agent stochastic game. We also noticed that Q learning based algorithm can improve the average data rate of the network, and can reduce the user satisfaction variance i.e., improve fairness among cognitive nodes. We further showed that convergence time and data rate improve for cooperative learning.

To further improve the channel utilization, we extended our study to include MIMO techniques in Chapter 5. We investigated the performance of a cross-layer antenna selection algorithms for cognitive networks. Our simulation and analytical results indicate that cross-layer antenna selection improves the transmission efficiency significantly compared to conventional systems. Furthermore, we proposed an antenna selection algorithm applied with beamforming to gain high throughput in cognitive radio networks. The proposed algorithm allows cognitive users to access the channel with no interference effect on primary users using beamforming. Our proposed cross-layer algorithm is shown to offer high throughput using low number of RF chains. The results also show that the effect of imperfect channel-state information and delayed estimates is not significant where the system still able to outperform other schemes.

For the above mentioned studies we assumed cognitive nodes have perfect knowledge of primary users presence information. In Chapter 6, we deviate from this assumption and investigated ANN methods to detect the presence of primary user presence during cognitive communication. For this purpose, we presented an algorithm for primary user identification using modulation class detection. We also evaluated the effect of multiple receive antennas on identification probability. We presented simulation results for both intra-class and inter-class identifications. Our results show that neural networks can be adopted to identify primary users' presence with very high accuracy while cognitive users are communicating.

7.2 Future Studies

In the sequel here we list some of the topics of interest.

- In Chapter 4 and 5, we have considered cognitive radios operate in a particular frequency channel at a particular time instant. In some recent works [96,97] multiple radio devices have been developed. For that, nodes can operate in multiple frequency channels simultaneously instead of adopting a single channel. Channel allocation problem for such system is an important research direction.

- This also necessitates the investigation of appropriate MAC protocols for multi radio cognitive settings. Further, network performance parameters can be determined for multi-radio multi-band cognitive communications.

Bibliography

[1] "FCC Report of the Spectrum Efficiency Working Group," FCC Spectrum Policy Task Force, Tech. Rep., Nov. 2002 [accessed Jan. 2013]. [Online]. Available: http://www.fcc.gov/sptf/files/SEWGFinalReport_1.pdf

[2] M. A. McHenry, "Nsf spectrum occupancy measurements project summary," *Shared spectrum company report*, 2005, [accessed Mar. 2013]. [Online]. Available: http://www.sharedspectrum.com/wp-content/uploads/ NSF_Chicago_2005-11_measurements_v12.pdf

[3] S. Haykin, "Cognitive Radio: Brain-empowered Wireless Communications," *IEEE J. Sel. Areas Comm.*, vol. 23, no. 2, pp. 201–220, Feb. 2005.

[4] "Unlicensed Operation in the TV Broadcast Bands," Federal Communications Commission, Tech. Rep., May 2004 [accessed Jan. 2013]. [Online]. Available: http://fjallfoss.fcc.gov/edocs_public/attachmatch/FCC-04-113A1.pdf

[5] Ofcom, "A Statement on Our Approach to Awarding the Digital Dividend," Digital Dividend Review, Tech. Rep., Dec. 2007 [accessed Oct. 2012]. [Online]. Available: http://stakeholders.ofcom.org.uk/binaries/consultations/ddr/statement/ statement.pdf

[6] *European Harmonized Technical Conditions and Band Plans for Broadband Wireless Access in the 790-862 MHz Digital Dividend Spectrum*, 2010.

[7] C.-J. Kim, S. won Kim, J. Kim, and C. Pyo, "Dynamic Spectrum Access/Cognitive Radio Activities in Korea," in *Proc. IEEE Symp. New Frontiers in Dynamic Spectrum*, 2010, pp. 1–5.

[8] K. G. Shin, H. Kim, A. W. Min, and A. Kumar, "Cognitive Radios for Dynamic Spectrum Access: from Concept to Reality," *IEEE Wireless Communications Magazine*, vol. 17, no. 6, pp. 64–74, 2010.

[9] I. F. Akyildiz, W.-Y. Lee, M. C. Vuran, and S. Mohanty, "A Survey on Spectrum Management in Cognitive Radio Networks," *IEEE Comm. Mag.*, vol. 46, no. 4, pp. 40–48, Apr. 2008.

[10] A. Paulraj, R. Nabar, and D. Gore, *Introduction to Space-Time Wireless Communications*. UK: Cambridge University press, 2003.

[11] T. M. Duman and A. Ghrayeb, *Coding for MIMO Communication Systems*. John Wiley & Sons Ltd, 2007.

[12] P. Venkatraman and B. Hamdaoui, "Cooperative Q - learning for Multiple Secondary Users in Dynamic Spectrum Access," in *Proc. 7th Int. Wireless Communications and Mobile Computing Conf. (IWCMC)*, 2011, pp. 238–242.

[13] H. Li, "Multi-agent Q-learning of Channel Selection in Multi-user Cognitive Radio Systems: A Two by Two Case," in *Proc. IEEE Int. Conf. Systems, Man and Cybernetics SMC 2009*, 2009, pp. 1893–1898.

[14] Y. Xu, J. Wang, Q. Wu, A. Anpalagan, and Y.-D. Yao, "Opportunistic Spectrum Access in Cognitive Radio Networks: Global Optimization Using Local Interaction Games," *IEEE Journal of Selected Topics in Signal Processing*, vol. 6, no. 2, pp. 180–194, 2012.

[15] N. Nie and C. Comaniciu, "Adaptive Channel Allocation Spectrum Etiquette for Cognitive Radio Networks," in *Proc. First IEEE Int. Symp. New Frontiers in Dynamic Spectrum Access Networks DySPAN 2005*, Baltimore, MD, USA, Nov. 2005, pp. 269–278.

[16] Q. Cheng and B. Kollimarla, "Joint Channel and Power Allocation Based on User Satisfaction for Cognitive Radio," in *Proc. 43rd Annual Conf. Information Sciences and Systems CISS 2009*, Baltimore, MD, Mar. 2009, pp. 579–584.

[17] G. L. L. J. C. G. F. Daquan Feng, Chenzi Jiang and G. Y. Li, "A Survey of Energy-Efficient Wireless Communications," *IEEE Communications Surveys & Tutorials*, vol. 15, no. 1, pp. 167–178, 2013.

[18] A. A. El-Sherif and K. Liu, "Cooperation in Random Access Networks: Protocol Design and Performance Analysis," *IEEE Journal on Selected Areas in Communications*, vol. 30, no. 9, pp. 1694–1702, 2012.

[19] D. K. Navid Tadayon, Honggang Wang and L. Xing, "Analytical Modeling of Medium-Access Delay for Cooperative Wireless Networks Over Rayleigh Fading Channels," *IEEE Transactions on Vehicular Technology*, vol. 62, no. 1, pp. 349–359, 2013.

[20] J. J. Popoola and R. van Olst, "A Novel Modulation-Sensing Method," *IEEE Vehicular Technology Magazine*, vol. 6, no. 3, pp. 60–69, 2011.

[21] B. Ramkumar, T. Bose, and M. S. Radenkovic, "Combined Blind Equalization and Automatic Modulation Classification for Cognitive Radios," in *Proc. IEEE 13th Digital Signal Processing Workshop and 5th IEEE Signal Processing Education Workshop DSP/SPE 2009*, 2009, pp. 172–177.

[22] U. Phuyal, A. Punchihewa, V. K. Bhargava, and C. Despins, "Power Loading for

Multicarrier Cognitive Radio with MIMO Antennas," in *Proc. IEEE Wireless Comm. and Networking Conf. WCNC 2009*, Budapest, Apr. 2009, pp. 1–5.

[23] N. Reisi, M. Ahmadian, and S. Salari, "Performance Analysis of Energy Detection-Based Spectrum Sensing over Fading Channels," in *Proc. 6th Int Wireless Communications Networking and Mobile Computing (WiCOM) Conf*, 2010, pp. 1–4.

[24] A. Ghosh and W. Hamouda, "Cross-layer Antenna Selection and Channel Allocation for MIMO Cognitive Radios," *IEEE Transactions on Wireless Communications*, vol. 10, no. 11, pp. 3666–3674, 2011.

[25] ——, "Multiple-Input Multiple-Output Cross-layer Antenna Selection and Beamforming for Cognitive Networks," *IET Wireless Sensor Systems*, vol. 2, no. 3, pp. 170–175, 2012.

[26] ——, "Game Theory for Channel Assignment of Cognitive Radios," in *IEEE International Symposium on a World of Wireless Mobile and Multimedia Networks (WoWMoM)*, 2010, pp. 1–2.

[27] ——, "Cross-layer Design for Cognitive MIMO Ad-hoc Networks," in *IEEE International Conference on Communications (ICC)*, 2011, pp. 1–5.

[28] ——, "Combined Antenna Selection and Beamforming in Cross-layer Design for Cognitive Networks," in *IEEE International Conference on Communications (ICC)*, 2012, pp. 4949–4953.

[29] ——, "Channel Selection for Heterogeneous Nodes in Cognitive Networks," in *IEEE International Conference on Communications (ICC 2013)*, Budapest, Jun. 2013.

[30] A. Ghosh, W. Hamouda, and I. Dayoub, "Blind Primary User Identification in MIMO Cognitive Networks," in *IEEE International Conference on Communications (ICC 2013)*, Budapest, June 2013.

[31] A. Ghosh and W. Hamouda, "Performance Analysis of Interference Aware Cognitive Ad-hoc Networks," in *IEEE Global Telecommunications Conference (Globecom 2013)*, Atlanta, GA, Dec 2013, accepted.

[32] I. F. Akyildiz, W.-Y. Lee, M. C. Vuran, and S. Mohanty, "NeXt Generation/dynamic Spectrum Access/cognitive Radio Wireless Networks: A Survey," *Comput. Netw.*, vol. 50, no. 13, pp. 2127–2159, Sep. 2006.

[33] J. M. III and J. Gerald Q. Maguire, "Cognitive Radio: Making Software Radios more Personal," *IEEE Personal Communications*, vol. 6, no. 4, pp. 13–18, 1999.

[34] Supervised Learning. [accessed Mar. 2013]. [Online]. Available: http://en.wikipedia. org/wiki/Supervised_learning

[35] E. Alpaydin, *Introduction to Machine Learning.* The MIT Press, 2004.

[36] Fictitious play. [accessed Mar. 2013]. [Online]. Available: http://en.wikipedia.org/ wiki/Fictitious_play

[37] T. M. Narendra K., "Learning Automata A Survey," *IEEE Transactions on Systems, Man, and Cybernetics*, vol. SMC-4, No. 4, p. 323334, July 1974.

[38] Artificial Neural Networks/Neural Network Basics. [accessed Feb. 2013]. [Online]. Available: http://en.wikibooks.org/wiki/Artificial_Neural_Networks/ Neural_Network_Basics

[39] P. F. Baldi and K. Hornik, "Learning in Linear Neural Networks: A Survey," *IEEE Transactions on Neural Networks*, vol. 6, no. 4, pp. 837–858, 1995.

[40] G. P. Zhang, "Neural Networks for Classification: A Survey," *IEEE Transactions on Systems, Man, and Cybernetics, Part C: Applications and Reviews*, vol. 30, no. 4, pp. 451–462, 2000.

[41] M. Felegyhazi and J.-P. Hubaux, "Game Theory in Wireless Networks: A Tutorial," *Technical report: LCA-REPORT-2006-002, EPFL*, Feb. 2006.

[42] Prisoner's Dilemma. [accessed Mar. 2013]. [Online]. Available: http://en.wikipedia.org/wiki/Prisoner%27s_dilemma

[43] L. C. Emna Charfi and L. Kamoun, "PHY/MAC enhancements and QoS mechanisms for very high throughput WLANs: A survey," *IEEE Communications Surveys & Tutorials*, to be published, early Access.

[44] Q. Li, G. Li, W. Lee, M.-i. Lee, D. Mazzarese, B. Clerckx, and Z. Li, "MIMO Techniques in WiMAX and LTE: a Feature Overview," *IEEE Communications Magazine*, vol. 48, no. 5, pp. 86–92, 2010.

[45] T. R. Ramya and S. Bhashyam, "Using Delayed Reedback for Antenna Selection in MIMO Systems," *IEEE Transactions on Wireless Communications*, vol. 8, no. 12, pp. 6059–6067, 2009.

[46] H. A. A. Saleh and W. Hamouda, "Cross-layer Based Transmit Antenna Selection for Decision-feedback Detection in Correlated Ricean MIMO Channels," *IEEE Trans. Wireless Comm.*, vol. 8, no. 4, pp. 1677–1682, Apr. 2009.

[47] A. De Domenico, E. C. Strinati, and M.-G. Di Benedetto, "A Survey on MAC Strategies for Cognitive Radio Networks," *IEEE Communications Surveys & Tutorials*, vol. 14, no. 1, pp. 21–44, 2012.

[48] C. Cordeiro and K. Challapali, "C-MAC: A Cognitive MAC Protocol for Multi-Channel Wireless Networks," in *Proc. 2nd IEEE Int. Symp. New Frontiers in Dynamic Spectrum Access Networks DySPAN 2007*, 2007, pp. 147–157.

[49] D.-J. Lee and H. Wu, "Spectrum Sensing Time Minimizing Access Delay of IEEE

802.11-Like MAC in Cognitive Radio Networks," *IEEE Communications Letters*, vol. 15, no. 11, pp. 1249–1251, 2011.

[50] A. S. Zahmati, X. Fernando, and A. Grami, "Steady-state Markov Chain Analysis for Heterogeneous Cognitive Radio Networks," in *Proc. IEEE Sarnoff Symp*, April 2010, pp. 1–5.

[51] J. Gao, W. Ahmed, J. Yang, and M. Faulkner, "Throughput Comparison in Cognitive Radio Networks," in *Proc. Int Electrical Engineering/Electronics Computer Telecommunications and Information Technology (ECTI-CON) Conf*, May 2010, pp. 794–798.

[52] S. M. Kannappa and M. Saquib, "Performance Analysis of a Cognitive Network with Dynamic Spectrum Assignment to Secondary Users," in *Proc. IEEE Int Communications (ICC) Conf*, May 2010, pp. 1–5.

[53] D. T. C. Wong and F. Chin, "Sensing-Saturated Throughput Performance in Multiple Cognitive CSMA/CA Networks," in *Proc. IEEE 71st Vehicular Technology Conf. (VTC 2010-Spring)*, May 2010, pp. 1–5.

[54] X. Li, Q. Zhao, X. Guan, and L. Tong, "Optimal Cognitive Access of Markovian Channels under Tight Collision Constraints," in *Proc. IEEE Int Communications (ICC) Conf*, May 2010, pp. 1–5.

[55] M. Wadhwa, C. Xin, M. Song, and E. K. Park, "Throughput Analysis for a Contention-based Dynamic Spectrum Sharing Model," *IEEE Transactions on Wireless Comm.*, vol. 9, no. 4, pp. 1426–1433, April 2010.

[56] E. Felemban and E. Ekici, "Single Hop IEEE 802.11 DCF Analysis Revisited: Accurate Modeling of Channel Access Delay and Throughput for Saturated and Unsaturated Traffic Cases," *IEEE Transactions on Wireless Communications*, vol. 10, no. 10, pp. 3256–3266, 2011.

[57] L. Dai and X. Sun, "A Unified Analysis of IEEE 802.11 DCF Networks: Stability, Throughput and Delay," *IEEE Transactions on Mobile Computing*, to be published, early Access.

[58] G. Wang, Y. Shu, L. Zhang, and O. W. W. Yang, "Delay Analysis of the IEEE 802.11 DCF," in *Proc. 14th IEEE Personal, Indoor and Mobile Radio Communications PIMRC 2003*, vol. 2, 2003, pp. 1737–1741.

[59] G. Bianchi, "Performance Analysis of the IEEE 802.11 Distributed Coordination Function," *IEEE J. on Sel. Areas in Comm.*, vol. 18, no. 3, pp. 535–547, Mar. 2000.

[60] E. P. C. Kao, *An introduction to stochastic processes.* Duxbury Press, 1997.

[61] L. Busoniu, R. Babuska, and B. De Schutter, "A Comprehensive Survey of Multiagent Reinforcement Learning," *IEEE Transactions on Systems, Man, and Cybernetics, Part C: Applications and Reviews*, vol. 38, no. 2, pp. 156–172, 2008.

[62] K.-L. A. Yau, P. Komisarczuk, and P. D. Teal, "Context-awareness and Intelligence in Distributed Cognitive Radio Networks: A Reinforcement Learning Approach," in *Proc. Australian Communications Theory Workshop (AusCTW)*, Canberra, ACT, Feb. 2010, pp. 35–42.

[63] M. Ma and D. H. K. Tsang, "Impact of Channel Heterogeneity on Spectrum Sharing in Cognitive Radio Networks," in *Proc. IEEE Int. Conf. Comm. ICC '08*, Beijing, May 2008, pp. 2377–2382.

[64] Z. Jiang, Y. Ge, and Y. Li, "Max-utility Wireless Resource Management for best-effort Traffic," *IEEE Trans. Wireless Comm.*, vol. 4, no. 1, pp. 100–111, Jan. 2005.

[65] A. Jafari, A. R. Greenwald, D. Gondek, and G. Ercal, "On No-Regret Learning, Fictitious Play, and Nash Equilibrium," in *ICML '01: Proc. of the Eighteenth Inter-*

national Conf. on Machine Learning. San Francisco, CA, USA: Morgan Kaufmann Publishers Inc., Jun. 2001, pp. 226–233.

[66] C. J. Watkins and P. Dayan, "Technical Note Q - Learning," *Machine Learning*, vol. 8, pp. 279–292, 1992.

[67] Y. Xu, J. Wang, Q. Wu, A. Anpalagan, and Y.-D. Yao, "Opportunistic Spectrum Access in Unknown Dynamic Environment: A Game-Theoretic Stochastic Learning Solution," *IEEE Transactions on Wireless Communications*, vol. 11, no. 4, pp. 1380–1391, 2012.

[68] D. Monderer. and L. S. Shapley, "Potential Games," *Games and Economic Behavior*, vol. 14, pp. 124–143, 1996.

[69] E. R. Gomes and R. Kowalczyk, "Dynamic Analysis of Multiagent Q -learning with ϵ-greedy Exploration," in *Proceedings of the 26th International Conference on Machine Learning*, 2009, pp. 369–376.

[70] P. Papadimitratos, S. Sankaranarayanan, and A. Mishra, "A Bandwidth Sharing Approach to Improve Licensed Spectrum Utilization," *IEEE Comm. Magazine*, vol. 43, no. 12, Dec. 2005.

[71] S. Lal and A. Mishra, "A Look Ahead Scheme for Adaptive Spectrum Utilization," in *Proc. Radio and Wireless Conf. RAWCON '03*, Aug. 2003, pp. 83–86.

[72] G. Zheng, S. Ma, K. kit Wong, and T.-S. Ng, "Robust Beamforming in Cognitive Radio," *IEEE Transactions on Wireless Comm.*, vol. 9, no. 2, pp. 570–576, February 2010.

[73] N. Noori, S. M. Razavizadeh, and A. Attar, "Limiting Harmful Interference to the Primary Users through Joint Power Allocation and Beamforming in the Uplink of

Cognitive Radio Networks," in *Proc. IEEE 20th Int Personal, Indoor and Mobile Radio Communications Symp*, Sept. 2009, pp. 1246–1250.

[74] S. Yiu, M. Vu, and V. Tarokh, "Interference and Noise Reduction by Beamforming in Cognitive Networks," *IEEE Transactions on Comm.*, vol. 57, no. 10, pp. 3144–3153, October 2009.

[75] L. Bixio, G. Oliveri, M. Ottonello, M. Raffetto, and C. S. Regazzoni, "Cognitive Radios With Multiple Antennas Exploiting Spatial Opportunities," *IEEE Trans. on Signal Proc.*, no. 99, p. 1, Apr. 2010, early Access.

[76] S. Hua, H. Liu, M. Wu, and S. S. Panwar, "Exploiting MIMO Antennas in Cooperative Cognitive Radio Networks," in *Proc. IEEE INFOCOM*, 2011, pp. 2714–2722.

[77] Y. Jiang and M. K. Varanasi, "The Effect of Ordered Detection and Antenna Selection on Diversity Gain of Decision Feedback Detector," in *Proc. IEEE Int. Conf. Comm. ICC '07*, Glasgow, Jun. 2007, pp. 5383–5388.

[78] G. D. Golden, C. J. Foschini, R. A. Valenzuela, and P. W. Wolniansky, "Detection Algorithm and Initial Laboratory Results Using V-BLAST Space-time Communication Architecture," *Electronics Letters*, vol. 35, no. 1, pp. 14–16, 1999.

[79] A. Leon-Garcia and I. Widjaja, *Communication Networks: Fundamental Concepts and Key Architectures*, 2nd ed. McGraw-Hill, 2004.

[80] H. Li, "Blind Channel Estimation for Multicarrier Systems with Narrowband Interference Suppression," *IEEE Comm. Lett.*, vol. 7, no. 7, pp. 326–328, Jul. 2003.

[81] C. Shen, Y. Zhu, S. Zhou, and J. Jiang, "On the Performance of V-BLAST with Zero-forcing Successive Interference Cancellation Receiver," in *Proc. IEEE Global Telecommunications Conf. GLOBECOM '04*, vol. 5, 2004, pp. 2818–2822.

[82] W. Peng, F. Adachi, S. Ma, J. Wang, and T.-S. Ng, "Effects of Channel Estimation Errors on V-BLAST Detection," in *Proc. IEEE Global Telecommunications Conf. IEEE GLOBECOM 2008*, 2008, pp. 1–5.

[83] K. Ben Letaief and W. Zhang, "Cooperative Communications for Cognitive Radio Networks," *Proceedings of the IEEE*, vol. 97, no. 5, pp. 878–893, 2009.

[84] N. S. Shankar, C. Cordeiro, and K. Challapali, "Spectrum Agile Radios: Utilization and Sensing Architectures," in *Proc. First IEEE Int. Symp. New Frontiers in Dynamic Spectrum Access Networks DySPAN 2005*, 2005, pp. 160–169.

[85] O. A. Dobre, A. Abdi, Y. Bar-Ness, and W. Su, "Survey of Automatic Modulation Classification Techniques: Classical Approaches and New Trends," *IET Communications*, vol. 1, no. 2, pp. 137–156, 2007.

[86] W. Wei and J. M. Mendel, "Maximum-likelihood Classification for Digital Amplitude-phase Modulations," *IEEE Transactions on Communications*, vol. 48, no. 2, pp. 189–193, 2000.

[87] W. Su, J. L. Xu, and M. Zhou, "Real-time Modulation Classification Based on Maximum Likelihood," *IEEE Communications Letters*, vol. 12, no. 11, pp. 801–803, 2008.

[88] M. L. D. Wong and A. K. Nandi, "Automatic Digital Modulation Recognition Using Artificial Neural Network and Genetic Algorithm," *Signal Processing*, vol. 84, p. 351365, 2004.

[89] A. Ebrahimzadeh and A. Ranjbar, "Intelligent Signal-type Identification," *Engineering Applications of Artificial Intelligence*, vol. 21, p. 569577, 2008.

[90] B. Mobasseri, "Digital Modulation Classification Using Constellation Shape," *Signal Processing*, vol. 8, p. 2000, 2000.

[91] P. Prakasam and M. Madheswaran, "Modulation Identification Algorithm for Adaptive Demodulator in Software Defined Radios Using Wavelet Transform," *International Journal of Signal Processing*, vol. 5, p. 7481, 2009.

[92] A. Swami and B. M. Sadler, "Hierarchical Digital Modulation Classification using Cumulants," *IEEE Transactions on Communications*, vol. 48, no. 3, pp. 416–429, 2000.

[93] M. Riedmiller and H. Braun, "A Direct Adaptive Method for Faster Backpropagation Learning: the RPROP Algorithm," in *Proc. IEEE Int Neural Networks Conf*, 1993, pp. 586–591.

[94] K. Hassan, I. Dayoub, W. Hamouda, C. N. Nzeza, and M. Berbineau, "Blind Digital Modulation Identification for Spatially-Correlated MIMO Systems," *IEEE Transactions on Wireless Communications*, vol. 11, no. 2, pp. 683–693, 2012.

[95] E. C. P. Ying-Chang Liang, Yonghong Zeng and A. T. Hoang, "Sensing-Throughput Tradeoff for Cognitive Radio Networks," *IEEE Transactions on Wireless Communications*, vol. 7, no. 4, pp. 1326–1337, 2008.

[96] R. E. Irwin, A. B. MacKenzie, and L. A. DaSilva, "Resource-Minimized Channel Assignment for Multi-Transceiver Cognitive Radio Networks," *IEEE Journal on Selected Areas in Communications*, vol. 31, no. 3, pp. 442–450, 2013.

[97] P. Wang, J. Matyjas, and M. Medley, "Joint Spectrum Allocation and Scheduling in Multi-radio Multi-channel Cognitive Radio Wireless Networks," in *IEEE Sarnoff Symposium, 2010.* IEEE, 2010, pp. 1–6.